

Noble gases as tracers for mixing and gas exchange processes in lakes and oceans

Christian P. Holzner



Noble gases as tracers for mixing and gas exchange processes in lakes and oceans

A dissertation submitted to
ETH ZURICH

for the degree of
DOCTOR OF SCIENCES

presented by
CHRISTIAN PETER HOLZNER
Dipl. Umwelt-Natw. ETH
born 14 July 1972
citizen of Tartar (GR)

accepted on the recommendation of
Prof. Dr. Dieter M. Imboden, examiner
Prof. Dr. Bernhard Wehrli, co-examiner
Prof. Dr. Rolf Kipfer, co-examiner

2008

Chapter 4 has been published as:

Holzner C. P., McGinnis D. F., Schubert C. J., Kipfer R., and Imboden D. M. Noble gas anomalies related to high-intensity methane gas seeps in the Black Sea. *Earth. Planet. Sci. Lett.*, 265(3-4):396–409, 2008. doi: 10.1016/j.epsl.2007.10.029.

Chapter 5 has been submitted for publication and is currently under review:

Holzner C. P., Aeschbach-Hertig W., Simona M., Veronesi M., Kipfer R., and Imboden D. M. Exceptional mixing events in Lake Lugano, Switzerland, studied using environmental tracers. *Limnol. Oceanogr.*, submitted, 2008.

Acknowledgements

I would like to express my gratitude to the referees of my thesis: *Dieter Imboden*, *Bernhard Wehrli* and *Rolf Kipfer* aka. *RoKi*. Dieter's sound and critical reviews of my work helped to improve this thesis considerably. I thank Bernhard for consenting to be co-referee on my thesis and for valuable discussions. The enthusiasm and continuous support of RoKi, his broad knowledge and his inspiring unconventional ideas were a big help in completing this work.

It was a great pleasure working at the Eawag W+T department. My thanks go to all the colleagues at Eawag, especially to the current and former members of the Environmental Isotopes Group: *Werner Aeschbach-Hertig* (who guided my first steps in research during my diploma thesis on Lake Lugano), *Helena Amaral*, *Matthias Brennwald*, *Nora Graser* (who contributed substantially to the studies in Lake Hallwil and in the Black Sea with her diploma thesis), *Markus Hofer*, *Edi Höhn*, *Thomas Jankowski*, *Stephan Klump*, *David Livinstone* (who thoroughly checked and corrected the English of all my manuscripts), *Lars Mächler*, *Yvonne Scheidegger*, *Yama Tomonaga*. I always enjoyed the helpful collaboration, the interesting discussions (about science and other exciting things in life), the lunch-time running exercises, the nice company at conferences, and the good working atmosphere in general.

Thanks are due to *Arno Stöckli* from the Department of Environment of the Canton of Argovia for the detailed introduction to Lake Hallwil and for letting me use their boat. I would also like to thank *Lee Bryant*, *Theresa Edmonds*, *John Little*, and *Vickie Singleton* from Virginia Tech, USA for the cooperation during sampling on Lake Hallwil.

It was a unique opportunity to contribute to the European Union project CRIMEA and to join a research cruise on the Black Sea. I greatly appreciated the support by the officers and crew of the *R/V Professor Vodjanitskiy* during the cruise. The scientific contacts and private friendships within the CRIMEA team that were made during the cruise and the following meetings are very valuable. In particular, I would like to thank the following "CRIMEAns": *Stan Beaubien*, *Marilena Calarco*,

Marc De Batist, Jens Greinert, Matthias Haeckel, Lucia Klauser, Peter Linke, Dan McGinnis, Lorenz Moosmann, Lieven Naudts, Sonia Papili, Martin Pieper, Angelika Rohrbacher, Frank Schellig, Olivier Schmale, and Carsten Schubert.

Further thanks go to *Marco Simona* and *Mauro Veronesi* from the Earth Science Institute of the University of Applied Sciences of Southern Switzerland, Cannobio for making the water sampling in Lake Lugano possible and for giving me access to their large archive of CTD data.

Thanks are due to the members of the noble-gas group at ETH Zürich, especially to *Heiri Baur* and *Urs Menet* for their great work in keeping the noble-gas mass spectrometers running and for always assisting me when something broke.

I would like to acknowledge the funding of this thesis by the Swiss Federal Office of Education and Science (within the framework of the European Union project CRIMEA) and by the ETH methane research cluster TUMSS.

Last but not least, I thank *my family, Franziska* and *my friends* for their huge support, their everlasting encouragement, and for distracting me from work at the right times.

Contents

Summary	iii
Zusammenfassung	v
1 Introduction	1
1.1 Investigation of mixing and gas exchange in lakes and oceans using noble gases	1
1.2 Outline	2
2 Conceptual aspects	5
2.1 Origin of noble gases in surface water bodies	6
2.2 Atmospheric equilibrium concentrations in water	8
2.3 Gas exchange across the air-water interface	10
2.4 Injection of gas bubbles into lakes and oceans	13
2.5 Vertical mixing in stratified waters	16
2.6 Tritium decay and water ages	18
2.7 Two simple models for noble gas concentrations in lakes and oceans .	19
3 Aeration of Lake Hallwil	23
3.1 Introduction	23
3.1.1 Restoration of eutrophic Lake Hallwil	23
3.1.2 Effect of aeration on dissolved noble gases in lakes	26
3.2 Methods	27
3.2.1 Sampling	27
3.2.2 Noble gas analyses	28
3.3 Results and discussion	29
3.3.1 Differences in the noble gas concentration profiles along the lake axis	30
3.3.2 Noble gas profiles observed at different aeration gas flow rates	34
3.3.3 Mass balance calculations	36
3.4 Conclusions	39

4	Methane gas seeps in the Black Sea	41
4.1	Introduction	42
4.2	Methods	43
4.2.1	Study area	43
4.2.2	Noble gases and tritium	45
4.3	Results and Discussion	47
4.3.1	Reference profiles of tritium and noble gases	47
4.3.2	Depletion of heavy noble gases above high-intensity CH ₄ gas seeps	51
4.3.3	Proposed mechanism of noble gas depletion	53
4.3.4	Helium concentrations and isotopic composition in the water column	56
4.3.5	Helium emanation from the sediment	57
4.4	Conclusions	60
4.5	Appendix: Tables of the noble gas data	62
4.5.1	Water samples	62
4.5.2	Sediment samples	66
5	Mixing events in Lake Lugano	67
5.1	Introduction	68
5.2	Methods	69
5.2.1	Sampling	69
5.2.2	Transient tracers	70
5.3	Results and discussion	71
5.3.1	Temperature, conductivity and dissolved oxygen	71
5.3.2	Density and stability	73
5.3.3	Transient tracer concentrations	75
5.3.4	Apparent water ages	79
5.3.5	Quantification of deep-water renewal	80
5.4	Conclusions	84
6	Synthesis and outlook	87
	Bibliography	91
	Curriculum vitae	101

Summary

This work focuses on specific mixing and gas exchange processes that affect the concentrations of dissolved noble gases in lakes and oceans. As a common first-order generalization, the concentrations of noble gases in open waters are expected to correspond to the respective atmospheric equilibrium concentrations. Nevertheless, deviations from gas-exchange equilibrium with the atmosphere – so-called noble gas concentration anomalies – have been detected in various lakes and oceans, e.g. due to the radiogenic production of noble gases or due to the injection of air by breaking waves. The observed magnitudes of the noble gas concentration anomalies allow the rates of the prevailing physical processes to be estimated. Three case studies that use noble gases as tracers to investigate the effects of mixing and gas exchange processes in different water bodies are discussed in this thesis.

- In *Lake Hallwil*, the aeration system that was installed to prevent anoxic conditions in the water has been found to inject noble-gas enriched aeration gas bubbles into the lake. The aeration process results in a characteristic supersaturation of dissolved noble gases in the water body. A noble-gas mass balance suggests that the injected aeration gas is efficiently dissolved in the lake during summer stratification and gas loss to the atmosphere appears to be negligible.
- In the *Black Sea*, high-intensity methane gas seeps influence the concentrations of dissolved noble gases in the water column above the seep sites. Profiles sampled at active seep sites were characteristically depleted in noble gases. Because the noble gas depletions cannot be explained solely by gas exchange with methane gas bubbles rising in the water, a concurrent injection of fluids depleted in noble gases from the active seeps is postulated. The injected fluids seem to undergo vertical transport in the water column due to small density differences and mix with the surrounding water, causing the observed noble-gas depletions. Elevated helium concentrations in the deep water of the Black Sea are due to the release of helium from the solid earth. Analyses of the helium isotope ratios in

water samples as well as in the pore water of sediments suggest that the helium release is spatially heterogeneous and might be related to the methane seepage at certain active seep sites.

- In *Lake Lugano*, two exceptional mixing events triggered considerable vertical water exchange and subsequent gas exchange with the atmosphere. Existing time-series of data on noble gases and other transient tracers, which extend more than ten years back in time, have been prolonged to cover the recent mixing events. The deep water of Lake Lugano was permanently stratified over the last four decades, which resulted in small changes of the dissolved tracer concentrations and a gradual increase of the corresponding apparent water ages in the earlier measurements. During the recent mixing events, however, the tracer concentrations and apparent water ages changed dramatically in response to mixing and gas exchange with the atmosphere. Numerical modeling of the tracer concentrations shows that the deep-water renewal rates increased by at least an order of magnitude during the mixing events.

In conclusion, the presented case studies illustrate that noble gases are very suitable tracers to study gas exchange and mixing processes in lakes and oceans. The tracer data are a useful complement to the standard measurements which are commonly used to characterize the physical conditions in lakes and oceans as they allow secondary gas exchange processes such as the gas exchange with bubbles injected into a water body to be analyzed.

Zusammenfassung

Diese Arbeit befasst sich mit spezifischen Mischungs- und Gasaustauschprozessen, welche die Konzentrationen gelöster Edelgase in Seen und Meeren beeinflussen. Als gebräuchliche Näherung kann angenommen werden, dass die Edelgaskonzentrationen in Oberflächengewässern den jeweiligen atmosphärischen Gleichgewichtskonzentrationen entsprechen. Abweichungen vom Gasaustauschgleichgewicht mit der Atmosphäre – sogenannte Edelgas-Konzentrationsanomalien – wurden aber in verschiedenen Seen und Meeren beobachtet, z.B. aufgrund radiogener Produktion von Edelgasen oder wegen dem Eintrag von Luftblasen durch brechende Wellen. Anhand der Grösse der beobachteten Edelgas-Konzentrationsanomalien lassen sich Raten der vorherrschenden physikalischen Prozesse abschätzen. In dieser Dissertation werden drei Fallstudien behandelt, in welchen Edelgase als Tracer verwendet werden, um die Effekte von Mischungs- und Gasaustauschprozessen in verschiedenen Gewässern zu untersuchen.

- Im *Hallwilersee* werden von der Belüftungsanlage, welche anoxische Bedingungen im Wasser verhindert, Edelgas-angereicherte Gasblasen in den See eingebracht. Der Belüftungsbetrieb führt zu charakteristischen Anreicherungen gelöster Edelgase im Wasserkörper. Eine Massenbilanz der Edelgase deutet darauf hin, dass das eingeblasene Belüftungsgas während der Sommerstratifikation zum grössten Teil im See gelöst wird und dass der direkte Gasverlust in die Atmosphäre vernachlässigbar ist.
- Im *Schwarzen Meer* beeinflussen Gasaustritte am Seegrund, welche mit hoher Intensität Methangas freisetzen, die Konzentrationen gelöster Edelgase in der darüberliegenden Wassersäule. Profile von Wasserproben, die oberhalb solcher Gasaustritte gesammelt wurden, zeigten charakteristische Abreicherungen der Edelgase. Da die vorliegenden Edelgasabreicherungen nicht allein von Gasaustauschprozessen mit den aufsteigenden Methanblasen verursacht sein können, wird spekuliert, dass zusätzlich zur Gasfreisetzung am Seegrund auch Fluide

ausströmen, welche abgereichert sind an Edelgasen. Aufgrund geringer Dichteunterschiede scheinen diese Fluide in der Wassersäule aufzusteigen und sich schliesslich mit dem umgebenden Wasser zu vermischen. Daraus könnten die beobachteten Edelgasanreicherungen resultieren.

Erhöhte Heliumkonzentrationen im Tiefenwasser des Schwarzen Meeres weisen auf die Freisetzung von Helium aus dem Erdinneren hin. Analysen der Heliumisotopenverhältnisse in Wasserproben und auch in Porenwässern von Sedimenten deuten darauf hin, dass die Heliumfreisetzung räumlich heterogen stattfindet und möglicherweise mit dem Ausströmen von Methan aus gewissen aktiven Gasaustritten verknüpft ist.

- Im *Luganersee* führten zwei aussergewöhnliche Mischungsereignisse zu bedeutendem vertikalen Wasseraustausch und erhöhtem Gasaustausch mit der Atmosphäre. Zeitreihen von Edelgaskonzentrationen und anderen transienten Tracern, welche mehr als zehn Jahre zurückreichen, wurden erweitert, um die aktuellen Mischungsereignisse zu erfassen. Das Tiefenwasser des Luganersees war über die letzten vier Jahrzehnte permanent geschichtet, was sich in geringen Veränderungen der gelösten Tracerkonzentrationen und einer allmählichen Zunahme der entsprechenden scheinbaren Wasseralter niederschlug. Im Gegensatz dazu veränderten sich die Tracerkonzentrationen und die scheinbaren Wasseralter während der kürzlichen Mischungsereignisse schlagartig aufgrund der verstärkten Mischung und des Gasaustausches mit der Atmosphäre. Ein numerisches Modell der Tracerkonzentrationen zeigt, dass die Tiefenwassererneuerung während der Mischungsereignisse um mindestens eine Grössenordnung zugenommen hat.

Zusammenfassend lassen die präsentierten Fallstudien den Schluss zu, dass Edelgase sehr geeignet sind als Tracer um Mischungs- und Gasaustauschprozesse in Seen und Meeren zu untersuchen. Die Tracerdaten sind eine sinnvolle Ergänzung der Standardmessungen, die üblicherweise angewendet werden um die physikalischen Bedingungen in Oberflächengewässern zu charakterisieren, weil sie erlauben, Aussagen über sekundäre Gasaustauschprozesse zu machen, welche stattfinden wenn Blasen in einem Gewässer freigesetzt werden.

Introduction

1.1 Investigation of mixing and gas exchange in lakes and oceans using noble gases

Dissolved noble gases are often used to trace mixing dynamics and to analyze water residence times in lacustrine and marine systems. Kipfer et al. (2002) and Schlosser and Winckler (2002) review and summarize the governing processes and common applications of noble gases in lakes and oceans.

The concentrations of dissolved noble gases in open waters normally correspond to the atmospheric equilibrium concentrations determined by the temperature, salinity and pressure prevailing at the surface of the water body. As noble gases are biochemically inert, only physical processes or “non-atmospheric” inputs can change the noble-gas concentrations in lakes and oceans and hence are responsible for deviations from the gas-partition equilibrium with the atmosphere. For instance, helium excesses due to the input of helium from the earth’s crust or mantle (e.g. Aeschbach-Hertig et al., 2002; Bieri et al., 1966; Clarke et al., 1969; Craig et al., 1975), or due to the accumulation of helium-3 produced by the radioactive decay of tritium (e.g. Jenkins and Clarke, 1976) are common features in water bodies with a relatively long residence time. Oceans and some large lakes have also been found to be slightly supersaturated with noble gases due to the injection of air by breaking waves (e.g. Craig and Weiss, 1971; Peeters et al., 2000a).

The aim of this work is to further investigate noble gas concentration anomalies in lakes and oceans that are related to specific mixing and gas exchange processes. A main focus is laid on the effect that gas injection from natural gas reservoirs in the

subsurface (Chapter 4) or from technical installations like aeration systems (Chapter 3) has on the noble gas concentrations in lakes and oceans.

Gas bubbles that are released at the bottom of a water body and rise in the water column will induce secondary gas-exchange processes with the surrounding water. At the same time, the gas bubbles cause buoyancy that affects the mixing regime of the water column. Earlier studies of aeration systems and natural gas sources in lakes and oceans only analyzed the main gas species contained in the bubbles, like oxygen or methane, but did not consider noble gases (e.g. Clark et al., 2003; Leifer et al., 2006; McGinnis et al., 2006a; Wüest et al., 1992b). The present work aims to study the influence that gas bubbles injected from aeration systems and natural gas sources have on the concentrations of dissolved noble gases in the water column. Noble gases are expected to be particularly useful to determine the rates of the induced gas exchange and mixing processes because their concentrations in natural waters are not altered by biogeochemical transformation processes and because their physical properties, which control gas-exchange processes, cover a wide range of physical properties of the gases typically injected into surface waters from natural gas reservoirs or aeration systems. Simultaneous measurements of the five noble gases helium, neon, argon krypton and xenon (Beyerle et al., 2000) are therefore expected to provide detailed insights that make a thorough analysis of the gas exchange between the water and the injected bubbles feasible.

Apart from bubble-related processes, this work also investigates large-scale mixing and gas exchange in a stratified lake that underwent a sudden transition in the mixing regime (Chapter 5). The aim of this part is to explore the use of time-series of noble gas measurements to assess changes in the rate of deep water renewal and to monitor the gas exchange with the atmosphere.

1.2 Outline

This thesis comprises the results of three noble gas studies carried out in two Swiss lakes – Lake Hallwil and Lake Lugano – and in the Black Sea. In these applications, noble gas concentration changes and/or deviations from gas exchange equilibrium with the atmosphere are interpreted in terms of gas exchange and mixing processes taking place in the respective water bodies. Mass balance calculations and numerical models are developed and applied to determine the relevant process rates based on the noble gas data obtained.

Conceptual aspects (Chapter 2) This chapter summarizes the main sources and processes that determine noble gas concentrations in lakes and oceans. It also includes a brief introduction on the modeling of noble gas concentrations in surface water bodies.

Aeration of Lake Hallwil (Chapter 3) Lake Hallwil (Switzerland), a small eutrophic lake, is equipped with an artificial aeration system to prevent anoxic conditions developing in the deep water during stratification in summer. The aeration system consists of diffusers releasing oxygen-rich gas bubbles into the deep water at the bottom of the lake. The concentrations of the noble gases He, Ne and Ar in the deep water are found to be strongly supersaturated, while Kr and Xe concentrations correspond to their respective atmospheric equilibrium concentrations. The observed noble gas excesses seem to be related to the operation of the aeration system and to the composition of the injected aeration gas. Based on this, it is demonstrated that the noble gas data can be utilized to estimate the proportion of the injected aeration gas that effectively remains as dissolved gas in the water body.

Methane gas seeps in the Black Sea (Chapter 4) In some areas of the Black Sea, high-intensity gas seeps release considerable volumes of gaseous methane from the sediment into the water column. As methane is a significant greenhouse gas, the fate of the gas injected into the water column and its potential release to the atmosphere is relevant for the atmospheric methane cycle. The noble gas profiles measured in the water column show characteristic concentration anomalies above active seep sites as compared to reference sites unaffected by gas release. These noble gas anomalies seem to be caused by gas exchange between the rising bubbles and the water, or by advective vertical water transport induced by the seepage. The noble gas data allow specific processes occurring in the seepage areas to be identified. In contrast, the concentrations of other dissolved substances in the water column, such as the methane itself, show no significant differences between seep and reference sites, as the accuracy of the measurements is too low to detect the methane-gas input directly.

Mixing events in Lake Lugano (Chapter 5) Strong eutrophication resulted in the deep northern basin of Lake Lugano (Ticino, Switzerland) being meromictic for much of the last ~40 years, with a permanent stratification that inhibited seasonal mixing and deep water renewal below ~100 m depth, leading to permanent deep-water anoxia. Two strong mixing events that extended to the entire water column took place in the winters of 2004/2005 and 2005/2006, and led to drastic changes in the distribution of oxygen and nutrients in the water column. Traces of oxygen were measured even at the bottom of the lake for the first time in decades. Noble gas measurements carried out before and after the mixing events showed strong concentration changes due to the intensive water turnover and subsequent gas exchange with the atmosphere. Numerical modeling of the noble gas concentrations allowed quantification of the deep-water renewal that accompanied the mixing events.

Concepts regarding noble gases in lakes and oceans

Noble gases make excellent tracers to study the physical processes that occur in lakes and oceans, because they are unaffected by biological and chemical transformation processes. Helium isotopes in combination with tritium provide time information related to the water dynamics (i.e. the ^3H - ^3He age, see Sec. 2.6), which is useful in estimating vertical water exchange in deep lakes, e.g., Lake Lucerne (Aeschbach-Hertig et al., 1996), Lake Baikal (Hohmann et al., 1998; Peeters et al., 1997, 2000b), Lake Issyk-Kul (Hofer et al., 2002; Vollmer et al., 2002), the Caspian Sea (Peeters et al., 2000a), the Great Lakes of North America (Torgersen et al., 1977), and in chemically stratified lakes, e.g., Green Lake (Torgersen et al., 1981), Lake Lugano (Aeschbach-Hertig et al., 2007; Holzner, 2001; Wüest et al., 1992a), Lake Zug (Aeschbach-Hertig, 1994), and Lac Pavin (Aeschbach-Hertig et al., 2002). In addition to vertical mixing, horizontal water exchange between different lake basins can be studied (Aeschbach-Hertig et al., 1996; Peeters et al., 1997; Zenger et al., 1990). Measurements of noble gases in combination with tritium may also be applied to determine rates of oxygen consumption in a water body and terrigenous helium fluxes from the sediments (Aeschbach-Hertig, 1994; Aeschbach-Hertig et al., 1996, 2002, 2007; Hohmann et al., 1998; Holzner, 2001; Mamyrin and Tolstikhin, 1984; Peeters et al., 2000b; Top et al., 1981). Large programs were realized in oceans that used helium isotopes (^3He and ^4He), frequently in combination with tritium, to study water mass formation, circulation and variability (e.g. Jenkins, 1987; Schlosser et al., 1991a,b). The atmospheric noble gases neon, argon, krypton and xenon carry information on the physical conditions prevailing at the water surface

during gas exchange. Aeschbach-Hertig et al. (1999) use noble gas data from Lake Baikal (Hohmann et al., 1998) and the Caspian Sea (Peeters et al., 2000a) to reconstruct equilibration temperatures. Atmospheric noble gases have also been used to study lake level fluctuation in Lake Tanganyika (Kipfer et al., 2000).

The behavior of the noble gas radon differs from that of the other noble gases as it is lost rapidly by radioactive decay. The most stable isotope ^{222}Rn (half-life 3.8 d) has been employed to study horizontal and vertical mixing in the region near the sediment of lakes and oceans (Broecker et al., 1968; Chung and Craig, 1972; Colman and Armstrong, 1987; Imboden, 1977; Imboden and Emerson, 1978; Imboden and Joller, 1984; Weiss et al., 1984) and to trace river inflow, e.g. in Lake Constance (Weiss et al., 1984).

This chapter will give an brief overview of the processes and sources (Fig. 2.1) that are relevant in determining the noble gas concentrations in the water bodies being analyzed in this work. The main noble gas components found in lakes and oceans are defined (Sec. 2.1); which are the atmospheric, terrigenic (i.e. originating from the solid earth), and radiogenic noble gases. Typical atmospheric equilibrium concentrations of noble gases in water are given (Sec. 2.2) and the process of air-water gas exchange is discussed (Sec. 2.3). The anticipated effects of gas bubbles injected into water bodies on the concentrations of dissolved noble gases are discussed conceptually (Sec. 2.4). It is shown how vertical mixing affects the noble gas concentrations (Sec. 2.5) and how the radioactive decay of tritium assigns a time information to a water mass that can be interpreted as an apparent water age (Sec. 2.6). Two types of models that were used in the current work to analyze the effect of mixing processes on noble gas concentrations are introduced in the last part of this chapter (Sec. 2.7).

2.1 Origin of noble gases in surface water bodies

The most dominant noble gas component – the *atmospheric* noble gases helium (He), neon (Ne), argon (Ar), krypton (Kr) and xenon (Xe) – is introduced into lakes and oceans by gas exchange at the surface, and to a far lesser extent by the (complete or partial) dissolution of entrapped air bubbles that were injected into the water by breaking waves (e.g. Craig and Weiss, 1971; Peeters et al., 2000a). In polar regions, melting of shelf ice that contains entrapped air bubbles also injects atmospheric noble gases into the oceans (Hohmann et al., 2002; Schlosser, 1986; Schlosser et al., 1990).

The non-atmospheric components comprise *terrigenic* (originating from defined geochemical reservoirs within the solid earth) and *radiogenic* noble gases (produced either by radioactive decay or by α -particle induced secondary nuclear reactions). The terms “terrigenic” and “radiogenic” are often used synonymously although they do not necessarily describe exactly the same noble gas component. Radiogenic ^3He

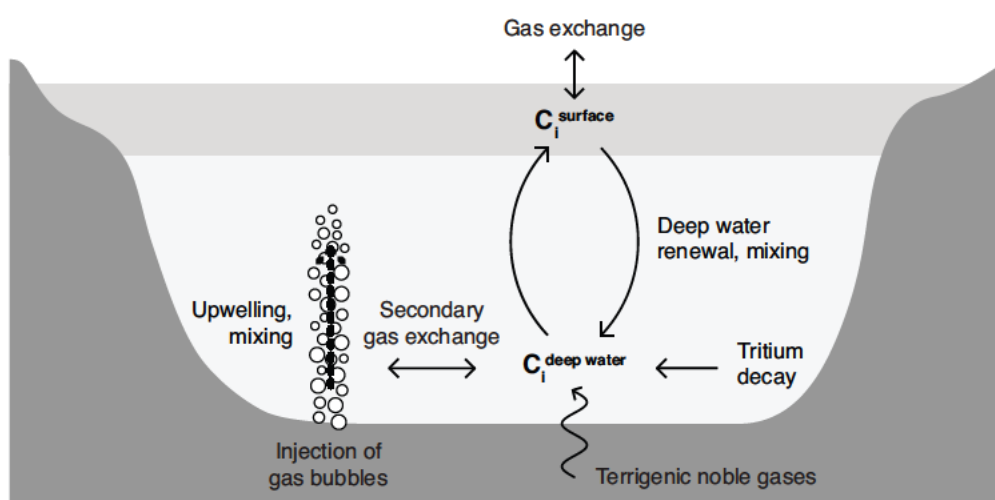


Figure 2.1 Illustration of the processes analyzed in this thesis that affect noble gas concentrations C_i ($i = \text{He, Ne, Ar, Kr, Xe}$) in lakes and oceans.

and ^4He that are produced within the earth's crust and released to lakes and oceans are therefore of terrigenous origin. Primordial ^3He (i.e. ^3He that originates from the time of the formation of the solid earth) from the earth's mantle is non-radiogenic, but terrigenous. The most important radiogenic ^3He component in surface waters is *tritogenic* ^3He that is produced in the water body by the radioactive decay of tritium (^3H). Since the half-life time of ^3H (4500 d \cong 12.32 yr; Lucas and Unterwieser, 2000) is comparable to the typical renewal times of many surface water bodies, ^3H and ^3He can be used to analyze water exchange in lakes and oceans (see Sec. 2.6). A further non-atmospheric noble gas that can be used as environmental tracer in aquatic systems is radon (Rn). Rn isotopes are formed in the decay chains of uranium and thorium and emanate from mineral surfaces in the sediments into the overlying water bodies. As all Rn isotopes are radioactive (^{222}Rn : half-life of 3.8 d, ^{220}Rn : 56 s, ^{219}Rn : 4 s), they are in principle suitable to trace physical processes on very short time scales. Most Rn studies (e.g. Broecker et al., 1968; Chung and Craig, 1972; Colman and Armstrong, 1987; Imboden, 1977; Imboden and Emerson, 1978; Imboden and Joller, 1984; Weiss et al., 1984) use the relatively stable isotope ^{222}Rn , as it is comparatively easy to measure due to the longer half-life. Only recently, ^{220}Rn was applied as a tracer in groundwater studies (E. Hoehn, pers. comm.). The noble gas Rn has not been analyzed in this work and will not be discussed further. Note that for noble gases other than He and Rn, non-atmospheric components in surface waters are commonly negligible.

2.2 Atmospheric equilibrium concentrations in water

The concentrations of noble gases dissolved in water bodies that are in phase partitioning equilibrium with a corresponding gas phase are given by *Henry's Law*:

$$p_i = H_i(T, S) \cdot C_i^{eq} \quad i = \text{He, Ne, Ar, Kr, Xe} \quad (2.1)$$

where p_i is the partial pressure of the noble gas i in the gas phase, H_i is the *Henry coefficient*, which depends on the water temperature T and salinity S , and C_i^{eq} is the noble gas concentration dissolved in the water at equilibrium. Solubility coefficients $\lambda_i = 1/H_i$ are often used in the literature instead of the Henry coefficients. In this work, the noble gas solubilities – or the Henry coefficients – are calculated from the parameterizations recommended by Kipfer et al. (2002); i.e. those of Weiss (1971) for He and Ne, Weiss (1970) for Ar, Weiss and Kyser (1978) for Kr, and Clever (1979) for Xe. The Henry coefficients H_i and the atmospheric equilibrium concentrations of the noble gases for typical water temperatures T and salinities S are listed in Tab. 2.1 and Tab. 2.2. The concentrations of dissolved noble gases are usually denoted as gas volumes (cm^3) at standard conditions (STP: $T_0 = 273.15 \text{ K} = 0^\circ\text{C}$, $p_0 = 1 \text{ atm}$) per unit water mass (g); i.e. in units of $\text{cm}^3\text{STP g}^{-1}$. Aqueous noble gas concentrations can be converted into molar units using:

$$\begin{aligned} 1 \text{ cm}^3\text{STP} &= 2.6868 \times 10^{19} \text{ atoms} = 4.4615 \times 10^{-5} \text{ mol} \\ \text{or } 1 \text{ mol} &= 22414 \text{ cm}^3\text{STP}. \end{aligned} \quad (2.2)$$

Gas concentrations in the atmosphere are specified in terms of partial pressures in atm ($1 \text{ atm} = 101325 \text{ N m}^{-2}$). The partial pressures p_i are given by:

$$p_i = (p_{\text{atm}} - e) \cdot v_i \quad (2.3)$$

Table 2.1 Henry coefficients H_i of the noble gases $i = \text{He, Ne, Ar, Kr, Xe}$ at different water temperatures T and salinities S ($1\text{‰} = 1 \text{ g kg}^{-1}$).

T	0°C		10°C		20°C	
S^*	0‰	20‰	0‰	20‰	0‰	20‰
i	$H_i [\text{atm (cm}^3\text{STP g}^{-1})^{-1}]$					
He	106.86	120.60	112.80	126.16	117.05	129.93
Ne	80.82	92.75	90.11	101.89	98.22	109.97
Ar	18.76	21.88	24.19	27.92	29.94	34.22
Kr	9.18	10.76	12.52	14.54	16.36	18.82
Xe	4.52	5.39	6.60	7.74	9.14	10.58

* Fresh water: 0‰, typical salinity of the Black Sea: $\sim 20\text{‰}$ (Chapter 4).

Table 2.2 Atmospheric equilibrium concentrations C_i^{eq} of the noble gases $i = \text{He, Ne, Ar, Kr, Xe}$ calculated for different water temperatures T and salinities S (1‰ = 1 g kg⁻¹) using the Henry coefficients in Tab. 2.1.

T	0°C		10°C		20°C	
S^*	0‰	20‰	0‰	20‰	0‰	20‰
i	C_i^{eq} [cm ³ STP g ⁻¹]					
He ($\times 10^{-8}$)	4.90	4.35	4.65	4.15	4.48	4.03
Ne ($\times 10^{-7}$)	2.25	1.96	2.02	1.78	1.85	1.65
Ar ($\times 10^{-4}$)	4.98	4.27	3.86	3.35	3.12	2.73
Kr ($\times 10^{-7}$)	1.24	1.06	0.91	0.78	0.70	0.61
Xe ($\times 10^{-8}$)	1.92	1.61	1.32	1.12	0.95	0.82

* Fresh water: 0‰, typical salinity of the Black Sea: ~20‰ (Chapter 4).

where p_{atm} is the total atmospheric pressure, e is the water vapor pressure, and v_i is the volume fraction of the noble gas i in dry air (Tab. 2.3).

The noble gas solubilities in water, or the atmospheric equilibrium concentrations, respectively, are important determinants of the air-water gas exchange process (Sec. 2.3). Because the air-water gas exchange is fast compared to mixing processes in lakes and oceans, the concentrations of dissolved noble gases in surface waters typically correspond to the solubility equilibrium concentrations that are set by gas partitioning during air-water exchange. Deviations of the actual noble gas concentrations in a water body from the equilibrium concentrations are referred to as *noble gas anomalies*. The atmospheric equilibrium concentrations calculated from the mea-

Table 2.3 Characteristic properties of the noble gases $i = \text{He, Ne, Ar, Kr, Xe}$: atomic mass M_i (Lide, 1994), volume fraction in dry air v_i (Ozima and Podosek, 2002) and diffusivities in water $D_i(T)$ (Jähne et al., 1987).

i	M_i	v_i	$D_i(0^\circ\text{C})$	$D_i(10^\circ\text{C})$	$D_i(20^\circ\text{C})$
	[g mol ⁻¹]	[-]	[10 ⁻⁹ m ² s ⁻¹]		
He	4.0026	$(5.24 \pm 0.05) \times 10^{-6}$	4.735	5.680	6.730
Ne	20.179	$(1.818 \pm 0.004) \times 10^{-5}$	2.336	2.942	3.648
Ar *	39.948	$(9.34 \pm 0.01) \times 10^{-3}$	1.443	1.870	2.381
Kr	83.80	$(1.14 \pm 0.01) \times 10^{-6}$	0.877	1.200	1.608
Xe	131.30	$(8.7 \pm 0.1) \times 10^{-8}$	0.664	0.929	1.271

* The diffusivities of Ar are calculated by scaling the diffusivities of the other noble gases.

sured water temperature and salinity are therefore used as natural threshold against which the noble gas concentrations observed in Lake Hallwil (Chapter 3), in the Black Sea (Chapter 4), and in Lake Lugano (Chapter 5) are interpreted.

2.3 Gas exchange across the air-water interface

The transfer of noble gases across the air-water boundary leads to gas partition equilibrium between the atmosphere and surface waters (Section 2.2). Gas exchange between the water and a gas phase also occurs if gas bubbles are introduced into a water body (see Sec. 2.4). This section gives a brief overview of the physics of the gas exchange across the air-water interface. For a detailed discussion of these exchange processes in open waters, see Schwarzenbach et al. (2003). For the specific case of gas exchange in porous media (i.e. gas transfer between entrapped air bubbles and ground water) refer to Holocher (2002) and Klump (2007).

At the surface of lakes and oceans, air-water exchange processes of gases other than noble gases are of great importance for the ecological balance of the water bodies (e.g. oxygenation of Lake Hallwil and Lake Lugano; Chapters 3 and 5) or for the release of greenhouse gases to the atmosphere (e.g. methane release from the Black Sea; Chapter 4 and Schmale et al., 2005). Gas exchange across the air-water interface can be expressed as a function of physical properties of the respective noble gas species (e.g. diffusivity) and of parameters that depend on the water body and are independent of the gas considered (e.g. wind speed; see below). Hence, air-water gas exchange rates determined for noble gases can be used to estimate the rates for other gases like oxygen (e.g. Aeschbach-Hertig, 1994; Peeters et al., 1997).

The oldest and conceptually simplest representation of gas-liquid exchange is the *stagnant film model* (Whitman, 1923). This model assumes that the gas transfer at the air-water interface is controlled by a water-side and a air-side stagnant boundary layer which separate the two turbulently mixed phases (Fig. 2.2). Mass transport within the stagnant boundary layers is thought to be driven only by molecular diffusion. The mass flux F in the boundary layers can therefore be described by *Fick's First Law*, e.g. for the water-side transfer:

$$F_{iw} = -D_{iw} \frac{dC_{iw}}{dz} \cong -D_{iw} \frac{C_{iw}^{eq} - C_{iw}}{\delta_w} \quad (2.4)$$

$i = \text{He, Ne, Ar, Kr, Xe} \quad w: \text{water phase}$

where D_{iw} is the molecular diffusivity of the noble gas i in water and $dC_{iw}/dz \cong (C_{iw}^{eq} - C_{iw})/\delta_w$ is the concentration gradient within the water boundary layer of thickness δ_w . Combining Eq. 2.4 with the equivalent equation for the air boundary layer

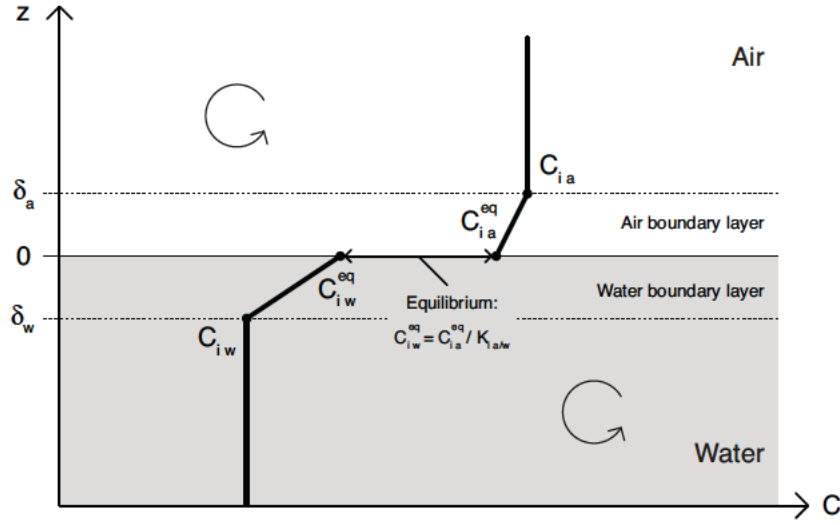


Figure 2.2 Illustration of the stagnant film model, adopted from (Schwarzenbach et al., 2003). The formulation of the air-water gas exchange flux in this model is given in Eqs. 2.5 to 2.7. The symbols are defined in the text.

yields the following expression for the total mass flux $F_{ia/w}$ across the air-water interface:

$$F_{ia/w} = v_{ia/w} \cdot (C_{iw} - C_{iw}^{eq}) \quad \text{where} \quad (2.5)$$

$$\frac{1}{v_{ia/w}} = \frac{1}{v_{iw}} + \frac{1}{v_{ia} \cdot K_{ia/w}} \quad \text{and} \quad (2.6)$$

$$v_{iw} = \frac{D_{iw}}{\delta_w}, \quad v_{ia} = \frac{D_{ia}}{\delta_a}, \quad K_{ia/w} = \frac{H_i}{T \cdot R}.$$

In this equation, $K_{ia/w}$ denotes the air-water partition equilibrium constant (i.e. the nondimensional Henry's Law constant) that can be related to the Henry coefficient H_i using the prevailing temperature T and the universal gas constant R . $v_{ia/w}$ is the total air-water transfer velocity which depends on the two single-phase transfer velocities v_{iw} and v_{ia} in the water and air boundary layer, respectively.

Eq. 2.6 allows the contributions of water-side and air-side boundary layers to the total transfer velocity to be separated out. For gases with small Henry coefficients H_i (i.e. highly soluble gases with small $K_{ia/w}$), the gas-phase (i.e. air) transfer dominates and the total transfer velocity is $v_{ia/w} \cong v_{ia} \cdot K_{ia/w}$. By contrast, for volatile gases with high H_i (and high $K_{ia/w}$) the gas transfer is limited by the water boundary layer only and the transfer velocity is $v_{ia/w} \cong v_{iw}$. Schwarzenbach et al. (2003) define a critical value for the equilibrium air-water partition constant $K_{ia/w}^{critical} \approx 10^{-3}$ (corresponding to $H_i^{critical} \approx 5.5 \times 10^{-6} \text{ atm (cm}^3\text{STP g}^{-1})^{-1}$), which allows gas-phase controlled

transfer to be distinguished from water-phase controlled transfer. Noble gases have large Henry coefficients H_i in the range of 4–130 atm (cm³STP g⁻¹)⁻¹ (see Tab. 2.1) that are considerably higher than the critical value. Hence, the air-water exchange of noble gases virtually depends on the water-phase transfer velocity alone, and the equation for the gas exchange velocity across the air-water interface can be simplified to:

$$v_{ia/w} \cong v_{iw} = \frac{D_{iw}}{\delta_w}, \quad i = \text{He, Ne, Ar, Kr, Xe.} \quad (2.7)$$

Eqs. 2.5 and 2.7 illustrate two important features of the transfer of noble gases from a gaseous phase into an aqueous phase:

- The concentration difference ($C_{iw} - C_{iw}^{eq}$) determines the magnitude and direction of the flux. Therefore, the noble-gas solubilities that govern their equilibrium concentrations C_{iw}^{eq} in water (Section 2.2) are important determinants of the air-water exchange.
- The speed of the air-water exchange is given by the transfer velocity $v_{ia/w} = D_{iw}/\delta_w$, which depends on the diffusivities D_{iw} of the noble gases in water and on the thickness δ_w of the stagnant boundary layer. The diffusivities D_{iw} are elemental properties of the noble gases that vary with temperature (Tab. 2.3). δ_w is a typical length scale in the environmental system that governs diffusive transport in the water boundary layer. The dimension δ_w depends on the ambient wind speed, on the flow velocity of the water and on other characteristic parameters of the environmental system (Schwarzenbach et al., 2003).

The specific environmental and physical conditions that determine the exchange rate at the air-water interface must be incorporated into the transfer velocity $v_{ia/w}$. Other models proposed in the literature differ in the assumptions they make about the nature and the relevant transport behavior of the interface between the gaseous and the aqueous phase. In the following, two other classical models from the literature will be compared to the stagnant film model.

The different conceptual models can be characterized in terms of the dependence of the transfer velocity $v_{ia/w}$ on the diffusivity of the exchanged gas D_i . For the stagnant film model, the relation is $v_{ia/w} \propto D_i$. In the *surface renewal model* (Danckwerts, 1951; Higbie, 1935), the water in the boundary layer is periodically replaced with water from the turbulently mixed water phase. This model is characterized by $v_{ia/w} \propto D_i^{1/2}$. The *boundary layer model* (Deacon, 1977) lies in-between with $v_{ia/w} \propto D_i^{2/3}$. It incorporates the effect of the viscosity of water on the transport in the boundary layer. Due to the assumption of a rigid boundary (i.e. a smooth water surface), this model – as well as the stagnant film model – is only valid at low wind speeds. The surface renewal model, in contrast, is mainly applicable for higher wind speeds (i.e. “turbulent” conditions).

In addition to the theoretical gas exchange models discussed above, empirical models have been developed to describe gas exchange between the atmosphere and the ocean (e.g. Liss and Merlivat, 1986; Wanninkhof, 1992). These models generally relate the gas exchange velocities to the prevailing wind speed. Such parameterizations account for the fact that the water surface becomes “rough” at higher wind speeds due to breaking waves, which enhances gas transfer. Livingstone and Imboden (1993) discuss the non-linear effect of wind speed variability on gas exchange in lakes that has to be considered when calculating mean gas exchange velocities from time-series of wind-speed data. A recent review evaluates a large number of parametrizations of air-water gas exchange depending on wind speed, including those by Liss and Merlivat (1986) and Wanninkhof (1992), to determine oxygen transfer into lakes and ponds (Ro et al., 2007). In conclusion, the authors propose a new equation for “wind-driven superficial oxygen transfer into stationary water bodies” which can also be adjusted to other gases (Ro and Hunt, 2006; Ro et al., 2007). In the present thesis, however, the widely-used parameterizations of Wanninkhof (1992) were applied to calculate the gas exchange between surface waters and the atmosphere as function of the measured wind speed at the Black Sea (Chapter 4) and at Lake Lugano (Chapter 5). This choice appears justified, as the models that were developed for noble gas concentrations in lakes and oceans (Sec. 2.7) showed low sensitivity on the type of gas exchange parameterization used.

2.4 Injection of gas bubbles into lakes and oceans

The effect of gas bubbles injected into lakes and oceans on the dissolved noble gas concentrations is of particular interest in this thesis. Two specific studies deal with gas injections from either technical systems (aeration system in Lake Hallwil; Chapter 3) or from natural sources (methane gas seeps in the Black Sea; Chapter 4). Previous work on aeration systems (e.g. McGinnis et al., 2004; Wüest et al., 1992b) and methane gas seeps (e.g. Clark et al., 2003; CRIMEA Project, 2006; Leifer and Patro, 2002; Leifer et al., 2000; McGinnis et al., 2006a) documented and studied gas exchange processes between the rising bubbles and water column, as well as mixing processes within the water body being induced by the injected gas bubbles. These studies, however, did not analyze noble gases as tracers for the gas exchange processes with the injected bubbles.

The processes that occur when gas bubbles are injected at the bottom of a water body and rise in the water column are illustrated on a conceptual level in Fig. 2.3 A. The rising bubbles force “secondary gas exchange” with the surrounding water (i.e. gas exchange with a gas phase other than the atmosphere). During this process, dissolved gases in the water are stripped by the bubbles while the main gas contained

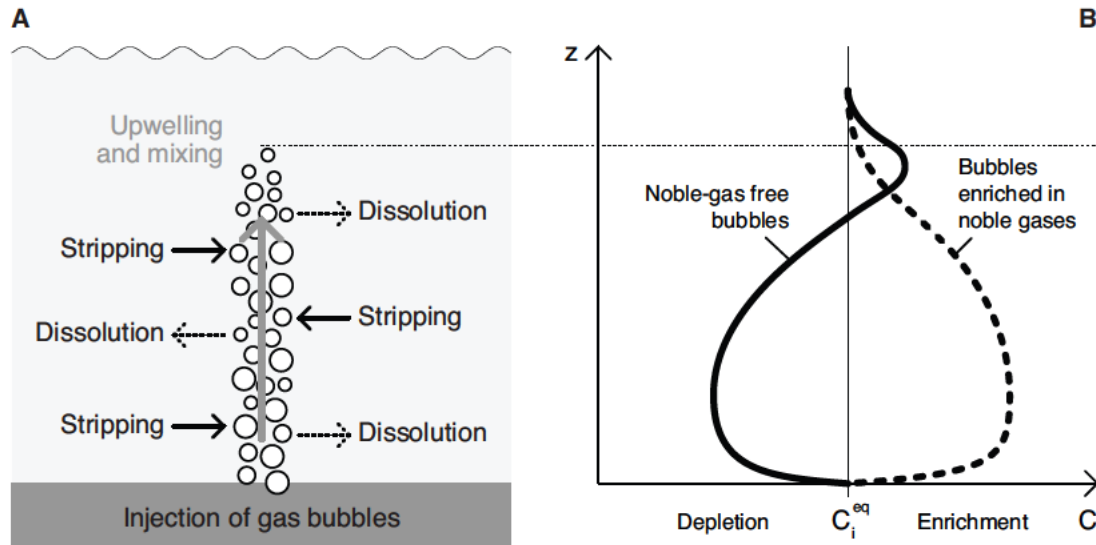


Figure 2.3 (A) Illustration of the processes occurring due to the injection of gas bubbles into a water body and (B) expected concentration profiles of the noble gas i ($i = \text{He, Ne, Ar, Kr, Xe}$) dissolved in the water due to secondary gas exchange with the injected bubbles (stripping and dissolution). The case of the injection of noble-gas free bubbles (solid line) is compared to the case of bubbles enriched in noble gases (broken line). For a detailed discussion, see also Graser (2006).

in the bubbles (e.g. oxygen, methane) continuously dissolves from the bubbles. The gas exchange between the bubbles and the surrounding water continues until an equilibrium is reached or the bubbles dissolve completely. The injected gases also cause buoyancy and the bubbles, together with the surrounding water, may rise as a plume if the bubble release rate is high enough to overcome the density stratification in the water column (e.g. McDougall, 1978; Wüest et al., 1992b). The formation of a bubble plume leads to upwelling and mixing of water from different depths, resulting in a homogenization in the concentrations of dissolved substances within the plume.

Fig. 2.3 B shows the qualitative shape of the profile of a dissolved noble gas i ($i = \text{He, Ne, Ar, Kr, Xe}$) in the water column expected if dissolution and stripping occur due to the injection of gas bubbles (see also Graser, 2006). This illustration and the discussion below are based on the assumption that no vertical water transport by a plume occurs and only the gas exchange processes between the rising bubbles and the surrounding water affect the noble gas concentrations. The bubbles are expected to dissolve completely within the water body (i.e. no gas contained in the bubbles may escape directly to the atmosphere), as indicated in Fig. 2.3 A. It is further assumed that without the injection of bubbles, the noble gas concentrations in the water column would correspond to their respective atmospheric equilibrium concentrations

C_i^{eq} (i.e. no relevant radiogenic or terrigenous components are present). Two cases are considered: (1) the injected gas bubbles are depleted with respect to noble gases or free of noble gases (2) the injected gas bubbles are enriched in noble gases.

In case (1), stripping by the rising bubbles would lead to depletion of the dissolved noble gases in the lower part of the water column, near the source of the bubbles. As the bubbles dissolve completely, the stripped noble gases would again be transferred to the water and would cause noble gas enrichment at the top of the stream of bubbles. In contrast, if the bubbles would reach the water surface, part of the stripped noble gases might be lost to the atmosphere. It should be noted that bubbles escaping at the water surface will generally have a composition that is very different from the initially injected gas phase due to the effects of stripping and dissolution in the water column (e.g. Clark et al., 2003; Graser, 2006; McGinnis et al., 2006a).

In case (2), the bubbles enriched in noble gases are expected to continuously release noble gases to the water as they dissolve, resulting in an accumulation of dissolved noble gases in the depth range where bubble dissolution occurs.

The noble gas analyses for Lake Hallwil revealed noble gas excesses in the water column in response to the injection of aeration gas bubbles that are enriched in noble gases (Chapter 3). The noble gas depletions found in profiles sampled at the Black Sea, however, could not be explained by the effect of stripping by (noble-gas free) methane bubbles released from gas seeps at the sea floor alone. As shown in Chapter 4, the observed noble gas anomalies make a strong case that water depleted in noble gases is released from the seeps together with the methane gas, causing noble gas depletions in the water column.

The effect of the secondary gas exchange processes (dissolution and stripping) – which are induced by injected gas bubbles – on the concentrations of dissolved noble gases are expected to vary with the diffusivities and solubilities of the respective noble gases in water. Similar to the exchange of noble gases across the surface of a water body (Eq. 2.7), the noble gas flux $F_{ib/w}$ from a spherical gas bubble into the water can be expressed as (Schwarzenbach et al., 2003):

$$F_{ib/w} = v_{ib/w} \cdot (C_{iw} - C_{iw}^{eq}) \quad \text{with} \quad v_{ib/w} = D_{iw} \cdot \left(\frac{1}{\delta_w} + \frac{1}{r_b} \right) \quad (2.8)$$

where the transfer velocity $v_{ib/w}$ depends on the diffusivity D_{iw} of the noble gas i in water, the thickness δ_w of the water boundary layer, and the bubble radius r_b . As the mixing processes within the bubble can be considered to be fast enough to keep the concentrations homogeneous, the gas transfer is limited only by the water-side boundary layer. C_{iw} is the noble gas concentration prevailing in the ambient water and C_{iw}^{eq} the concentration in equilibrium with the bubble gas phase, which depends on the water depth (that controls the total gas pressure in the bubble) and especially on the solubility of the respective noble gas i in water (Eq. 2.1).

Stripping by bubbles depleted with respect to noble gases or free of noble gases would therefore mainly affect the lighter noble gases (i.e. He and Ne). Because, in comparison to the heavy noble gases Ar, Kr and Xe, the gas transfer of He and Ne is considerably faster (by a factor >2 , due to their higher diffusivities) and they are preferentially enriched in the gas bubbles (due to their lower solubilities). On the other hand, the complete dissolution of bubbles enriched in noble gases would also lead to stronger enrichment of He and Ne dissolved in the water, relative to the atmospheric equilibrium concentrations, than of Ar, Kr and Xe, due to the difference in solubilities.

The differences in the effect of stripping and dissolution on the concentrations of the five noble gases He, Ne, Ar, Kr and Xe were investigated in depth to interpret the noble gas depletions observed above gas seeps in the Black Sea (Graser, 2006). For this purpose, a bubble dissolution model that was initially developed for ground-water studies (Holocher, 2002; Holocher et al., 2003) was adopted to reproduce the gas exchange processes taking place when a methane bubble rises in the water column of the Black Sea. The model predicts that stripping by methane bubbles would preferentially remove the lighter noble gases from the water. The noble gas depletion patterns detected in the Black Sea showed exactly the opposite, i.e. the heavy noble gases were found to be the most depleted in the water column, which indicates that stripping and dissolution alone cannot explain the observed noble gas anomalies (see Chapter 4).

2.5 Vertical mixing in stratified waters

In lakes and oceans, the distributions of dissolved substances, and therefore of noble gases, depend strongly on the mixing processes occurring in the water body. Substance transport in natural waters occurs mainly by turbulent diffusion, convective mixing and – if basin-scale currents are present – by large-scale advection. Lakes and oceans typically show a distinct density stratification due to vertical temperature and/or salinity gradients (e.g. Lake Hallwil, the Black Sea and Lake Lugano are all seasonally or permanently stratified; see Chapters 3–5). The stratification inhibits vertical mixing processes, and in consequence, the vertical substance transport is slow. Horizontal transport processes, in contrast, are orders of magnitude faster than vertical exchange as horizontal transport occurs along lines of equal density and is therefore unaffected by the density stratification. Hence, lakes (and also some parts of oceans) can be considered as horizontally homogeneous and vertically stratified with respect to the concentrations of dissolved substances like noble gases (e.g. Imboden and Wüest, 1995).

The seasonal change of the density stratification in lakes is typically controlled by the water temperature. An exception are lakes that contain relatively high concentrations of dissolved ions which causes chemical stratification (see below). In temperate climate zones (e.g. in Switzerland), the water body of thermally stratified lakes can generally be divided into three distinct horizontal layers. The deep water has a temperature close to the temperature of maximum density of pure water ($\sim 4^{\circ}\text{C}$) and is referred to as the *hypolimnion*. The water temperatures in the well-mixed surface layer, the *epilimnion*, follow the seasonal climate cycle, because the lake surface temperatures are strongly and directly coupled to air temperatures (Livingstone and Lotter, 1998; Livingstone et al., 1999). During most of the year, epilimnion and hypolimnion are separated by a transition zone, the *metalimnion*, characterized by a strong gradient in temperature (and hence in density), the *thermocline*.

In winter, surface cooling supported by stronger turbulent mixing due to wind forcing lead to a decrease in the epilimnion temperature. This effect weakens the temperature gradient, and therefore also the density gradient in the metalimnion, and shifts the thermocline downwards. When the temperature difference between epilimnion and hypolimnion disappears (i.e. the entire water column becomes homogeneous in temperature and typically approaches the temperature of maximum density of $\sim 4^{\circ}\text{C}$) and if the water column stratification is not controlled by the concentration of dissolved ions (see below), large-scale circulation and advective transport of dissolved substances can take place in the entire basin and over the full depth of the water body. The basin-wide circulation induces small-scale turbulence due to friction which finally leads to complete elimination of the vertical concentration gradients. The process of winter mixing is of great importance for the supply of atmospheric gases to the hypolimnion, which enter the lake by gas exchange at the surface (Sections 2.2 and 2.3). Winter mixing is a prerequisite for the ecologically relevant oxygenation of the hypolimnion, and also has a profound effect on noble gas concentrations in the water column by resetting them to their respective atmospheric equilibrium concentrations, which are given by the temperature and salinity of the exchanged water mass.

Historically, lakes which undergo full circulation every winter are called *holomictic*. In contrast, in *meromictic* lakes the winter circulation does not reach the lake bottom, so that the deepest water layers are more or less isolated from the rest of the lake and from gas exchange with the atmosphere. Hence, oxygen is usually depleted and non-atmospheric noble gases are enriched in the stagnant deep water of meromictic lakes. Meromixis is often caused by a chemical stratification of the water column due to an increase in the concentration of dissolved ions (i.e. “salinity”) with depth.

In fresh waters, the effect of temperature changes on the water density is small near the density maximum at $\sim 4^{\circ}\text{C}$. Hence, the small gradients in the concentration of dissolved solids (i.e. “salinity”) that occur in meromictic lakes may over-

compensate the density effects of the cooling of the water column in winter and can therefore stabilize the water column. High nutrient inputs from municipal waste water and agriculture lead to increased primary production, subsequent decomposition of organic matter and finally to increased mineralization. These processes often result in chemical (i.e. “salinity”-controlled) stratification and oxygen depletion in lakes, for instance in Lake Hallwil (Chapter 3; Märki and Schmid, 1983) and Lake Lugano (Chapter 5; Wüest et al., 1992a). Apart from meromictic lakes, permanent stratification also occurs in ocean basins like the Black Sea, when fresh water input from rivers and precipitation leads to the formation of a surface layer with relatively low salinity (and therefore low density) that overlays the more saline deep water (Sorokin, 2002). The effect of the stratification on mixing conditions in the Black Sea is reflected in the distribution of noble gases in the water column (Chapter 4).

2.6 Tritium decay and water ages

The β -decay of ^3H is the main source of non-atmospheric ^3He in meteoric waters. As the half-life of ^3H ($4500 \text{ d} \cong 12.32 \text{ yr}$; Lucas and Unterweger, 2000) is of similar size as the water renewal times in many natural water bodies, ^3H is often used to analyze mixing and water exchange in lakes, oceans and groundwaters. ^3H , the radioactive isotope of hydrogen, is produced naturally in the upper atmosphere by the interaction of cosmic radiation with nitrogen and oxygen nuclei (Craig and Lal, 1961). In addition to the natural background, thermonuclear bomb tests in the atmosphere during the 1960s released large amounts of ^3H to the environment and increased the terrestrial ^3H inventory by several orders of magnitude (e.g. IAEA/WMO, 2004; Weiss et al., 1979). Atmospheric ^3H is immediately oxidized to tritiated water and subsequently becomes part of the global hydrological cycle. On a regional scale, ^3H concentrations in aquatic systems can be above average in industrial areas where ^3H is used or produced in technical applications. Time-series of ^3H concentrations in precipitation measured at numerous stations worldwide are available from the GNIP database (IAEA/WMO, 2004). ^3H concentrations are usually expressed as tritium units (TU), i.e. as the isotopic ratio of ^3H to ^1H :

$$1 \text{ TU} = 1 \text{ } ^3\text{H} \text{ atom per } 10^{18} \text{ } ^1\text{H} \text{ atoms.} \quad (2.9)$$

^3H decays to $^3\text{He}_{\text{tri}}$ (tritogenic ^3He) with a half-life of $\tau_{1/2} = 4500 \pm 8 \text{ d} \cong 12.32 \text{ yr}$ (Lucas and Unterweger, 2000). In an isolated water parcel, the concentration of $^3\text{He}_{\text{tri}}$ increases to the same degree as the concentration of ^3H decreases due to radioactive decay. If these two concentrations are known, the so-called ^3H - ^3He water age τ (Tolstikhin and Kamenskiy, 1969; Torgersen et al., 1977, 1979), which

is an estimate of the time since the water has last been in gas exchange equilibrium with the atmosphere, can be calculated as:

$$\tau = \frac{\tau_{1/2}}{\ln(2)} \cdot \ln \left(1 + \frac{[^3\text{He}_{\text{tri}}]}{[^3\text{H}]} \right) \quad (2.10)$$

where $[^3\text{He}_{\text{tri}}]$ and $[^3\text{H}]$ are the concentrations of tritiogenic ^3He and ^3H respectively, in the water parcel. For the determination of ^3H - ^3He water ages, $^3\text{He}_{\text{tri}}$ concentrations need to be converted into tritium units by using the formula (Roether, 1989):

$$1 \text{ cm}^3 \text{STP g}^{-1} = \frac{4.0193 \times 10^{14}}{1 - S/1000} \text{ TU} \quad (2.11)$$

with the salinity S in g kg^{-1} . Note that the ^3H - ^3He water age is nonlinear with respect to mixing (Jenkins and Clarke, 1976; Kipfer et al., 2002; Schlosser and Winckler, 2002). Mixing of water with different ^3H concentrations and different ages always leads to a bias of the apparent age of the mixture toward the age of the mixture with the higher ^3H concentration.

The ^3H - ^3He tracer pair has been widely used to analyze water renewal in lakes and oceans, partly in combination with CFCs and SF_6 (e.g. Aeschbach-Hertig et al., 1996, 2007; Hofer et al., 2002; Hohmann et al., 1998; Schlosser et al., 1991a; Torgersen et al., 1977). SF_6 and CFCs are other environmental tracers that can provide information on mixing rates and water residence times. See Chapter 5 for a description of the SF_6 and CFC-12 method and for a comparison of apparent water ages determined from ^3H - ^3He and from SF_6 . Apparent ^3H - ^3He tracer ages for the Black Sea are reported in Chapter 4.

2.7 Two simple models for noble gas concentrations in lakes and oceans

Various numerical models that reconstruct the evolution of noble gas concentrations in lakes have been used in earlier studies to analyze mixing rates, deep water renewal, water flow between different lake basins, gas exchange at the surface, and the input of terrigenous He (e.g. work of our group: Aeschbach-Hertig, 1994; Aeschbach-Hertig et al., 2002; Holzner, 2001; Peeters et al., 1997, 2000b). Similar models were developed in this work to estimate rates of mixing and deep water renewal in the water column using the noble gas data. The models were implemented using AQUASIM, a simulation software for aquatic systems (Eawag/SIAM, 2007; Reichert, 1994), which also allows to perform parameter estimations and sensitivity analyses.

Generally, to model the concentrations of dissolved noble gases in a water body, the following processes must be considered:

- Gas exchange with the atmosphere at the water surface
- Noble gas and tritium input by rivers and precipitation
- Noble gas and tritium loss via the outflow
- Input of terrigenic He from the sediments
- Production of tritiogenic ^3He by the radioactive decay of tritium
- Vertical transport by turbulent diffusion and advection

Note that the effects that gas bubble injection into a water body exerts on the noble gas concentrations are not within the scope the models discussed here. Specific models of gas exchange and mixing processes induced by bubbles injected into lakes and oceans are treated elsewhere (e.g. Graser, 2006; Leifer and Patro, 2002; McGinnis and Little, 2002; Wüest et al., 1992b).

Depending on the available data, the model structure used to estimate the rates of vertical transport can be simpler or more complex. Two types of model were used in this work: (1) classical box models (Fig. 2.4 A) and (2) n -box models with large n that approximate continuous one-dimensional models of the water column (Fig. 2.4 B). The discretization of the governing equations used in numerical models implies that a vertical one-dimensional lake model is evaluated as a system of n horizontal layers (i.e. n boxes). The software AQUASIM provides so-called “compartments” that can be combined to models of aquatic systems. A two-box model (Fig. 2.4 A) can therefore be set up combining two “mixed-reactor compartments” in AQUASIM. The n -box lake model (Fig. 2.4 B) corresponds to the “lake compartment” in AQUASIM.

In box models, vertical transport is represented as water fluxes that carry dissolved substances, and the water exchange rates between the boxes are fitted using the noble gas data. In continuous one-dimensional models, or their numerical approximation as n -box models in AQUASIM, all vertical transport is described in terms of turbulent mixing, and a profile of mixing rates is estimated using the noble gas profiles. For this work, a three-box model was used to study deep-water renewal in Lake Lugano during extreme mixing events (Chapter 5), and a “one-dimensional” (i.e. n -box) water column model was set up to estimate mixing rates and the terrigenic He input in the Black Sea (Chapter 4).

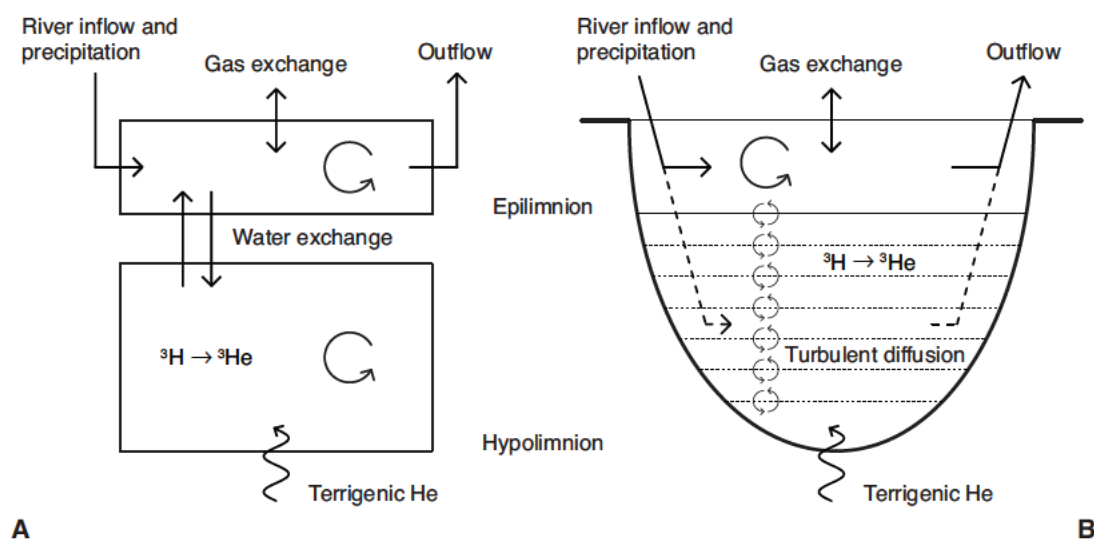


Figure 2.4 Schematic illustration of (A) a two-box lake model and (B) a n -box lake model, adopted from (Aeschbach-Hertig, 1994).

3

Using noble gases to trace bubble gas-exchange in the artificially aerated Lake Hallwil, Switzerland

3.1 Introduction

3.1.1 Restoration of eutrophic Lake Hallwil

Lake Hallwil is a medium-sized lake located on the border between the Cantons of Argovia and Lucerne, Switzerland (47°17'N, 8°13'E, 449 m above sea level; see Fig. 3.1 and Tab. 3.1). The lake became eutrophic around the beginning of the 20th century due to the increasing phosphorus input from municipal waste water and agriculture (Märki and Schmid, 1983). The high nutrient input to the lake led to extensive algal production and subsequent mineralization which led to oxygen depletion in the

Table 3.1 Characteristic features of Lake Hallwil.

Volume	285×10^6	m^3
Surface area	9.95×10^6	m^2
Maximum depth	46.5	m
Mean depth	28.6	m
Mean outflow	2.34	$\text{m}^3 \text{s}^{-1}$
Hydrological residence time	3.9	yr

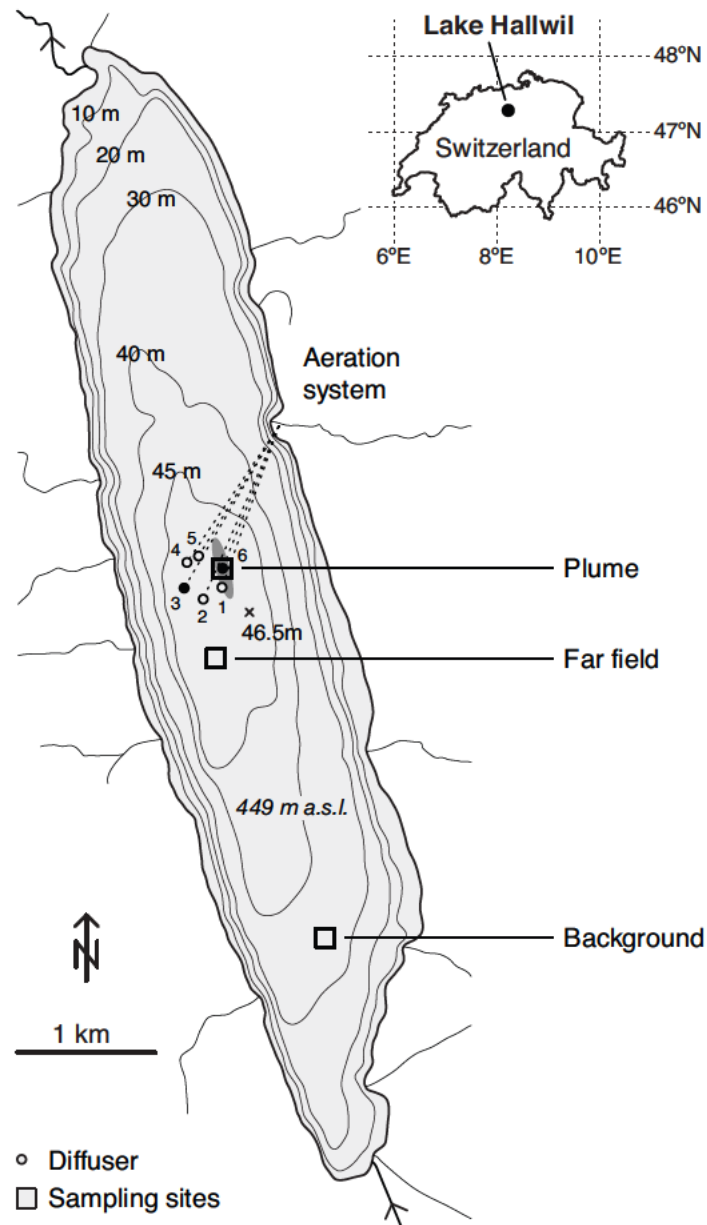


Figure 3.1 Map of Lake Hallwil, showing the positions of the diffusers (1–6) and of the three sampling sites. The inset shows the location of Lake Hallwil on a map of Switzerland.

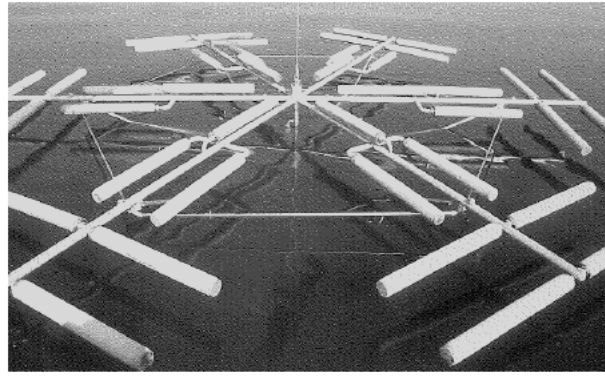


Figure 3.2 One diffuser of the “Tanytarsus” system. Photograph from Gächter and Stadelmann (1993).

hypolimnion. As external restoration measures to reduce the nutrient input to the lake were not sufficient to prevent anoxic conditions developing, an aeration system was installed in 1985 (Schaffner, 1987; Stöckli and Schmid, 1987; Wehrli and Wüest, 1996) to guarantee minimum oxygen concentrations in the water column. This system consists of six 6.5-m diffusers of the “Tanytarsus” type (Fig. 3.2) that are installed in a 300-m circular configuration near the deepest point of the lake (Fig. 3.1). The aeration gas is compressed on the shore and directed to the diffusers through six pipes at the lake bottom. The diffuser system aims to increase oxygen (O_2) concentrations in Lake Hallwil in two different ways (Fig. 3.3; Scheidegger et al., 1994). In winter, pressurized air is injected as large bubbles to support the vertical water circulation. This forces a plume of bubbles to rise above the aeration system and results in the advective upwelling of deep water with low O_2 concentrations due to the buoyancy of the injected air. The transport of O_2 depleted deep water to the surface enhances oxygenation by gas partitioning with the atmosphere. Note that the large-scale seasonal mixing in Lake Hallwil, and therefore the natural oxygenation in

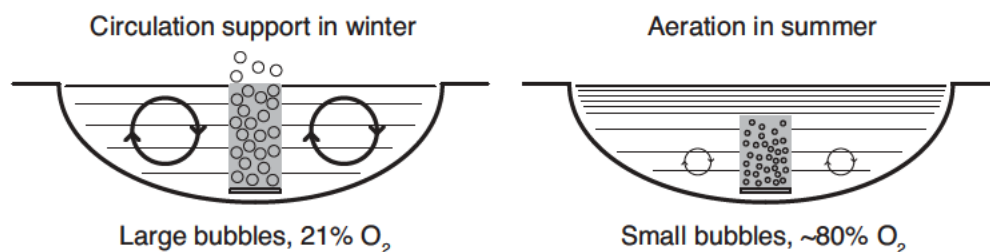


Figure 3.3 Illustration of the operation modes of the aeration system in winter and summer. Adapted from Stöckli and Schmid (1987).

winter, is limited due to the location of the lake in a north-south oriented valley, which protects the lake from the energy input of the predominant westerly winds. During summer, the system injects smaller, oxygen-enriched gas bubbles that dissolve virtually completely in the hypolimnion (see Sec. 3.3.1). The gas flow rate of the system is regulated such that the rising bubble plume does not affect the stratification of the water column but the O₂ input is sufficient to prevent anoxic conditions. Due to the relatively high productivity and subsequent decomposition of organic matter in Lake Hallwil, injected O₂ is consumed very fast in the hypolimnion and no significant O₂ accumulation within the plume is directly detectable (see Fig. 3.6). The aeration system is equipped with on-site O₂ enrichment that produces aeration gas containing ~80% O₂ by removing most of the nitrogen from compressed air.

The progress of the restoration measures in Lake Hallwil is monitored by the Department of Environment of the Canton of Argovia (AfU, 2007), based on regular measurements of various physical, chemical and biological variables in the lake. The internal (diffusor system) and external (reduction of nutrient input) measures resulted in a significant improvement in lake water quality since the start of the remediation program. Despite the reduced nutrient concentrations in the lake, the oxygen consumption again increased considerably after 1999, because a massive outbreak of *planktothrix rubescens* occurred (Stöckli, 2005). This blue-algae was common in Lake Hallwil in the first half of the 19th century and had disappeared as the nutrient concentrations became very high. In this context, the re-appearance of *planktothrix rubescens* is indicative of a better water quality, but the nutrient concentrations in the lake need to be reduced further to make the aeration system obsolete. Currently, the circulation support in winter and oxygenation in summer are still needed to fulfill the legal water quality objective of 4 mg/l O₂ in the entire water column (Der Schweizerische Bundesrat, 1998).

3.1.2 Effect of aeration on dissolved noble gases in lakes

The concentrations of dissolved atmospheric noble gases in lakes generally correspond to the equilibrium concentrations calculated for the atmospheric pressure at the altitude of the lake, and the temperature and salinity that prevail during atmospheric gas exchange. As noble gases are chemically inert, only physical processes and non-atmospheric noble gas inputs can change the noble gas concentrations and are therefore responsible for any deviations from atmospheric equilibrium (Kipfer et al., 2002). Gas bubbles that are injected into a lake will affect the concentrations of dissolved gases in the water column, as the bubbles strip gases from the surrounding water and dissolve simultaneously during their ascent. The effect of these secondary gas exchange processes on the concentrations of dissolved gases varies according to the solubility and diffusivity of the respective gas and depending on the initial gas

concentrations in the bubbles. We therefore expect dissolved noble gas signals in Lake Hallwil that are characteristic in relation to the prevailing aeration gas flow rate and the composition of the aeration gas. Especially during summer stratification, when gas exchange with the atmosphere only can only affect the concentrations in the mixed epilimnion, noble gases dissolved in the hypolimnion are expected to form an “archive” that records the history of the preceding aeration operation. In winter, the noble gas concentrations in the lake are expected to be reset to atmospheric equilibrium concentrations due to vertical mixing and gas exchange with the atmosphere. We measured helium (He), neon (Ne), argon (Ar), krypton (Kr) and xenon (Xe) both in the aeration gas and dissolved in the water of the lake, to study the effect of aeration gas injection on the noble gas concentrations in Lake Hallwil during summer stratification.

3.2 Methods

3.2.1 Sampling

Samples for the analysis of noble gas concentrations were collected during one week in July 2005. Our sampling was coordinated with a series of physical measurements in Lake Hallwil (transects of CTD profiles, vertical current velocity profiles using an acoustic Doppler velocimeter, thermistor moorings) to collect data to refine a bubble plume model (Edmonds and Singleton, 2005; McGinnis et al., 2004). In the course of this field campaign, the gas flow of the aeration system was either set to higher rates than used during normal oxygenation operation in summer or was switched off completely (see Tab. 3.2). We collected three depth profiles of water samples for noble gas analyses and two aeration gas samples on 08 July 2005, prior to the physical measurements when the system was still operated at the normal aeration gas flow rate used during the summer season. The water samples were taken at three sites that lay approximately along the longitudinal axis of the lake (Fig. 3.1). The “plume” site was located above diffuser number 6 of the aeration system. The “far field” site was located ~ 600 m and the “background” site ~ 2.7 km south of the aeration system. Water sampling at all three sites was repeated on 13 July 2005, after the aeration system had been inactive for ~ 1 day, and on 15 July 2005, after ~ 2 days of increased aeration gas flow rate. During this high flow phase, the aeration gas was only directed to diffusers number 3 and number 6 to increase the gas flow per diffuser by a factor of ~ 3 , but to keep the total gas flux into the lake virtually constant. We also sampled the aeration gas on 13 July 2005 (after water sampling, when the aeration system had been switched on again) and 15 July 2005 (at high aeration gas flow rate).

Table 3.2 Operation of the aeration system during the sampling campaign.

Time interval	J_{tot} [Nm ³ /hr]	J_{diff} [Nm ³ /hr]	Remarks
05 April – 11 July 2005 10:20	73	12	normal flow rate to all 6 diffusers, sampling on 08 July
11 – 12 July 2005 10:30	61	31	high flow rate to diffusers 3 and 6 only
12 – 13 July 2005 12:30	0	0	aeration off for 26 hours, sampling on 13 July
13 – 15 July 2005 14:35	55	28	high flow rate to diffusers 3 and 6 only, sampling on 15 July
After 15 July 2005	71	12	normal flow rate to all 6 diffusers

J_{tot} : gas flow rate to all diffusers; 1 Nm³ (i.e. gas at 0°C and 1 atm) \triangleq 10⁶ cm³STP

J_{diff} : gas flow rate to each active diffuser

Water samples for noble gas analyses were taken using Niskin bottles, avoiding any air contamination during sampling. On the ship, the water samples were immediately transferred to copper tubes that were sealed gas-tight using pinch-off clamps. Gas samples were withdrawn from the gas supply of the aeration system on the shore of Lake Hallwil and likewise stored in sealed copper tubes.

CTD profiles measured using a Seabird SBE19 probe at the positions of the water sampling stations were provided by A. Stöckli (Department of Environment, Canton of Argovia) for 08 July 2005 and by the team of the physical measurement campaign for 13 July 2005 and 15 July 2005 (Edmonds and Singleton, 2005).

3.2.2 Noble gas analyses

He, Ne, Ar, Kr and Xe concentrations both in the aeration gas and dissolved in the water samples were determined by mass-spectrometry (Beyerle et al., 2000). In total, 48 water samples and 4 gas samples were analyzed. Typical overall errors of the noble gas concentration measurements (1 σ errors) are ± 1 –2%. The analysis of Ar, Kr and Xe failed for one water sample due to experimental problems. The measurements for the aeration gas sampled on 15 July 2005 were not used in this study, because of the occurrence of a technical problem in the aeration system during gas sampling that prevented reliable noble gas determination.

To calculate the atmospheric equilibrium concentrations of the different noble gases in the water column, we used the parameterizations recommended by Kipfer et al. (2002). The dissolved noble gas concentrations presented in this study are normalized to the equilibrium concentrations corresponding to the measured temperature and salinity, and to a mean atmospheric pressure of 0.95 atm at 449 m a.s.l..

The water sampling and noble gas analyses were carried out as part of the diploma thesis of N. Graser (Graser, 2006).

3.3 Results and discussion

The noble gas data collected for this study are summarized in Tab. 3.3 (08 July 2005), Tab. 3.4 (13 July 2005) and Tab. 3.5 (15 July 2005).

Table 3.3 Concentrations of He, Ne, Ar, Kr and Xe in Lake Hallwil on 08 July 2005 (normal aeration gas flow rate) in units of $\text{cm}^3\text{STP g}^{-1}$. The overall measurement errors (1σ errors) are $\pm 0.7\%$ for He, $\pm 1.7\%$ for Ne, $\pm 0.6\%$ for Ar, $\pm 1.3\%$ for Kr, and $\pm 2.2\%$ for Xe.

Depth [m]	He [10^{-8}]	Ne [10^{-7}]	Ar [10^{-4}]	Kr [10^{-7}]	Xe [10^{-8}]
Plume site					
1	4.41	1.80	3.02	0.67	0.94
10	4.72	2.06	3.97	0.92	1.37
15	6.51	2.72	4.54	1.01	1.48
20	7.27	3.02	4.85	1.02	1.51
30	8.59	3.47	5.31	1.03	1.54
40	7.95	3.18	5.18	1.02	1.52
Far field site					
1	4.37	1.79	3.02	0.67	0.94
10	4.66	2.03	3.90	0.90	1.33
20	6.05	2.59	4.60	1.03	1.49
25	6.62	2.80	4.72	1.03	1.54
35	6.48	2.75	4.75	1.04	1.55
40	6.20	2.66	4.68	1.04	1.54
Background site					
1	4.37	1.78	2.98	0.66	0.93
20	5.58	2.44	4.50	1.04	1.55
25	5.74	2.48	4.50	1.02	1.53
32	6.00	2.52	4.49	1.00	1.49

Table 3.4 Concentrations of He, Ne, Ar, Kr and Xe in Lake Hallwil on 13 July 2005 (aeration off) in units of $\text{cm}^3\text{STP g}^{-1}$. The overall measurement errors (1σ errors) are $\pm 0.7\%$ for He, $\pm 1.7\%$ for Ne, $\pm 0.6\%$ for Ar, $\pm 1.3\%$ for Kr, and $\pm 2.2\%$ for Xe.

Depth [m]	He [10^{-8}]	Ne [10^{-7}]	Ar [10^{-4}]	Kr [10^{-7}]	Xe [10^{-8}]
Plume site					
1	4.34	1.77	3.02	0.68	0.92
10	4.76	2.07	3.98	0.94	1.40
15	6.19	2.58	4.63	1.02	1.51
20	7.05	2.94	4.87	1.05	1.58
30	6.82	2.85	4.78	1.03	1.56
40	6.08	2.61	*	*	*
Far field site					
1	4.28	1.76	3.00	0.67	0.94
10	4.68	2.05	3.93	0.93	1.36
20	5.93	2.67	4.63	1.04	1.51
25	5.95	2.55	4.57	1.03	1.55
35	6.20	2.60	4.58	1.01	1.51
40	5.98	2.59	4.60	1.04	1.53
Background site					
1	4.30	1.74	2.94	0.64	0.90
20	5.40	2.36	4.46	1.04	1.52
25	5.76	2.47	4.56	1.04	1.53
32	6.17	2.63	4.66	1.04	1.55

* Lost as a result of experimental problems.

3.3.1 Differences in the noble gas concentration profiles along the lake axis

The noble gas profiles sampled on 08 July 2005 (normal aeration gas flow rate) at three sites in Lake Hallwil show a distinct variation in the He, Ne and Ar concentrations with distance from the aeration system (Tab. 3.3, Fig. 3.4). Deep-water samples from all three stations are supersaturated in He, Ne and Ar, i.e. the observed concentrations exceed the local equilibrium concentrations. The magnitude of the enrichment decreases with increasing distance from the bubble plume. No enrichment of He, Ne and Ar occurs above the thermocline at 10–15 m. In contrast, the Kr and Xe concentrations are in equilibrium with the atmosphere at all depths and the profiles from the three sites agree within analytical errors.

Table 3.5 Concentrations of He, Ne, Ar, Kr and Xe in Lake Hallwil on 15 July 2005 (high aeration gas flow rate) in units of $\text{cm}^3\text{STP g}^{-1}$. The overall measurement errors (1σ errors) are $\pm 0.7\%$ for He, $\pm 1.7\%$ for Ne, $\pm 0.6\%$ for Ar, $\pm 1.3\%$ for Kr, and $\pm 2.2\%$ for Xe.

Depth [m]	He [10^{-8}]	Ne [10^{-7}]	Ar [10^{-4}]	Kr [10^{-7}]	Xe [10^{-8}]
Plume site					
1	4.28	1.72	2.94	0.65	0.91
5	4.49	1.82	2.99	0.67	0.94
10	4.88	2.12	4.04	0.95	1.41
15	9.97	3.92	5.60	1.06	1.57
25	10.89	4.23	5.93	1.06	1.57
40	10.30	4.02	6.03	1.05	1.59
Far field site					
1	4.30	1.75	2.98	0.66	0.93
7.5	4.50	1.90	3.47	0.79	1.13
15	5.11	2.25	4.30	1.00	1.48
20	6.15	2.64	4.66	1.03	1.53
30	6.64	2.80	4.79	1.05	1.54
40	5.96	2.55	4.63	1.04	1.55
Background site					
1	4.12	1.68	2.84	0.63	0.89
17.5	5.26	2.32	4.43	1.04	1.51
22.5	5.74	2.47	4.54	1.04	1.56
32	5.55	2.39	4.37	1.00	1.49

The observed supersaturations of He, Ne and Ar in the hypolimnion correspond to the relative elemental composition of the aeration gas (Tab. 3.6). Noble gases in the injected bubbles are strongly fractionated with respect to air. He, Ne and Ar in the aeration gas are enriched by a factor of 3–4, whereas Kr and Xe are virtually absent (i.e. their volume fractions are nearly zero). Hence, the enrichment of He, Ne and Ar relative to the composition of air is in the same range as the enrichment of O_2 . The on-site O_2 enrichment unit of the aeration system that is active during oxygenation in summer, together with the removal of nitrogen, seem also to cause the prominent mass fractionation of the injected noble gases. Apparently, the heavy noble gases Kr and Xe are removed from the aeration gas, while the lighter noble gases He, Ne and Ar are enriched together with the O_2 .

To summarize, the injection of the aeration gas (enriched in O_2 , He, Ne and Ar) into the lake and the dissolution of the resulting bubbles in the water column seems to

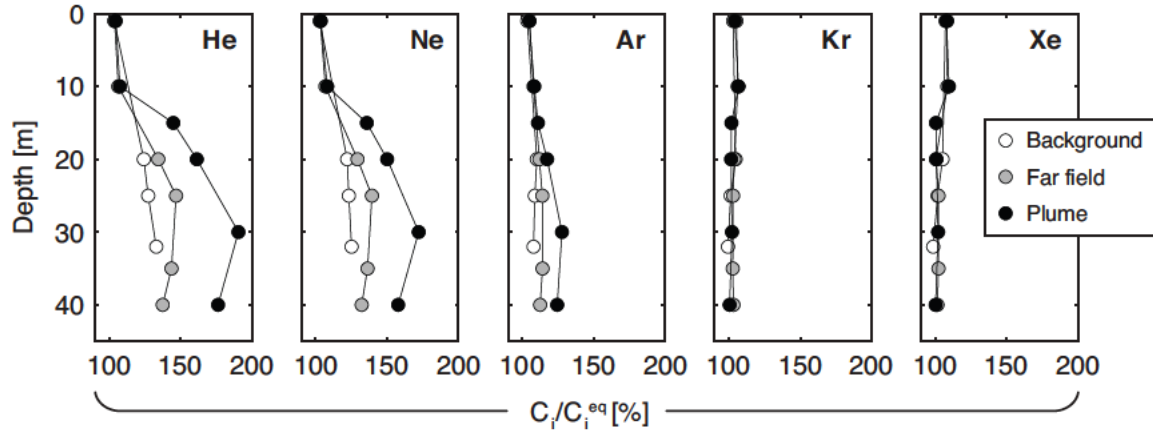


Figure 3.4 Comparison of the observed noble gas concentration profiles at the three sites while the aeration system was operated at normal gas flow rate (8 July 2005). See Fig. 3.1 for location of the profiles. The dissolved noble gas concentrations C_i ($i = \text{He, Ne, Ar, Kr, Xe}$) are normalized to their respective atmospheric equilibrium concentrations C_i^{eq} .

Table 3.6 Elemental composition of the aeration gas. O_2 data were provided by the Department of Environment of the Canton of Argovia (A. Stöckli, pers. comm.). The volume fractions of the noble gases in the aeration gas are mean values for the samples collected on 08 July 2005 and 13 July 2005, immediately before or after water sampling. The noble gas content of the three analyzed aeration gas samples varies by less than 3%. Noble gases and O_2 comprise $\sim 81\%$ of the aeration gas volume; the composition of the remaining $\sim 19\%$ was not determined.

Gas i	v_i^{gas}	v_i^{gas}/v_i^{air}
He	1.66×10^{-5}	3.17
Ne	5.73×10^{-5}	3.15
Ar	3.80×10^{-2}	4.07
Kr	1.14×10^{-8}	0.01
Xe	2.96×10^{-9}	0.03
O_2	7.72×10^{-1}	3.69

v_i^{gas} : volume fraction in the aeration gas

v_i^{air} : volume fraction in air

cause an accumulation of He, Ne and Ar in the hypolimnion. This effect is maximal for the profile sampled directly above a diffuser of the aeration system, i.e. within the bubble plume. The observed noble gas enrichment is limited to the hypolimnion.

An analysis of the elemental ratios of He/Ne and Ne/Ar observed in the aeration gas and in the dissolved gas excess at the plume site emphasizes a causal relation between the aeration gas injection and the noble gas supersaturation in the lake. The measured noble gas ratios are presented in Table 3.7. At normal aeration gas flow rate, the elemental ratios of He/Ne and Ne/Ar in the gas excess of the hypolimnion agree (within analytical errors) with the ratios in the injected aeration gas. This observation suggests that the noble gases injected with the aeration gas either dissolve completely below the thermocline or escape from the lake in equal shares. If gas loss would occur, this effect would not affect all the noble gases equally, because of the considerable differences in the noble gas solubilities. Gas loss would mainly affect the poorly soluble light noble gases He and Ne and therefore lead to a preferential accumulation of Ar in the lake water. The accumulation of Ar would result in a Ne/Ar ratio of the noble gas excess in the water that is lower than the ratio in the injected gas. As the noble gas ratios in the aeration gas and in the noble gas excess of the hypolimnion closely match, the occurrence of considerable gas loss can be excluded. During oxygenation in summer, the aeration system is continuously monitored and adjusted to assure that the injected aeration gas bubbles dissolve in the hypolimnion. No visual observations of gas bubbles escaping at the lake surface, which would cause considerable gas loss, were made during the oxygenation period from 05 April 2005 to 08 July 2005 that preceded our sampling (A. Stöckli, pers. comm.). To sum up, the findings imply a rather complete dissolution of the injected aeration gas

Table 3.7 Comparison of He/Ne and Ne/Ar elemental ratios in the aeration gas and in the dissolved gas excess.

Gas reservoir	He/Ne $\times 10$	Ne/Ar $\times 1000$
Aeration gas	2.90 ± 0.05	1.51 ± 0.05
Excess (normal flow rate) *	2.83 ± 0.09	1.36 ± 0.20
Excess (high flow rate) *	2.87 ± 0.03	1.19 ± 0.10

* Mean ratio of the noble gas excess concentrations at the plume site $C_i^{ex} = C_i - C_i^{eq}$, where $i = \text{He, Ne, Ar}$. C_i is the observed noble gas concentration and C_i^{eq} is the atmospheric equilibrium concentration. Only samples from the hypolimnion (depths ≥ 15 m) were taken into account, as the noble gas supersaturations occur only in this depth range.

bubbles in the hypolimnion at the normal aeration gas flow rate and thus an efficient O_2 input.

The elemental ratios observed at high aeration gas flow rate (Tab. 3.7) will be discussed in Section 3.3.2.

3.3.2 Noble gas profiles observed at different aeration gas flow rates

The noble gas concentration profiles sampled at the plume site, i.e. above diffuser 6, on 08 July 2005 (normal aeration gas flow rate), 13 July 2005 (aeration off) and 15 July 2005 (high aeration gas flow rate) show a strong response of dissolved He, Ne and Ar concentrations to the variation of the aeration gas flow rate (Tab. 3.3, Tab. 3.4, Tab. 3.5, Fig. 3.5). Compared to the normal flow situation, the concentrations of He, Ne and Ar in the hypolimnion increase considerably for high aeration gas flow rates and decrease substantially when the aeration is turned off. Because Kr and Xe are missing in the injected gas (see Tab. 3.6), the concentrations of Kr and Xe in the lake are not affected by the aeration process. The relative increase of the concentrations of the light noble gases He and Ne that occurs with increasing aeration gas flow rate is much more pronounced than for Ar. As He and Ne are less soluble than Ar in water, the noble gas accumulation due to aeration contributes a larger share to the total mass of the light noble gases stored in the lake. The short periods of altered aeration gas flow rates did not lead to significant changes of the noble gas concentrations at the far field and background sites (Tab. 3.3, Tab. 3.4, Tab. 3.5).

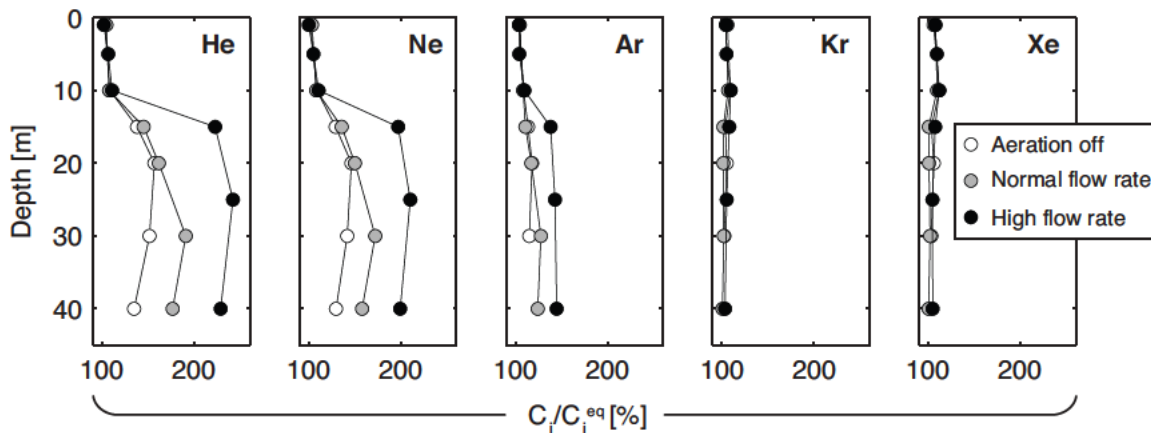


Figure 3.5 Comparison of the dissolved noble gas concentration profiles at the plume site for three different aeration gas flow rates (aeration off 13 July 2005; normal flow 8 July 2005; high flow 15 July 2005). See Fig. 3.1 for location of the profiles. The dissolved noble gas concentrations C_i ($i = \text{He, Ne, Ar, Kr, Xe}$) are normalized to the atmospheric equilibrium concentrations C_i^{eq} . The corresponding O_2 concentration profiles are shown in Fig. 3.6.

On 15 July 2005, when the aeration system was operated at high gas flow rate, the elemental ratios of Ne/Ar in the noble gas excess measured in the hypolimnion at the plume site are significantly lower than the Ne/Ar ratio in the injected aeration gas (Tab. 3.7). The He/Ne ratios, on the opposite, agree within experimental errors. At high aeration gas flow rate, the noble gas excess at the plume site contains therefore a disproportionately high Ar fraction that causes the low Ne/Ar ratio. The shift in the elemental ratios indicates incomplete dissolution of the injected aeration gas bubbles and loss of aeration gas at the lake surface. The solubility of Ar in water is considerably higher than the solubilities of He or Ne, which are similar. A partial loss of aeration gas to the atmosphere would mainly consist of gases with low solubilities that remain preferentially in the gas bubbles (e.g. He and Ne; see also Graser, 2006). Hence, the observed differences in the noble gas ratios suggest that, at high aeration gas flow rate used between 13 July 2005 and 15 July 2005, part of the injected gas bubbles did not dissolve completely and escaped to the atmosphere. This is in agreement with the visual observation of small gas bubbles reaching the lake surface at the plume site during sampling on 15 July 2005.

In contrast to the noble gas concentration profiles at the plume site, the profiles of dissolved O_2 remained virtually unchanged despite the strong variation in the aeration gas flow rate during the field campaign (Fig. 3.6). This implies that additional O_2 input by the aeration system due to the increased aeration gas flow rate is immediately compensated for by the high O_2 consumption rate in Lake Hallwil.

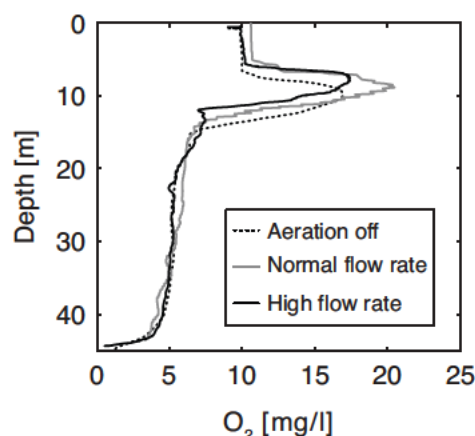


Figure 3.6 Comparison of the dissolved O_2 concentration profiles at the plume site for three different aeration gas flow rates (aeration off 13 July 2005; normal flow 8 July 2005; high flow 15 July 2005). See Fig. 3.1 for location of the profiles. The O_2 concentrations profiles at the plume site show now considerable changes in response to the variation of aeration gas flow rate, presumably due to the high O_2 consumption rate in Lake Hallwil. The corresponding noble gas concentration profiles are shown in Fig. 3.6.

3.3.3 Mass balance calculations

We performed simple noble gas mass balance calculations to gain a quantitative estimate of the dissolved gas accumulation in Lake Hallwil during the aeration phase. As discussed above, dissolved He, Ne and Ar in the hypolimnion is supersaturated due to the dissolution of injected aeration gas bubbles (Fig. 3.4 and Fig. 3.5). The observed noble gas excesses can therefore be interpreted as a measure of the fraction of the aeration gas that is stored in the water mass below the thermocline. To determine the noble gas excess concentrations $C_i^{ex} = C_i - C_i^{eq}$ ($i = \text{He, Ne, Ar}$), the measured noble gas concentrations C_i were reduced by the corresponding atmospheric equilibrium concentrations C_i^{eq} . Data from the water sample profiles collected on 08 July 2005 (normal aeration gas flow rate), 13 July 2005 (aeration off) and 15 July 2005 (high aeration gas flow rate) was used to derive a coarse estimate of the excess concentration distribution in the lake on each day. We interpolated noble gas excess concentration from the three sites linearly in two dimensions on a vertical plane that extends from the plume site to the background site and farther to the lake border. It was assumed that the noble gas concentrations at the lake surface and at the lake border are in equilibrium with the atmosphere and the noble gas excesses are therefore zero. We further assumed that the noble gas excess distributions are symmetric around the plume; i.e. that the excess concentrations are equal on ellipses which are centered at the bubble plume and have the same width-to-length ratio as Lake Hallwil. The interpolated concentration distributions were integrated over the entire lake volume to estimate the total mass of excess noble gases stored in the lake at the time of sampling. The mass balance calculations were carried out only for He, Ne and Ar, as Kr and Xe concentrations in Lake Hallwil are not affected by the aeration.

The resulting estimate of the mass of excess noble gases in Lake Hallwil on 08 July 2005 (normal aeration gas flow rate) was compared to the total noble gas mass flux into the lake during the preceding oxygenation period. On 05 April 2005, the aeration system was switched from “circulation support” mode to “oxygenation” mode. From that day until 08 July 2005, $\sim 138000 \text{ Nm}^3$ ($1 \text{ Nm}^3 \triangleq 10^6 \text{ cm}^3 \text{ STP}$) of O_2 -enriched aeration gas and $\sim 26000 \text{ Nm}^3$ of pressurized air were injected into the lake. A combination of O_2 -enriched aeration gas and pressurized air was used for the first three weeks of oxygenation mode to ensure a smooth transition from the preceding circulation support mode. Assuming that the composition of the aeration gas measured in July (Tab. 3.6) is representative for the entire oxygenation period in 2005, the total gas flux into Lake Hallwil from 05 April 2005 to 08 July 2005 corresponds to $\sim 160 \text{ t O}_2$. The masses M_i^{input} of He, Ne and Ar injected into the lake via the aeration gas input are listed in Tab. 3.8 side by side with the estimated masses M_i^{excess} of excess noble gases dissolved in the water body. This comparison suggests that the mass of He that was injected into Lake Hallwil by the aeration system from 05 April

Table 3.8 Comparison of the mass of He, Ne and Ar injected by the aeration system with the total mass of excess noble gases in Lake Hallwil.

Gas i	M_i^{input}	M_i^{excess}	$\Delta = M_i^{excess} / M_i^{input}$
He	434 g	439 g	$\sim 100\%$
Ne	7.6 kg	8.4 kg	$\sim 110\%$
Ar	9.8 t	14.8 t	$\sim 150\%$

M_i^{input} : total mass flux of gas i into Lake Hallwil from 05 April 2005 to 08 July 2005

M_i^{excess} : total mass of the excess of gas i in Lake Hallwil on 08 July 2005

2005 to 08 July 2005 is in good agreement with the observed excess of He dissolved in the lake. Direct loss of injected aeration gas bubbles to the atmosphere seems therefore to be negligible. Again, it has to be noted that the visual observation of the lake during the oxygenation period also confirmed the rather complete dissolution of the injected gas bubbles. For Ne and Ar, the gas excesses dissolved in the lake are slightly (Ne) and considerably (Ar) larger than the input by the aeration system. However, the approach used here to estimate the total mass of excess noble gases in Lake Hallwil from only three concentration profiles is subject to large uncertainties. The linear interpolation used to infer the noble gas excesses at positions between the profiles might bias the results. To explore this effect, the mass balance calculations were repeated using only the plume and background profiles in the interpolation and ignoring the data from the far field site. The total masses of excess He, Ne and Ar derived from these calculations differ by $\sim 20\%$ from the results obtained using all the profiles. We expect that the uncertainties of the mass balance calculations are in the range of these deviations. Given these uncertainties, the total masses of excess He and Ne in the lake appear to be equal to the noble gas mass injected by the aeration system whereas the Ar excess in the lake is significantly higher than the injected Ar mass (Tab. 3.8). For He and Ne, the injected gas mass seems therefore to be retained mostly or even completely in the lake during aeration at the normal gas flow rate. In contrast, the high excess of dissolved Ar in Lake Hallwil cannot be explained solely by the input of Ar from the aeration system between 05 April 2005 and 08 July 2005 and by the complete retention of the dissolved gas in the water column. As Ar is more soluble than He and Ne, it might also have partially dissolved from the larger bubbles of pressurized air that were injected into the lake during circulation support in the preceding winter and might even have accumulated in the “mixed” water column. In the case of Ar, it therefore appears that gas exchange at the lake surface is not fast enough to completely remove the gas being dissolved from the injected

bubbles during the circulation period. As a result, the concentrations of dissolved Ar might not be entirely set back to atmospheric equilibrium concentrations and the deep water of Lake Hallwil is expected to show a slight supersaturation with respect to Ar at the beginning of the oxygenation period. An excess of dissolved Ar remaining of the winter circulation might therefore account for the difference between the Ar mass injected by the aeration system and dissolved in the lake that was observed in summer (Tab. 3.8).

Between 13 July 2005 (aeration off) and 15 July 2005 (high aeration gas flow rate), the noble gas excess concentrations at the plume site increased substantially. However, this short term effect of the increased aeration gas flow rate did not affect the far field and background profiles and seems to occur only in a small volume at the center of the lake. We applied the same mass-balance approach as above to assess the accumulation of noble gases in the water column close to the bubble plume at diffuser 6. These mass balances were calculated for a vertical water column centered at the plume site with an elliptic base that has the same width-to-length ratio as Lake Hallwil (indicated as a dark gray area around diffuser 6 in Fig. 3.1). The size of the considered water volume was adjusted in order to match the mass of noble gases injected through diffuser 6 during the 2-day period of high gas flow rate (13 July 2005 to 15 July 2005) with the increase of the mass of dissolved noble gases stored in the water volume. The noble gas mass flux was calculated from the observed aeration gas flow rate and from the aeration gas composition (Tab. 3.2 and Tab. 3.6). The input of Ar that occurred during the high flow phase was found to be equal to the increase of the mass of excess Ar dissolved in a vertical water column with an elliptic base measuring 340×66 m. But the increase of the He and Ne excess in the same volume amounts to only $\sim 75\%$ of the gas mass injected by the aeration system. Part of the He and Ne input seems therefore to have been lost to the atmosphere. As mentioned in Sec. 3.3.2, small gas bubbles that reached the lake surface and escaped were observed during the phase of high aeration gas flow rate. The difference in the water-column accumulation of Ar compared to He and Ne is consistent with a partial loss of the aeration gas to the atmosphere. Due to the higher solubility, Ar is preferentially dissolved in water while He and Ne may remain in the escaping bubbles. The solubility of O_2 is similar to the solubility of Ar and therefore O_2 contained in the injected bubbles is also expected to dissolve virtually completely in the water column, even during the phase of high aeration gas flow rate.

The mass balance calculations for the phase of high aeration gas flow rate showed that the aeration gas mass injected through diffuser 6 between 13 July 2005 and 15 July 2005 results in a noble gas accumulation that is constrained to a relatively small vertical water column around the bubble plume with an elliptic base measuring 340×66 m. Under these conditions, the water volumes that are influenced by gas injection from each of the two diffusers that were in operation (diffuser 3 and 6; see

Fig. 3.1 and Tab. 3.2) do therefore not overlap. The horizontal extension of the noble gas enrichment seems to be controlled by currents in the hypolimnion. McGinnis et al. (2004) suggest that basin-wide internal seicheing leads to a dispersion of the “aeration plume signature” in Lake Hallwil. A period of ~ 6 hours and a mean horizontal velocity of $\sim 1 \text{ cm s}^{-1}$ were measured for the seiche-induced currents in the hypolimnion of Lake Hallwil. The horizontal water displacement due to the seiche-induced currents over a 6-hour period is therefore $\sim 220 \text{ m}$. Hence, the water volume that is affected by the increased noble gas accumulation during the 2-day period of high aeration gas flow rate is of similar size as expected due to dispersion caused by internal seicheing.

3.4 Conclusions

Noble gas concentrations measured in the aeration gas and in the water column of Lake Hallwil demonstrate that gas exchange between the water and the injected bubbles affects the noble gas concentrations in the water body. The specific noble gas enrichment signature of the aeration gas, being set by the on-site O_2 enrichment system, leads to a corresponding noble gas excess pattern in the lake water. As noble gases are chemically conservative, the “aeration signal” persists in the hypolimnion of Lake Hallwil during summer stratification. In contrast, the main aeration gas O_2 is consumed very fast and the observed O_2 concentration profiles are affected merely by variations in the aeration gas rate flow during the observation period. The noble gas concentrations in the lake that record the influence of the aeration operation seem to allow quantification of the efficiency of the aeration system; i.e. noble gas enrichment can be interpreted as a proxy for the transfer of O_2 to the lake water. At the normal gas flow rate used for summer aeration, the total injected noble gas mass seems to accumulate in the hypolimnion. Hence, the aeration gas bubbles appear to dissolve completely below the thermocline, as intended during the oxygenation mode. On a time-scale of days, the effects of the aeration are restricted to a small water volume (\ll lake volume) close to the bubble plume.

The relatively small number of samples and the considerable changes in aeration gas flow rates that occurred during the observation period only allow an approximate quantification of the bubble gas exchange based on the noble gas data presented. Nevertheless, the strong and distinct noble gas signals that we observed in the water column demonstrate the potential of noble gases as tracers to monitor aeration systems in lakes. Similar studies could help to understand processes in natural systems like gas seeps in lakes and oceans (see Chapter 4).

For future applications of this method of studying aeration systems, we recommend that the following points be considered:

- Preferably, such a study should cover the entire summer oxygenation period. The first noble gas profiles should be sampled immediately before the aeration system is switched from circulation support mode to aeration mode. Sampling should be repeated during the summer months, or at least at the end of the oxygenation period, to monitor the evolution of noble gas concentrations in the lake. In this case, the total increase in the concentrations of noble gases in the hypolimnion might be interpreted as a measure of the total aeration gas mass that was effectively transferred to the lake water by bubble gas exchange.
- Additional noble gas profiles in the near field of the aeration system could help to investigate the dispersion of the dissolved aeration gases in the lake. This would be a useful complement to the CTD and current velocity measurements that are usually performed to study the transport processes in the vicinity of the bubble plume.
- The noble gas study of the aeration system in Lake Hallwil should be combined with plume-modelling (e.g. McGinnis et al., 2004; Wüest et al., 1992b). Using noble gas concentration profiles as additional boundary conditions would help to better constrain these models.

4

Noble gas anomalies related to high-intensity methane gas seeps in the Black Sea

This chapter has been published in *Earth and Planetary Science Letters* (Holzner et al., 2008b).

Abstract Dissolved noble gases and tritium were analyzed at a series of high-intensity methane gas seeps in the Black Sea to study the transport and gas exchange induced by bubble-streams in the water column. These processes affect marine methane emissions to the atmosphere and are therefore relevant to climate warming. The seep areas investigated are located in the Dnepr paleo-delta, west of Crimea, and in the Sorokin Trough mud volcano area, south-east of Crimea. Noble gas concentration profiles at active seep sites revealed prominent anomalies compared to reference profiles that are unaffected by outgassing. Supersaturations of the light noble gases helium and neon observed relatively close to the sea floor are interpreted as effects of gas exchange between the water and the rising bubbles. Depletions of the heavy noble gases argon, krypton and xenon that were detected above an active, bubble-releasing mud volcano appear to be related to the injection of fluids depleted in noble gases that undergo vertical transport in the water column due to small density differences. In both cases, the noble gas anomalies clearly document seep-specific processes which are difficult to detect by other methods. Helium is generally enriched in the deep water of the Black Sea due to terrigenous input. Although exceptionally high helium concentrations observed in one seep area indicate a locally elevated helium flux, most of the seeps studied seem to be negligible sources of terrigenous helium. Noble gas analyses of sediment pore waters from the vicinity of a mud volcano showed large

vertical gradients in helium concentrations. The helium isotope signature of the pore waters points to a crustal origin for helium, whereas the deep water of the Black Sea also contains a small mantle-type component.

4.1 Introduction

Methane (CH_4) gas seeps in marine and lacustrine environments are currently of scientific interest due to their potential influence on global carbon cycles and climate warming (e.g. Judd, 2004; Walter et al., 2006). Gas release from seeps and rising bubbles in the water column can be detected by hydroacoustic systems (e.g. Artemov, 2006; Greinert et al., 2006; Hornafius et al., 1999; Naudts et al., 2006). Using this technology, marine CH_4 gas seeps have been documented worldwide, but detailed studies of gas exchange between rising CH_4 bubbles and the water column are rare (e.g. Clark et al., 2003; Leifer and Patro, 2002; Leifer et al., 2000; McGinnis et al., 2006a) and are commonly restricted to shallow seeps. Hence, more information on the processes controlling gas/water partitioning during the rising of CH_4 bubbles in the open water column is essential to better quantify the contribution of marine seeps to CH_4 in the atmosphere. We present noble gas analyses from different active seep sites that give new insights into CH_4 transport in the Black Sea.

In the Black Sea, intense gas seepage has been observed on the northern shelf and slope, as well as from mud volcanoes on the abyssal plain (Fig. 4.1). Within the EC-funded project CRIMEA (“Contribution of high-intensity gas seeps to the methane emission to the atmosphere”, <http://www.crimea-info.org/>), numerous seeps releasing gas bubbles into the Black Sea were characterized using various oceanographic and geochemical techniques to evaluate the potential effects of these “high-intensity gas seeps” on the atmosphere (Kourtidis et al., 2006; Schmale et al., 2005). The Black Sea is a unique environment in which to study marine CH_4 emissions because the water column is permanently stratified, with anoxic conditions and strong CH_4 accumulation below the chemocline at 100–150 m depth (e.g. Reeburgh et al., 1991). CH_4 concentrations in the isolated deep water body of the Black Sea reach values of up to $\sim 12 \mu\text{M}$. The majority of the CH_4 seeps observed during the CRIMEA cruises are situated at water depths shallower than 725 m. This depth limit corresponds to the upper boundary of the stability zone for pure methane hydrates at the ambient temperature and salinity conditions prevailing in the Black Sea (Naudts et al., 2006). Hence it appears that the seepage of CH_4 bubbles from the sediments is inhibited by the formation of gas hydrate layers in the sediment. Additionally, several gas-emitting mud volcanoes were studied south-east of the Crimea peninsula at about 2000 m water depth. These deep seeps occur within the gas hydrate stability zone. The mud volcano structures seem to provide migration pathways where gaseous or dissolved

CH₄ may be released from the sediments without being trapped in the gas-hydrates. Indications of CH₄ release and the presence of gas-hydrates have already been documented for neighboring mud volcanoes (Bohrmann et al., 2003). Hydroacoustically detectable bubble streams develop in the water column above the CH₄ seeps. Echo-sounder surveys of the deep mud volcanoes revealed bubble streams that rise up to 1300 m above the sea floor before they completely dissolve (Greinert et al., 2006). Rising bubbles do not only release gases to the water column during dissolution, but also force simultaneous stripping of dissolved gases which were initially absent in the gas phase (Clark et al., 2003). This process leads to characteristic anomalies of dissolved noble gases in the water column (Holzner et al., 2005, 2006). Studies of aeration systems and very intensive marine seeps describe upwelling flows induced by the bubble streams that reduce the bubble dissolution rate because dissolved gas concentrations in the rising water that surrounds the bubbles increase and may reach saturation (Clark et al., 2003; Leifer et al., 2006; Wüest et al., 1992b). However, in these studies the bubbling gas flow was much higher than observed in the Black Sea. Note that on the Black Sea shelf at depths ≤ 100 m, bubbles can reach the water surface, and might emit CH₄ directly to the atmosphere. CH₄ bubbles released from seeps located in the hydrate stability zone are expected to form a hydrate rim which may reduce gas exchange between bubbles and surrounding water (McGinnis et al., 2006a; Rehder et al., 2002). Nevertheless, the influence of such a hydrate rim on the noble gas abundance remains open and has to our knowledge not been investigated experimentally.

Dissolved noble gases in lakes and oceans are mainly of atmospheric origin. Therefore the concentrations in the water column generally correspond to atmospheric equilibrium concentrations, which are determined by the temperature and salinity prevailing during gas exchange at the water surface. As noble gases are chemically inert, only physical processes like radioactive decay and/or exchange with geochemical reservoirs other than the atmosphere can change the dissolved noble-gas abundance; hence such physical processes are responsible for any deviations from the initial partition equilibrium with the atmosphere. Due to these properties, noble gases are very useful for tracing water dynamics in marine and lacustrine systems (Kipfer et al., 2002).

4.2 Methods

4.2.1 Study area

Various high-intensity methane seeps situated in two areas south-east and west of the Crimea peninsula were investigated during the cruises of the CRIMEA project in 2003 and 2004 (Fig. 4.1 and Tab. 4.1). Part of the samples were collected at three

Table 4.1 Overview of the water column profiles and sediment cores sampled for noble gases. The noble gas data are listed in Sec. 4.5 (Tab. 4.2–4.5).

Water column profiles		
	Sampling date	Sample type *
<i>Reference 2003 (1700 m depth)</i>		
CTD064	08 June 2003	Reference
<i>Reference 2004 (2130 m depth)</i>		
CTD138	16 June 2004	Reference
<i>Dnepr paleo-delta</i>		
<i>Seep Area 1 (90 m depth)</i>		
CTD038	04 June 2003	Off-seep
CTD046	05 June 2003	On-seep
<i>Seep Area 2 (200 m depth)</i>		
CTD107	29 May 2004	On-seep
<i>Seep Area 3 (630 m depth)</i>		
CTD108	29 May 2004	Off-seep
CTD109	30 May 2004	On-seep
CTD110	30 May 2004	On-seep
<i>Sorokin Trough (Vodyanitskiy Mud Volcano, 2070 m depth)</i>		
CTD072	10 June 2003	On-seep
CTD115	03 June 2004	On-seep
CTD135	15 June 2004	On-seep
Sediment cores		
	Sampling date	Distance from VMV
<i>Reference 2003 (1700 m depth)</i>		
GC14	08 June 2003	~200 km
<i>Sorokin Trough (Vodyanitskiy Mud Volcano, 2070 m depth)</i>		
GC17	10 June 2003	~2700 m
GC41	15 June 2004	~400 m

* Reference: sampled at sites which are not affected by active seeps. On-seep: sampled above a seep. Off-seep: sampled in the vicinity of a seep but outside the current bubble stream.

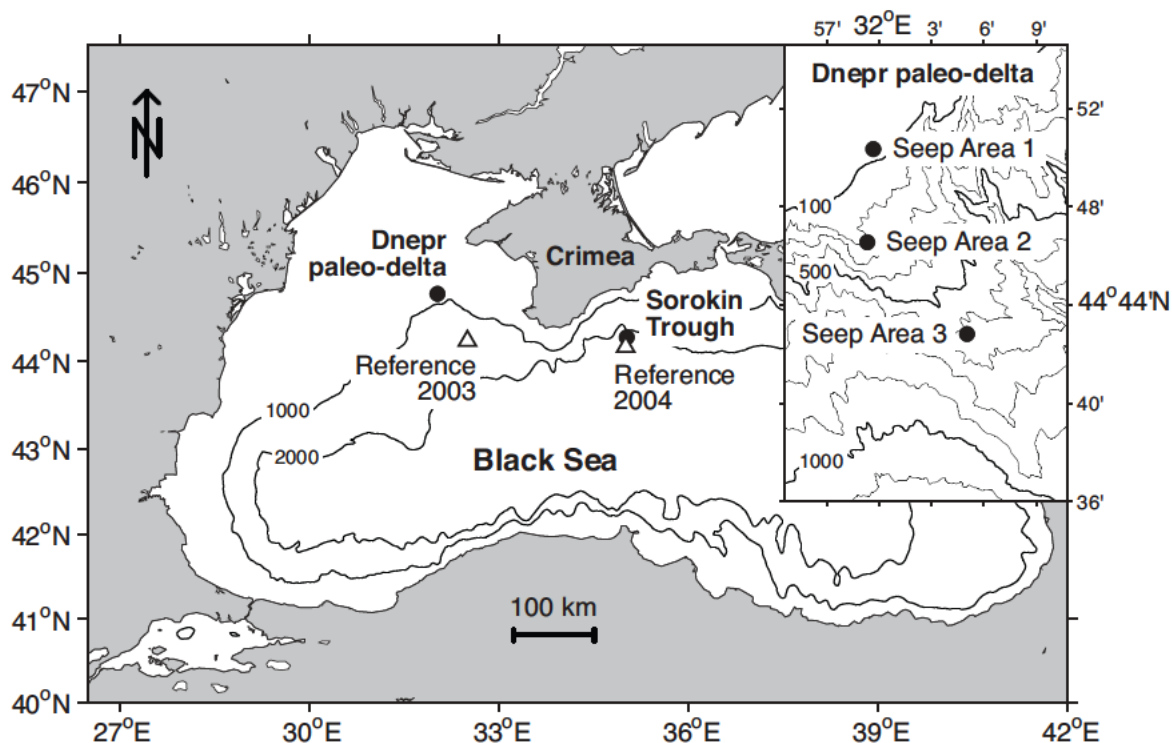


Figure 4.1 Map of the Black Sea showing the study sites. Our work focused on two areas of intense gas seepage (●): the Dnepr paleo-delta region and the Sorokin Trough. The inset shows a detailed map of the Dnepr paleo-delta with the locations of Seep Areas 1–3. The deep seep site in the Sorokin Trough (Vodyanitskiy mud volcano) and two reference sites (Δ, no influence of gas seepage) are indicated in the main panel.

sites in the Dnepr paleo-delta on the north-western Black Sea shelf and slope (Seep Area 1–3). Additionally, we studied the deep seep at the Vodyanitskiy mud volcano (VMV), located in the Sorokin Trough mud volcano area.

For comparison, samples were collected from sites in the open water away from active seeps, where no hydroacoustic signals of CH_4 gas seepage were detected. In the following, these sites will be referred to as “reference sites” and used as a baseline to interpret the results from the active seep sites. The 2003 reference site is situated between the two main study areas at a distance of ~ 70 km from the Dnepr paleo-delta and ~ 200 km from the Sorokin Trough. The 2004 reference site was chosen closer to one of the seep sites studied, i.e. ~ 9 km south of VMV.

4.2.2 Noble gases and tritium

Water samples for noble gas and tritium analysis as well as the corresponding CTD (Conductivity, Temperature, Depth) measurements were obtained using an SBE 911-plus CTD with a water-sampling rosette (12 Niskin bottles, 10 l volume each). Con-

tact of the water samples with air during sampling was avoided. The water samples (~ 23 g) were transferred to copper tubes on the ship immediately after recovery of the CTD probe, and the tubes were sealed gas-tight using pinch-off clamps. Noble gas concentrations and helium isotope ratios were measured using noble gas mass spectrometry in the Noble Gas Laboratory at ETH Zürich (Beyerle et al., 2000). Tritium concentrations were determined by the ^3He -ingrowth method using a high-sensitivity compressor-source noble gas mass spectrometer (Baur, 1999; Kipfer et al., 2002). Typical overall 1σ errors for the water analyses are $\sim 1\%$ for noble gas concentrations and $^3\text{He}/^4\text{He}$ ratios, and $\sim 3\%$ for ^3H . In total, 93 water samples were analyzed for this work. We partly or completely omitted 19 samples: 4 of those because gas extraction failed, 13 because our measurements indicate gas loss, contamination or analytical problems and 2 surface water samples were excluded from the interpretation because the results indicated solubility disequilibrium due to exceptionally high water temperatures.

Sediment cores for the analysis of noble gases in the pore water were taken using a gravity corer and sampled according to the procedures developed by Brennwald et al. (2003). Sub-samples for noble gas analysis were taken immediately after recovery of the sediment cores to minimize exsolution of supersaturated gases. The bulk sediment (~ 10 g, containing ~ 6 g of pore water) was transferred from the sediment cores into copper tubes without exposure to the atmosphere and sealed gas-tight. Dissolved noble gases in the sediment pore water were determined according the experimental protocols described by Brennwald et al. (2003) and Beyerle et al. (2000). This method consists of noble gas extraction from the pore water by degassing the sediment in an evacuated extraction vessel followed by noble gas analysis by mass spectrometry. Typical overall 1σ errors of the sediment pore water analyses are $\sim 4\%$ for noble gas concentrations and $\sim 9\%$ for $^3\text{He}/^4\text{He}$ ratios. We present noble gas data for 9 sediment samples from three Black Sea cores. Three other samples from these cores were omitted due to problems during sampling (degassing or air contamination).

Atmospheric equilibrium concentrations in the water column were calculated using the parameterizations recommended by Kipfer et al. (2002) for the measured salinity and potential temperature. A total atmospheric pressure of 1 atm was assumed for all partition equilibrium calculations, in accordance with measurements during the 2003 cruise (O. Schmale, pers. comm.). As pressure differences have a linear effect in the partition equilibrium concentrations, the given uncertainty in the average atmospheric pressure is negligible compared to the overall errors of the noble gas analyses.

4.3 Results and Discussion

4.3.1 Reference profiles of tritium and noble gases

The dissolved noble gas concentrations and tritium (^3H), as well as the apparent ^3H - ^3He ages determined for the two reference profiles (CTD064 and CTD138) agree within experimental error (Fig. 4.2). This is remarkable as the profiles were sampled in two consecutive years and at very different positions relative to the seep sites.

The tritium concentration profiles are indistinguishable for all sites studied (Fig. 4.2 A, D). In the mixed surface layer, ^3H concentrations were as high as ~ 9 TU (1 TU = 1 tritium unit = 1 ^3H atom per 10^{18} ^1H atoms), dropping below the detection limit (< 0.1 TU) at ~ 600 m depth. Large amounts of ^3H were released to the atmosphere by thermonuclear bomb tests in the 1960s. Atmospheric ^3H was oxidized to tritiated water and subsequently transported to the oceans by the hydrological cycle. The observed ^3H distribution in the water column is a result of ^3H transport by vertical mixing (turbulent or advective), deep intrusions of Bosphorus water or river inflows and ^3H decay (Özsoy et al., 2002). Therefore, the upper water layers with non-zero ^3H concentrations must have been exchanged within approximately the last 40 years; i.e. since bomb-tritium has been released to the atmosphere. The ^3H data suggests that within this time interval, vertical water transport was confined to the uppermost 600 m and did not significantly affect the deep water of the Black Sea.

The determination of concentrations of ^3H and Helium-3 (^3He ; see below) for the same water sample allow the so-called ^3H - ^3He water age to be calculated (Torgersen et al., 1977). For this calculation, tritiogenic ^3He was separated from the atmospheric and terrigenous components (Kipfer et al., 2002). We observed apparent ^3H - ^3He ages close to zero at the surface, and an increase to about 40 years at 500 m depth (Fig. 4.2 A). Below ~ 600 m depth, ^3H - ^3He age calculations become meaningless because the ^3H concentrations are virtually zero. The observed depth limit of measurable ^3H at ~ 600 m depth corresponds to distinct changes in other geochemical parameters (e.g. CH_4 concentration; see Schubert et al., 2006b). Yet, the shape of the ^3H distribution is hardly affected by the permanent chemocline, a hydro-chemical and density boundary in the Black Sea at about 100 m depth.

Dissolved helium (He) concentrations are in partition equilibrium with the atmosphere in the mixed surface layer, and increase continuously with depth (Fig. 4.2 B, E). As a result, He is supersaturated by $\sim 20\%$ in the deep water of the Black Sea. This supersaturation is caused mostly by the input of terrigenous He that emanates from the Black Sea sediments and accumulates in the deep water, since vertical transport is slow. In the deep water, the contribution of tritiogenic ^3He to the He excess is negligible, as ^3H was only detected down to about 600 m depth.

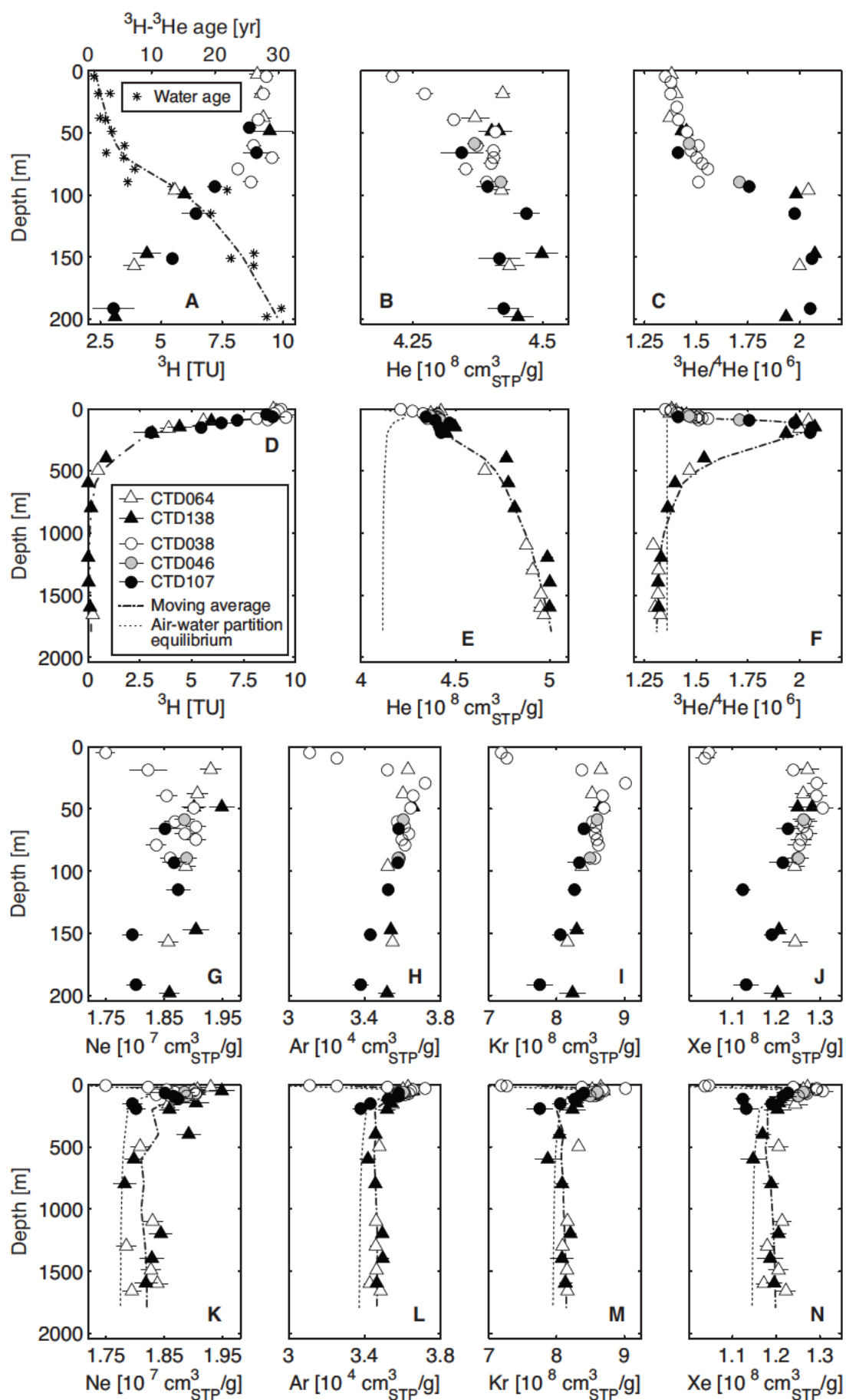


Figure 4.2 Reference profiles (figure caption continued on page 49).

Figure 4.2 (*continued from page 48*) Tritium (^3H) and dissolved noble gas data for the reference profiles (\blacktriangle) sampled in 2003 (CTD064) and 2004 (CTD138) and for the shallow profiles (\bullet) of Seep Area 1 (CTD038, CTD046) and Seep Area 2 (CTD107). He and Ne data for selected samples of the 2003 reference profile (CTD064) have already been presented by Schubert et al. (2006a). The noble gas data shown in this figure are listed in Sec. 4.5 (Tab. 4.2 and 4.3). (A–C) Tritium, helium (He) and apparent ^3H - ^3He ages in the uppermost 200 m of the water column. (D–F) ^3H and He profiles in the entire water column. The dotted lines indicate the calculated partition equilibrium concentrations with the atmosphere, the dash-dotted lines show moving-average concentrations and isotope ratios for the reference samples. ^3H concentrations are above the detection limit (>0.1 TU) in the upper 600 m of the water column. He concentrations are strongly supersaturated in the deep water and the $^3\text{He}/^4\text{He}$ isotope ratio shows a large positive anomaly around 150 m depth due to ^3H decay (“bomb peak”). (G–J) Neon (Ne), argon (Ar), krypton (Kr) and xenon (Xe) concentrations in the uppermost 200 m of the water column. (K–N) Full profiles of Ne, Ar, Kr and Xe. The reference profiles for these atmospheric noble gases show uniform, slightly supersaturated concentrations (2.5–4.5%) in the deep water.

The isotopic composition of dissolved He, i.e. the $^3\text{He}/^4\text{He}$ ratio, is in equilibrium with the atmosphere at the surface and increases down to ~ 150 m, where a strong positive anomaly (i.e. ^3He enrichment) is present. Below ~ 1000 m depth a slight negative anomaly (i.e. ^4He enrichment) is found (Fig. 4.2 C, F). The $^3\text{He}/^4\text{He}$ peak around 150 m depth is caused by the decay of ^3H and the accumulation of tritogenic ^3He . Low $^3\text{He}/^4\text{He}$ ratios near the sea floor indicate the input of isotopically heavy terrigenous He produced in the Earth’s crust ($^3\text{He}/^4\text{He} < 10^{-7}$; see Ballentine and Burnard (2002); Mamyrin and Tolstikhin (1984)).

To further investigate the terrigenous He input, we applied a 1-dimensional vertical transport model that was initially developed for lakes (Aeschbach-Hertig et al., 2002; Holzner, 2001; Kipfer et al., 2002). The model was numerically integrated using the simulation software for aquatic systems AQUASIM (Reichert, 1994). Our model describes the temporal evolution of ^3H and He concentrations in the Black Sea as a result of gas exchange at the sea surface (Wanninkhof, 1992), gain or loss of ^3H and He due to water in- and outflow, ^3He production by the radioactive decay of ^3H , vertical water transport, and terrigenous He input. The inverse fitting tools of AQUASIM were applied to tune the vertical mixing rates and to estimate the terrigenous He input. Only the ^3H and He data collected in this study were used as fitting targets. The resulting vertical mixing rates range from $3 \times 10^{-7} \text{ m}^2 \text{ s}^{-1}$ (below mixed surface layer) to $4 \times 10^{-4} \text{ m}^2 \text{ s}^{-1}$ (deep water). Assuming that He emanates homogeneously over the entire area of the Black Sea, we determine a terrigenous He flux of 7×10^9 atoms $\text{m}^{-2} \text{ s}^{-1}$ from the sediments into the water column. Our estimate of the terrigenous He input is in the range of the values given by Top and Clarke (1983) for the Black Sea ($1.3 \times 10^{10} \text{ atoms m}^{-2} \text{ s}^{-1}$) and for the mean world-ocean flux (3×10^9 atoms $\text{m}^{-2} \text{ s}^{-1}$; Craig et al., 1975).

Top and Clarke (1983) and Top et al. (1991) report He and ^3H concentrations for different stations in the central and southern Black Sea for the years 1975 and 1988, respectively, which agree remarkably well with our data. The earlier ^3H concentrations were much higher in the uppermost ~ 300 m, but no measurable ^3H was found below ~ 500 m depth with the exception of a few samples from 1975. According to Top et al. (1991), the observed non-zero ^3H concentrations cannot be representative of the entire deep water. The $^3\text{He}/^4\text{He}$ maximum due to ^3H decay also appears in the data from 1975 and 1988, but at shallower depths, because at that time the majority of the bomb- ^3H input was still concentrated in the surface waters. The sum of ^3H and tritogenic ^3He can be considered as a measure of the “total ^3H ” input into the water body. The “total ^3H ” content of a water body is unaffected by radioactive decay and only depends on input and output processes. We computed the budget of ^3H and tritogenic ^3He in the Black Sea by integrating the observed concentration profiles over depth. Using this method, the “total ^3H ” mass stored in the water column was calculated from the literature data (Top and Clarke, 1983; Top et al., 1991) and our new measurements. A comparison of the two results shows that “total ^3H ” has decreased by $\sim 35\%$ in the uppermost 600 m since 1975/88. Our measurements indicate that part of the tritogenic ^3He produced has been lost to the atmosphere due to vertical mixing and gas exchange.

Concentrations of the heavier noble gases neon (Ne), argon (Ar), krypton (Kr) and xenon (Xe) at the reference sites are close to partition equilibrium with the atmosphere (Fig. 4.2 G–N). Generally, Ne, Ar, Kr and Xe in lakes and oceans can only be of atmospheric origin because there are no other significant sources of these gases in natural waters (Kipfer et al., 2002). The profiles of dissolved Ne, Ar, Kr and Xe show similar shapes, and all these gases are slightly supersaturated in the deep water at the prevailing temperature and salinity conditions (Ne $\sim 2.5\%$, Ar $\sim 2.8\%$, Kr $\sim 2.3\%$, Xe $\sim 4.5\%$). Atmospheric noble gas supersaturations have been described for other marine waters (e.g. Craig and Weiss, 1971; Peeters et al., 2000a) and are commonly explained by air injection; i.e. air bubbles that are introduced by breaking waves and that dissolve partially or completely (Keeling, 1993). Air injection mainly affects lighter noble gases due to their low solubilities. Hence, the observed supersaturation of Ne is presumably caused by air injection. The enrichment of the heavier noble gases seems to be caused by the nonlinear effect of mixing saturated water masses at different temperatures and salinities. This process will cause supersaturations when Bosphorus inflow mixes with less saline and colder surface and intermediate waters. It is likely that the nonlinear effect of mixing also affects the noble gas concentrations in the deep water of the Black Sea because of the long water residence time (~ 2000 years; see Sorokin, 2002). The concentration profiles of Ne, Ar, Kr and Xe show shallow maxima at ~ 40 m depth that coincide with a minimum of $\sim 7^\circ\text{C}$ in the measured water temperature (data not shown), which corresponds to the mean winter

surface temperature of the Black Sea (Sorokin, 2002). Therefore, winter circulation reaching down to ~ 40 m seems to generate the cold, noble-gas-rich layer. Stanev et al. (2004) modeled convection in the Black Sea and found a mixed layer of the same thickness during winter.

Noble gas concentrations for three profiles from the shallow Seep Areas 1 (90 m water depth) and 2 (200 m water depth) are also included in Fig. 4.2 (CTD038, CTD046, CTD107). Although these profiles were sampled in active seep areas, the observed noble gas concentrations differ little from the reference concentrations. There are numerous shallow seeps (Naudts et al., 2006), but their gas flows are small, and so they do not significantly affect the noble gas concentrations in the water column on the Black Sea shelf.

4.3.2 Depletion of heavy noble gases above high-intensity CH_4 gas seeps

Three noble gas concentration profiles (Fig. 4.3) were sampled above Vodyanitskiy mud volcano (VMV, located in the Sorokin Trough at 2070 m water depth; see Fig. 4.1), which was active at the time of sampling. A stream of emitted gas bubbles rose up to 1300 m above the sea floor (Greinert et al., 2006). Despite this strong activity, no significant differences in CH_4 concentrations were observed between the Sorokin Trough and the reference sites (Fig. 4.3 H; see also Schubert et al., 2006b). Although the distribution and amount of bubbles released at VMV was continuously monitored with an echo-sounder during water sampling, samples were likely not always collected right at the intended positions within the bubble stream due to ship drift (up to several 100 m during a CTD cast) and/or displacement of the water sampling device by currents.

Noble gas data for 2003 (CTD072) and 2004 (CTD115) that cover the entire water column above VMV will be discussed first. Compared to the reference samples, the He and Ne concentrations are slightly depleted (maximum depletions: He $< 2\%$, Ne $< 3\%$; see Fig. 4.3 A, B). Remarkably, the concentrations of the heavy noble gases Ar, Kr and Xe are depleted to a much higher extent (maximum depletions: Ar $\sim 5\%$, Kr $\sim 10\%$, Xe $\sim 15\%$; see Fig. 4.3 E–G). All heavy noble gases show a distinct concentration minimum at ~ 1200 m depth. The maximum noble gas depletion above VMV increases with atomic mass, i.e. with increasing solubility and with decreasing diffusion coefficient respectively. Note that bubble-mediated gas transfer is controlled by the diffusivity and solubility of the gases (e.g. Keeling, 1993). The observed depletion anomaly disappears at ~ 1100 m above the sea floor, close to the depth where the bubble stream disappears, as observed hydro-acoustically (1300 m; see Greinert et al., 2006). The overall depletion pattern above VMV seems to persist over longer time scales, since the noble gas concentrations for the two profiles sampled about one year apart agree within analytical errors. Horizontal currents might reduce noble

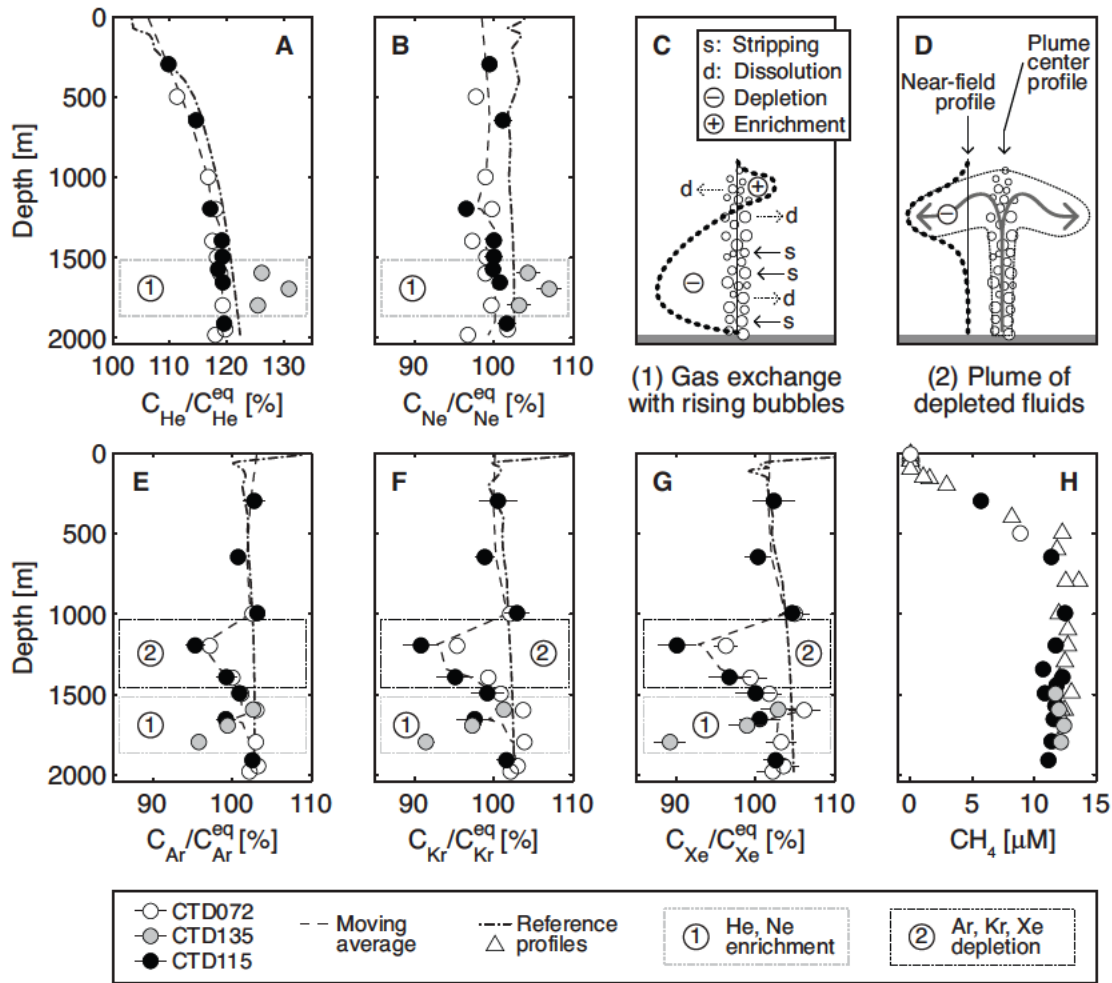


Figure 4.3 (A, B, E–G) Concentrations of dissolved noble gases at the deep seep site (normalized to atmospheric equilibrium concentrations C^{eq}). Helium (He) and neon (Ne) data for selected samples of the 2003 profile (CTD072) have already been presented by Schubert et al. (2006a). The dashed lines show moving-average concentrations of the deep seep profiles (CTD135 excluded). Mean reference profiles are shown as dash-dotted lines for comparison. The noble gas data shown in this figure are listed in Sec. 4.5 (Tab. 4.4). (C–D) Illustrations of the two mechanisms that might cause the observed noble gas anomalies at the deep seep site. The expected shape of the noble gas concentration profiles with areas of depletion (–) and enrichment (+) is indicated by the dashed line. (H) Concentration profiles of CH_4 at the deep seep site and at the reference sites (S. E. Beaubien, pers. comm.). In profiles CTD072 and CTD115, the water between ~ 1000 m and ~ 1400 m depth (zone 2) is strongly depleted in the heavy noble gases argon (Ar), krypton (Kr) and xenon (Xe). In contrast, samples from profile CTD135 are enriched in He and Ne below ~ 1500 m (zone 1) and depleted in heavy noble gases near the sea floor. Note that no significant differences in CH_4 concentrations were observed between the deep seep and the reference sites.

gas depletions due to mixing with ambient water, but currents in the deep Black Sea waters were found to be weak (Greinert et al., 2006; Korotaev et al., 2006) and seem to have a negligible effect on the observed depletion patterns.

CTD135 (Fig. 4.3) was sampled during very calm weather conditions with negligible ship drift. Hydroacoustic observations during sampling indicated that the water-sampling probe hit the bubble stream above VMV. Thus, we are quite confident that the deep-water samples for this profile were collected within the active bubble stream. The two other profiles from VMV were likely taken in the near-field of the bubble stream. As the CTD135 cast was focused on the root zone of the bubble stream, no samples were taken above 1500 m water depth.

The noble gas concentration profile CTD135 differs strikingly from the other profiles sampled at the deep seep site. He and Ne concentrations are above saturation levels and exceed their reference concentrations by 5–10% (Fig. 4.3 A, B). In contrast, Ar, Kr and Xe near the sea floor are depleted to a similar extent as in the previously discussed deep seep profiles at ~1200 m depth (Fig. 4.3 E–G). Farther from the sea floor, the concentrations of heavy noble gases increase towards the open-water reference concentrations.

4.3.3 Proposed mechanism of noble gas depletion

The prominent depletion in heavy noble gases found above VMV indicate that processes related to the activity of the mud volcano affect the concentrations of dissolved noble gases. There are only two plausible mechanisms that might deplete dissolved noble gases in the water column above a mud volcano:

(1) *Gas exchange with bubbles depleted with respect to noble gases (Fig. 4.3 C).*

Rising bubbles from marine gas seeps force a secondary gas exchange with the surrounding water (Clark et al., 2003). During this process, dissolved gases in the water are stripped by the bubbles while the host gas (e.g. CH₄) continuously dissolves from the bubbles until an equilibrium is reached between the bubbles and the surrounding water or the bubbles disappear. Therefore, gas exchange with bubbles depleted with respect to noble gases or free of noble gases would lead to noble gas depletions in the surrounding water in the depth range where stripping occurs. The effect of stripping on the concentrations of dissolved noble gases is expected to vary with diffusivity, with the highest impact on the elements with the highest diffusion coefficients (i.e. He and Ne).

(2) *Depleted fluid input (Fig. 4.3 D).*

As an alternative explanation for the observed noble gas profiles, an expulsion of fluids depleted in noble gases relative to the reference concentrations would locally decrease the noble gas concentrations in the water column. Such de-

pleted fluids might rise as a plume in the weakly stratified Black Sea deep water due to buoyancy caused by elevated temperature, injected bubbles, or a combination of both. The depleted fluids are transported vertically until the plume can no longer overcome the density gradient. As a consequence, the mud volcano fluids are injected into the water column and spread horizontally within a layer of equal density (McDougall, 1978; McGinnis et al., 2004; Wüest et al., 1992b). At this depth, the depleted water replaces or mixes with water which initially had the reference noble gas concentrations, thus causing the observed noble gas depletions.

In the following paragraphs, both mechanisms will be discussed. Considering only mechanism 1, it should be noted that the bubbles released from VMV dissolve completely within the water column (Greinert et al., 2006; McGinnis et al., 2006a). Therefore, all stripped gases redissolve. In this case, we would expect considerable noble gas enrichment to occur in the area of complete bubble dissolution. However, the profiles CTD072 and CTD115 (Fig. 4.3 A, B, E–G) show no noble gas enrichment relative to the reference profiles close to the top of the bubble stream (i.e. above ~ 1000 m water depth). The existence of a thin enrichment layer, as found for CH_4 in the north sea (Leifer and Judd, 2002), cannot be ruled out completely, given the coarse sampling resolution. Nevertheless, the observed increase in noble gas depletion with increasing atomic mass contradicts the fractionation expected by stripping. Stripping should be faster and more efficient for the light noble gases than for the heavier noble gases. It therefore appears unlikely that the depletion of heavy noble gases at ~ 1200 m depth is predominantly caused by mechanism 1, i.e. gas exchange between rising bubbles and the surrounding water column.

Profile CTD135, however, can be interpreted in terms of mechanism 1. The near-bottom noble gas anomalies observed for this profile (Fig. 4.3 A, B, E–G) seem to be directly related to bubble-driven gas exchange. During the sampling of CTD135, bubbles were tracked hydroacoustically up to ~ 1500 m water depth, which corresponds to the upper boundary of the He and Ne enrichment. The reduced bubble rise height follows a general decrease in mud volcano activity that was recorded between 2003 and 2004 (Greinert et al., 2006). The supersaturations of He and Ne as well as the concentration increase of Ar, Kr and Xe towards the reference values occur just below the depth where the bubble stream disappeared at the time of sampling. These structures can reasonably be interpreted as a signal of noble gas redissolution from collapsing bubbles containing noble gases stripped from the water column close to the sea floor.

The strong depletions in Ar, Kr and Xe at ~ 1200 m depth are conceptually consistent with mechanism 2, a rising plume of water depleted in noble gases. As the casts CTD072 and CTD115 most likely did not sample the center of the observed bubble

stream, the profiles probably represent the conditions prevailing in the near-field of the plume, which is not directly affected by bubble gas exchange (Fig. 4.3 D). The depleted mud-volcano fluid would be deposited at the equilibrium depth, where upwelling ceases and the plume water disperses horizontally over a larger area. At that depth range, the anticipated noble gas anomaly could hardly be missed even if ship positioning were inaccurate. Water-column profiles sampled relatively close to VMV should therefore always show a depletion signature if depleted fluids were expelled from VMV at that time.

Noble gas depletion of water within the mud volcano can either occur as a result of stripping during bubble emanation or because of gas hydrate formation. Stripping mainly affects the light noble gases, and could therefore account for the slight depletion of He and Ne detected in profiles CTD072 and CTD115. Gas hydrates were found in sediment cores sampled at VMV during the CRIMEA project and have also been discovered at various other mud volcanoes in the Sorokin Trough (Bohrmann et al., 2003). Winckler et al. (2002) showed that CH₄ hydrates from Hydrate Ridge (Pacific Ocean) contain significant amounts of Ar, Kr and Xe, but virtually no He and Ne. This specific fractionation occurs because the relatively large atoms of the heavier noble gases are preferentially incorporated as guest molecules into the gas hydrate structure. Gas hydrate formation in the sediments of the Sorokin Trough could therefore lead to depletion of the heavy noble gases in the remaining sediment pore water, which is then injected into the water column of the Black Sea by the mud volcanoes. Thus, the depletion of the heavy noble gases that were observed in the water column at the deep seep site might be linked to gas hydrate formation in the mud-volcano sediments.

To summarize, we propose that the expulsion of fluids depleted in noble gases from VMV, followed by the formation of an upwelling plume that disperses at an equilibrium depth of ~1200 m, leads to the observed depletion of heavy noble gases. Bubble-induced stripping also seems to fractionate the noble gases in the water column above VMV, but this effect is only relevant for samples from the center of the active bubble stream. The proposed mechanism of an upwelling plume is further supported by the detection of enhanced turbulence in water temperature profiles from the Sorokin Trough and by the results of plume modeling (McGinnis et al., 2006b). Strong upwelling flows caused by rising bubbles were previously documented for shallow, highly active marine seeps (e.g. Clark et al., 2003; Leifer et al., 2006).

For the profiles sampled at Seep Area 3 (630 m water depth), we observed a similar depletion in the heavy noble gases (shown for Xe in Fig. 4.4 C). These profiles show the same characteristic features that were found at VMV: a depletion in the heavy noble gases near the sea floor and a prominent concentration minimum of the heavy noble gases at the depth where the rising bubbles dissolve completely. These

similarities indicate that at the shallower site, seep-related processes also induce noble gas depletion in the water column.

4.3.4 Helium concentrations and isotopic composition in the water column

The highest concentrations of dissolved He were observed in three profiles (CTD108, CTD109 and CTD110) sampled at Seep Area 3 in 2004 (Fig. 4.4 A, B). These He maxima exceed the concentrations in the Black Sea deep water by more than 5%. Seep Area 3 also showed the highest dissolved CH_4 concentrations (up to $14 \mu\text{M}$ in 2004 and up to $16 \mu\text{M}$ in 2003). Total He in all three profiles is elevated within the lowermost $\sim 300 \text{ m}$ of the water column, where active bubble streams were detected. Above the bubble streams, He concentrations at Seep Area 3 match the concentrations found at the reference sites.

CTD108 was sampled “off-seep”, i.e. at a location where no gas bubbles were observed, but still within the far-field of various seeps. CTD109 and CTD110 were taken right above active gas seeps (“on-seep”). The shapes of the off-seep and on-seep He profiles (Fig. 4.4 A) differ considerably. The off-seep He concentration is maximal near the sea floor and decreases gradually towards the water surface. In

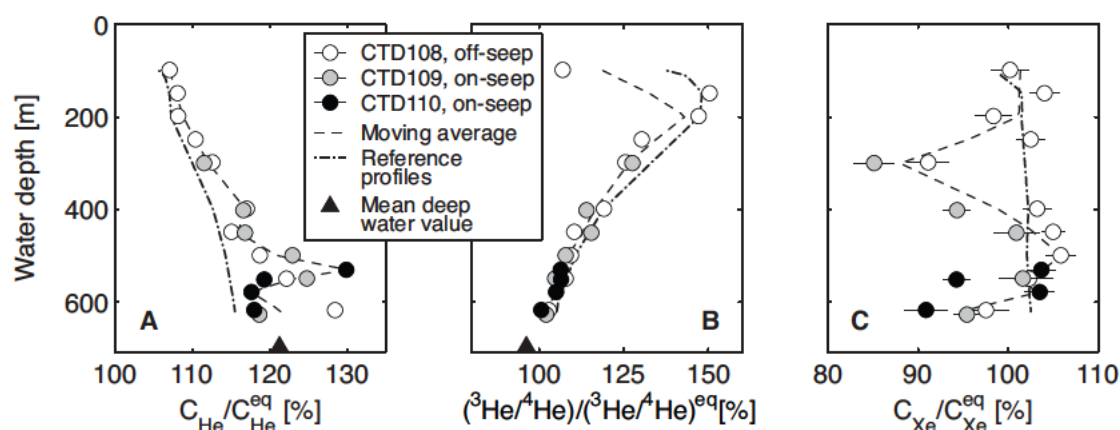


Figure 4.4 Helium (He) and xenon (Xe) data (normalized to atmospheric equilibrium concentrations) for profiles sampled at Seep Area 3 in the Dnepr paleo-delta region. The dashed lines show moving-average concentrations and isotope ratios for the data presented. Mean reference profiles are shown as dash-dotted lines for comparison. The symbol \blacktriangle indicates mean deep water He concentrations and isotope ratios. The noble gas data shown in this figure are listed in Sec. 4.5 (Tab. 4.3). (A) He concentrations at $\sim 500 \text{ m}$ depth exceed corresponding reference values and even exceed the concentrations found in the deep water of the Black Sea. (B) The $^3\text{He}/^4\text{He}$ isotope ratios do not differ considerably from those at the reference sites. (C) Depletion in the heavy noble gases (e.g. Xe) is similar to that at the deep seep site in the Sorokin Trough (Fig. 4.3 C–E). The concentration profiles of Ne, Ar and Kr (not shown) are qualitatively similar to the concentration profile of Xe.

contrast, the profiles sampled on-seep within a bubble stream show a distinctive He concentration maximum at ~ 500 m depth. In general, the positive He anomalies at Seep Area 3 occur at a greater depth than that of the maximum depletion of the heavy noble gases (Fig. 4.4 C).

The differences in He concentration between off-seep and on-seep profiles indicate that He emission is linked to the CH_4 gas seepage. We speculate that He emanates from the seeps together with CH_4 as free gas. The on-seep He enrichment seems to be caused by He dissolution from the rising bubbles. As He diffuses much faster out of the rising bubbles than CH_4 , it is expected to be transferred to the water column at an early stage of bubble dissolution, substantially below the top of the bubble stream. The observed He concentration maximum is similar to the positive He anomaly found near the sea floor at VMV (Fig. 4.3 A). The enrichment of dissolved He, which was observed for the off-seep profile CTD108, is most likely related to the emissions from the adjacent seeps. Horizontal mixing presumably transports He-enriched water from the active gas seep sites towards CTD108.

In contrast to the He concentrations, the He isotope ratios at Seep Area 3 are indistinguishable from those at the reference site (Fig. 4.4 B). Accordingly, the observed excess He shows a similar $^3\text{He}/^4\text{He}$ ratio to that generally found in the Black Sea, and seems to have the same terrigenous source (Fig. 4.2 E, F).

4.3.5 Helium emanation from the sediment

To gain further insight into the sources of terrigenous He in the Black Sea, we analyzed the sediment pore water for noble gases. Fig. 4.5 A, B shows He concentrations and $^3\text{He}/^4\text{He}$ ratios determined in pore-water samples from two cores collected close to VMV in the Sorokin Trough, and from one core from the 2003 reference site (locations are shown in Fig. 4.1). Sediment cores taken at the centre of VMV were not suitable for noble gas analysis as they contained CH_4 hydrates which dissociated and induced degassing during core recovery. Core GC41 and GC17 were taken ~ 400 m and ~ 2700 m, respectively, from the center of VMV. The reference core GC14 was taken ~ 200 km from VMV.

All He concentrations and $^3\text{He}/^4\text{He}$ ratios measured in the pore water of the reference core GC14 are the same within experimental errors (Fig. 4.5 A, B). The $^3\text{He}/^4\text{He}$ ratios correspond to the values found in the Black Sea deep water, indicating that non-atmospheric He in the pore water of this core and in the deep water have the same source. The pore waters are slightly enriched in He (by $\sim 15\%$) compared to the deep water, and therefore seem to emit He to the Black Sea.

In contrast, the pore waters of the cores from the Sorokin Trough show strong He concentration gradients and a characteristic decrease in the $^3\text{He}/^4\text{He}$ ratio with sediment depth (Fig. 4.5 A, B). The gradients in the He concentration and in the

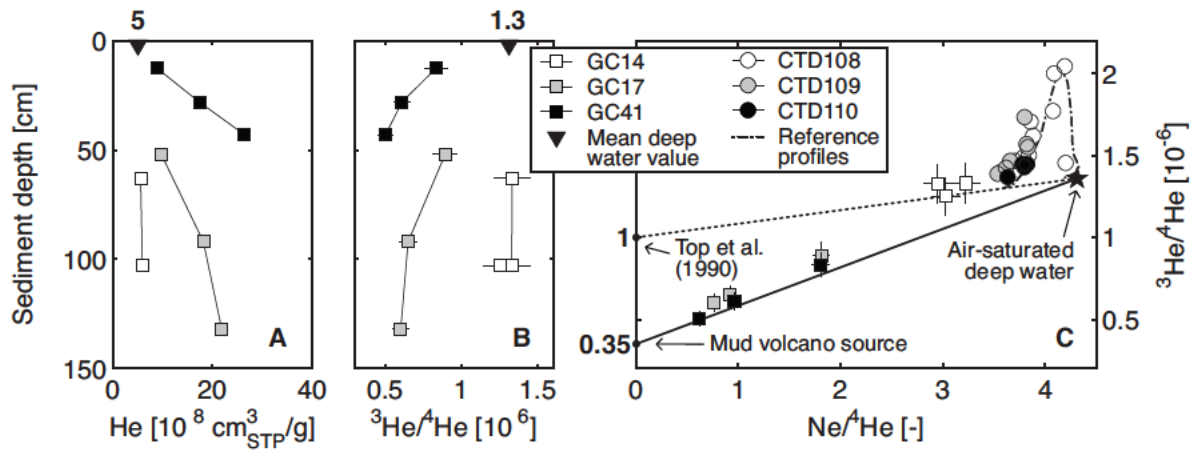


Figure 4.5 (A) Helium (He) concentrations and (B) $^3\text{He}/^4\text{He}$ isotope ratios in the pore water of three sediment cores from the Sorokin Trough (GC17, GC41) and the 2003 reference site (GC14). (C) $^3\text{He}/^4\text{He}$ ratio as a function of $\text{Ne}/^4\text{He}$ for the sediment pore water samples (■), the open water samples from Seep Area 3 (●; see also Fig. 4.4) and for the mean open water reference profile (dash-dotted line). The noble gas data shown in this figure are listed in Sec. 4.5 (Tab. 4.3 and 4.5). Straight lines indicate mixing between air-equilibrated Black Sea deep water and a seafloor source with a $^3\text{He}/^4\text{He}$ ratio of 1×10^{-6} (dotted line) as determined by Top et al. (1990) for the southern Black Sea, or with an estimated mud volcano source with a $^3\text{He}/^4\text{He}$ ratio of 3.5×10^{-7} (solid line). The data for the deep water samples and sediment pore water are in agreement with the higher $^3\text{He}/^4\text{He}$ ratio determined by Top et al. (1990), while the pore water results from the Sorokin Trough indicate a local source of helium with lower $^3\text{He}/^4\text{He}$.

$^3\text{He}/^4\text{He}$ ratio are steeper for GC41, which was taken closer to VMV, than for GC17. Pore-water He concentrations in the lower part of the cores from the Sorokin Trough are enriched by up to $\sim 400\%$ relative to the Black Sea deep-water concentrations. Towards the water/sediment interface, the pore-water He concentrations and $^3\text{He}/^4\text{He}$ ratios approach the water-column values, indicating that noble gases diffuse from the sediment into the water column. He transport within the sediment pore water can be estimated from the observed concentration gradients using the equations given by Strassmann et al. (2005). We assume a sediment porosity of 70% (e.g. Ross et al., 1978) and consider only diffusive fluxes. The estimate for GC17 of $9 \times 10^9 \text{ atoms m}^{-2} \text{ s}^{-1}$ is slightly higher than the terrigenous He flux that was derived from the water column data ($7 \times 10^9 \text{ atoms m}^{-2} \text{ s}^{-1}$; see above). The data for GC41 indicate a highly increased flux of $33 \times 10^9 \text{ atoms m}^{-2} \text{ s}^{-1}$.

As He transport within the Earth's crust occurs primarily by advection of fluids (Ballentine and Burnard, 2002), He release at the sea floor depends on the presence of geological structures which allow fluid migration. In the Sorokin Trough, mud volcanoes occur at the southern border of a diapiric zone/fold, formed by compressive deformation (Krastel et al., 2003), and provide possible migration pathways. The

sediment core with the highest He gradient (GC41) was taken right on the southern border of this active structure. Core GC17 was taken ~ 1 km NW of that border and shows a considerably smaller He gradient. At Seep Area 3, there are no clear indications of conduits for upward fluid migration. Seismic data showed no evidence of shallow faults in the uppermost 250 m of the sediment column (Naudts et al., 2006); however, the shallow seismic results do not rule out that deeper structures, such as the mud diapirs and deep faults documented in the region by Lüdmann et al. (2004) and Kutas et al. (2004), may enhance He transport.

A plot of $^3\text{He}/^4\text{He}$ against $\text{Ne}/^4\text{He}$ (Fig. 4.5 C) allows us to differentiate between atmospheric input (denoted by a ★) and non-atmospheric sources of He in the Black Sea. Water samples from depths around 150 m are shifted towards higher $^3\text{He}/^4\text{He}$ ratios due to the production and accumulation of tritiogenic ^3He (“bomb peak”). Deep-water samples and pore-water samples from the reference core have a $^3\text{He}/^4\text{He}$ ratio that is slightly lower than that of air-saturated deep water, and show lower $\text{Ne}/^4\text{He}$ ratios due to terrigenous He input. The much stronger accumulation of terrigenous He in the sediments from the Sorokin Trough leads to substantially lower $^3\text{He}/^4\text{He}$ ratios and $\text{Ne}/^4\text{He}$ ratios.

All samples shown in Fig. 4.5 C, except for the open-water samples containing tritiogenic ^3He , can be interpreted as binary mixtures of air-saturated deep water and virtually Ne-free terrestrial inputs. At least two types of terrigenous He determine the $^3\text{He}/^4\text{He}$ ratios of the non-atmospheric He excess in the Black Sea. Samples from the deep water of the Black Sea and from the reference core GC14 show a terrigenous He component with a $^3\text{He}/^4\text{He}$ ratio of $\sim 10^{-6}$. The existence of such a ^3He -rich terrigenous He source was postulated by Top et al. (1990) based on measurements of He isotopes in the water column. Using our water column model (see above), we estimated a similar $^3\text{He}/^4\text{He}$ ratio of 7×10^{-7} for the terrigenous He input. The sediment pore water samples from the Sorokin Trough (GC17 and GC41) indicate a different He source with a significantly lower $^3\text{He}/^4\text{He}$ ratio of $\sim 3.5 \times 10^{-7}$. Therefore, He in the sediment cores from the Sorokin Trough area must be of crustal origin ($^3\text{He}/^4\text{He} < 10^{-7}$; Ballentine and Burnard, 2002; Mamyrin and Tolstikhin, 1984), with the addition of small amounts of mantle-type He ($^3\text{He}/^4\text{He} > 10^{-5}$; Mamyrin and Tolstikhin, 1984). The deep water of the Black Sea as well as the reference core, however, are dominated by a terrigenous He component that is more enriched in ^3He .

Overall, He emission into the Black Sea is heterogeneous and originates from different terrigenous He sources. There are indications of enhanced He release in Seep Area 3 and at VMV. However, sediment pore-water analyses for the Sorokin Trough exclude VMV as a major source of terrigenous ^3He in the Black Sea.

4.4 Conclusions

We compiled a broad set of noble gas and ^3H data for the water column at active seep sites located on the shelf, on the slope and in the abyssal region of the Black Sea. The data gathered allowed us to assess the influence of gas seepage on the abundance of noble gases in the Black Sea. Reference profiles sampled at sites unaffected by seepage show Ne, Ar, Kr and Xe concentrations that are close to atmospheric equilibrium concentrations. In contrast, He is supersaturated due to the injection of terrigenous He. The concentrations of ^3H and tritiogenic ^3He imply that bomb- ^3H has penetrated the Black Sea to a depth of ~ 600 m. Compared to earlier measurements, “total ^3H ” (i.e. the sum of ^3H and tritiogenic ^3He) in this depth range has decreased by about one third due to the escape of ^3He to the atmosphere.

Profiles sampled at active gas seep sites demonstrate the clear effects of the bubble release on the noble gas concentrations in the water column. Two types of noble gas anomaly were identified. Relatively close to the sea floor, within active bubble streams, the water was found to be supersaturated with respect to the light noble gases and simultaneously to be depleted with respect to the heavy noble gases. These anomalies seem to be the result of gas exchange between the rising bubbles and the surrounding water column. Additional profiles from the deep seep in the abyssal zone of the Black Sea revealed no enrichment of light noble gases, but prominent depletions in Ar, Kr and Xe. We suggest that the depletion in the heavy noble gases is the result of the expulsion of fluids depleted in noble gases from a mud volcano. Because of their lower density, these fluids rise as a plume in the water column and disperse at their equilibrium depth by mixing with the surrounding water.

Sediment cores from the mud volcano area at the Sorokin Trough show strong He concentration gradients and characteristically low $^3\text{He}/^4\text{He}$ ratios, which seem to be related to the local geological structure. The $^3\text{He}/^4\text{He}$ signatures in the sediment pore waters of the Sorokin Trough, however, differ substantially from those found in the Black Sea deep-water body and in the pore-water of sediments sampled far from the mud volcano area. Both the latter are enriched in ^3He . Terrigenous sources that are not related to mud volcanoes must therefore account for the ^3He -enriched helium excess that prevails in the Black Sea.

The analysis of sediment pore-water for noble gases has proven useful to characterize the heterogeneity in subsurface He release at a gas and/or fluid emitting mud volcano. Water column He concentrations, in contrast, do not reflect the spatial variations of the terrigenous He flux, and hence can be used to determine the mean He input over the entire area of the Black Sea.

Acknowledgments We greatly appreciate the support by the officers and crew of the R/V Professor Vodyanitsky during the cruises. We are also grateful to the whole

CRIMEA team for their excellent collaboration during the project and particularly to S. E. Beaubien and S. Lombardi (Universita di Roma “La Sapienza”) for providing the CH₄ data. We thank H. Amaral, M. S. Brennwald, M. Hofer, S. Klump and Y. Tomonaga from the Environmental Isotopes Group at Eawag, as well as H. Baur and U. Menet from ETH for their support in the laboratory. We further thank D. M. Livingstone, M. L. Delaney (Editor EPSL) and two anonymous reviewers for their detailed comments that improved our manuscript. The CRIMEA project was funded by the European Union (Contract no. EVK2-CT-2002-00162) and by the Swiss Federal Office of Education and Science (Contract no. 02.0247). Further financial support came from TUMSS (the ETH methane cluster) to C. P. Holzner and R. Kipfer and from the Swiss National Science Foundation to D. F. McGinnis (Grant 200020-111763), C. J. Schubert (Grants 2100-068130 and 2160-067493) and R. Kipfer (Grants 200020-101725 and 200020-105263).

4.5 Appendix: Tables of the noble gas data

4.5.1 Water samples

Table 4.2 Profiles of ^3H concentrations, noble gas concentrations, and $^3\text{He}/^4\text{He}$ ratios in the water at the *reference sites* in the Black Sea. The overall measurement errors (1σ errors) are $\pm 3\%$ for ^3H concentrations, $\pm 1\%$ for noble gas concentrations, and $\pm 1\%$ for $^3\text{He}/^4\text{He}$ ratios.

Depth [m]	^3H [TU]	He † [10^{-8}]	$^3\text{He}/^4\text{He}$ [10^{-6}]	Ne † [10^{-7}]	Ar † [10^{-4}]	Kr † [10^{-8}]	Xe † [10^{-8}]
CTD064 (Reference 2003, 1700 m depth), date of sampling: 08 June 2003							
3	8.9	*	1.38	*	*	*	*
18	9.1	4.42	1.40	1.93	3.63	8.65	1.27
38	9.2	4.37	1.37	1.91	3.60	8.53	1.26
96	5.6	4.42	2.04	1.89	3.52	8.37	1.24
157	3.9	4.44	2.00	1.86	3.55	8.16	1.24
497	0.5	4.66	1.47	1.81	3.48	8.32	1.21
796	*	*	*	*	*	*	*
1097	–	4.88	1.29	1.83	3.46	8.16	1.21
1297	–	4.91	1.32	1.78	3.46	8.09	1.18
1490	–	4.95	1.32	1.83	3.46	8.15	1.21
1598	–	4.95	1.30	1.84	3.43	8.12	1.17
1658	0.2	4.97	1.33	1.79	3.48	8.16	1.22
CTD138 (Reference 2004, 2130 m depth), date of sampling: 16 June 2004							
49	9.4	4.42	1.43	1.95	3.66	8.65	1.28
49	–	4.40	1.45	1.90	3.65	8.69	1.25
99	5.9	*	1.98	*	*	*	*
147	4.4	4.50	2.07	1.90	3.54	8.30	1.21
198	3.1	4.45	1.93	1.86	3.52	8.23	1.20
398	0.9	4.77	1.54	1.89	3.46	8.04	1.17
598	0.0	4.78	1.40	1.80	3.42	7.87	1.15
796	0.1	4.81	1.36	1.78	3.46	8.08	1.19
997	*	*	*	*	*	*	*
1196	0.0	4.99	1.33	1.84	3.49	8.20	1.21
1396	0.0	5.00	1.32	1.83	3.49	8.08	1.19
1597	0.1	5.00	1.32	1.82	3.46	8.13	1.20
1795	*	*	*	*	*	*	*

† Noble gas concentrations are given in $\text{cm}^3\text{STP g}^{-1}$.

– Not analyzed.

* Omitted due to experimental problems.

Table 4.3 Profiles of ^3H concentrations, noble gas concentrations, and $^3\text{He}/^4\text{He}$ ratios in the water of the *Dnepr paleo-delta area* of the Black Sea. The overall measurement errors (1σ errors) are $\pm 3\%$ for ^3H concentrations, $\pm 1\%$ for noble gas concentrations, and $\pm 1\%$ for $^3\text{He}/^4\text{He}$ ratios. (continued on next page)

Depth [m]	^3H [TU]	He † [10^{-8}]	$^3\text{He}/^4\text{He}$ [10^{-6}]	Ne † [10^{-7}]	Ar † [10^{-4}]	Kr † [10^{-8}]	Xe † [10^{-8}]
CTD038 (Seep Area 1, 90 m depth, off-seep), date of sampling: 04 June 2003							
5	9.3	4.21	1.35	1.75	3.11	7.18	1.05
9	–	*	1.38	*	3.25	7.26	1.04
19	9.2	4.27	1.38	1.82	3.52	8.37	1.24
29	–	*	1.41	*	3.72	9.02	1.29
39	9.0	4.33	1.41	1.85	3.66	8.68	1.29
49	–	4.41	1.46	1.90	3.64	8.70	1.31
60	8.8	4.37	1.51	1.87	3.57	8.53	1.27
64	–	4.41	1.47	1.90	3.61	8.58	1.26
70	9.5	4.41	1.50	1.88	3.63	8.57	1.27
75	–	4.40	1.53	1.90	3.60	8.60	1.26
79	8.1	4.35	1.56	1.84	3.61	8.62	1.25
90	8.7	4.39	1.51	1.86	3.58	8.57	1.25
CTD046 (Seep Area 1, 90 m depth, on-seep), date of sampling: 05 June 2003							
59	–	4.37	1.47	1.88	3.60	8.60	1.26
90	–	4.42	1.71	1.89	3.58	8.50	1.25
CTD107 (Seep Area 2, 200 m depth, on-seep), date of sampling: 29 May 2004							
46	8.6	*	*	*	*	*	*
66	8.9	4.34	1.41	1.85	3.58	8.40	1.23
93	7.2	4.39	1.76	1.87	3.57	8.34	1.22
115	6.4	4.47	1.97	1.87	3.52	8.26	1.12
151	5.5	4.42	2.06	1.80	3.43	8.05	1.19
191	3.0	4.42	2.05	1.80	3.38	7.75	1.13

† Noble gas concentrations are given in $\text{cm}^3\text{STP g}^{-1}$.

– Not analyzed.

* Omitted due to experimental problems.

Table 4.3 (continued from previous page)

Depth [m]	^3H [TU]	He † [10^{-8}]	$^3\text{He}/^4\text{He}$ [10^{-6}]	Ne † [10^{-7}]	Ar † [10^{-4}]	Kr † [10^{-8}]	Xe † [10^{-8}]
CTD108 (Seep Area 3, 630 m depth, off-seep), date of sampling: 29 May 2004							
98	8.5	4.52	1.45	1.90	3.62	8.56	1.23
149	4.8	4.48	2.04	1.88	3.51	8.25	1.22
198	2.9	4.48	2.00	1.83	3.37	7.80	1.14
248	2.1	4.57	1.77	1.86	3.46	8.13	1.19
298	1.8	4.65	1.71	1.79	3.22	7.26	1.05
398	1.1	4.83	1.62	1.88	3.46	8.12	1.19
448	1.0	4.75	1.50	1.82	3.52	8.18	1.21
499	0.9	4.90	1.49	1.85	3.38	7.83	1.22
549	0.3	5.04	1.47	1.86	3.47	8.02	1.18
617	0.3	5.29	1.40	1.89	3.36	7.69	1.12
CTD109 (Seep Area 3, 630 m depth, on-seep), date of sampling: 30 May 2004							
299	1.8	4.61	1.74	1.75	3.08	6.89	0.98
401	0.9	4.81	1.55	1.84	3.28	7.54	1.09
450	1.5	4.82	1.57	1.84	3.43	7.98	1.16
499	0.1	5.07	1.47	1.85	*	*	*
548	0.4	5.14	1.43	1.86	3.47	8.11	1.17
627	0.2	4.89	1.39	1.73	3.32	7.58	1.10
CTD110 (Seep Area 3, 630 m depth, on-seep), date of sampling: 30 May 2004							
530	0.6	5.35	1.45	2.05	3.57	8.31	1.19
551	0.5	4.92	1.45	1.86	3.32	7.67	1.08
578	0.4	4.85	1.43	1.84	3.50	8.28	1.19
617	0.0	4.86	1.37	1.77	3.22	7.30	1.04

† Noble gas concentrations are given in $\text{cm}^3\text{STP g}^{-1}$.

– Not analyzed.

* Omitted due to experimental problems.

Table 4.4 Profiles of ^3H concentrations, noble gas concentrations, and $^3\text{He}/^4\text{He}$ ratios in the water column above *Vodyanitskiy mud volcano (VMV)*, which is located in the Sorokin Trough area of the Black Sea. The overall measurement errors (1σ errors) are $\pm 3\%$ for ^3H concentrations, $\pm 1\%$ for noble gas concentrations, and $\pm 1\%$ for $^3\text{He}/^4\text{He}$ ratios.

Depth [m]	^3H [TU]	He † [10^{-8}]	$^3\text{He}/^4\text{He}$ [10^{-6}]	Ne † [10^{-7}]	Ar † [10^{-4}]	Kr † [10^{-8}]	Xe † [10^{-8}]
CTD072 (VMV, 2070 m depth, on-seep), date of sampling: 10 June 2003							
6	9.2	*	1.39	*	*	*	*
497	0.9	4.59	1.50	1.74	*	*	*
997	–	4.81	1.33	1.76	3.46	8.13	1.20
1198	–	4.86	1.31	1.77	3.28	7.59	1.10
1397	–	4.84	1.33	1.73	3.37	7.90	1.14
1497	–	4.87	1.34	1.76	3.41	8.02	1.17
1598	–	4.89	1.26	1.76	3.47	8.24	1.22
1679	*	*	*	*	*	*	*
1798	0.1	4.91	1.32	1.77	3.47	8.26	1.18
1898	*	*	*	*	*	*	*
1947	–	4.93	1.34	1.81	3.48	8.19	1.19
1981	–	4.86	1.30	1.72	3.44	8.12	1.17
CTD115 (VMV, 2070 m depth, on-seep), date of sampling: 03 June 2004							
295	–	4.53	1.68	1.77	3.49	8.05	1.18
645	0.3	4.72	1.36	1.80	3.40	7.88	1.15
995	–	*	1.36	*	3.48	8.19	1.20
1195	0.0	4.82	1.31	1.71	3.22	7.23	1.03
1344	0.0	*	*	*	*	*	*
1393	0.0	4.90	1.30	1.78	3.35	7.57	1.11
1443	0.0	*	1.32	*	*	*	*
1493	0.0	4.91	1.35	1.78	3.40	7.89	1.15
1573	0.0	4.88	1.31	1.77	*	*	*
1655	0.0	4.91	1.29	1.79	3.34	7.76	1.15
1793	0.0	*	1.32	*	*	*	*
1911	0.1	4.92	1.30	1.80	3.46	8.07	1.17
CTD135 (VMV, 2070 m depth, on-seep), date of sampling: 15 June 2004							
1496	*	*	*	*	*	*	*
1596	–	5.19	1.33	1.85	3.46	8.05	1.18
1695	–	5.39	1.31	1.90	3.35	7.73	1.13
1798	–	5.16	1.33	1.83	3.23	7.27	1.02

† Noble gas concentrations are given in $\text{cm}^3\text{STP g}^{-1}$.

– Not analyzed.

* Omitted due to experimental problems.

4.5.2 Sediment samples

Table 4.5 Concentrations of noble gases and $^3\text{He}/^4\text{He}$ ratios in the pore water of Black Sea sediments. GC14 was taken at the *reference site* of the 2003 expedition. GC17 and GC41 are sediment cores collected close to *Vodyanitskiy mud volcano (VMV)* in the Sorokin Trough area of the Black Sea. The overall measurement errors (1σ errors) are $\pm 4\%$ for noble gas concentrations and $\pm 9\%$ for $^3\text{He}/^4\text{He}$ ratios.

Sediment depth [cm]	He † [10^{-8}]	$^3\text{He}/^4\text{He}$ [10^{-6}]	Ne † [10^{-7}]	Ar † [10^{-4}]	Kr † [10^{-8}]	Xe † [10^{-8}]
GC14 (Reference 2003, 1700 m depth, ~200 km away from VMV)						
Date of sampling: 08 June 2003						
43	*	*	*	*	*	*
63	*	*	*	*	*	*
63	5.57	1.33	1.79	3.18	7.33	1.25
103	5.89	1.33	1.74	3.56	8.63	1.58
103	5.96	1.25	1.80	3.58	8.45	1.50
GC17 (VMV, 2070 m depth, ~2700 m away from VMV)						
Date of sampling: 10 June 2003						
12	*	*	*	*	*	*
52	9.74	0.89	1.76	3.39	7.81	1.25
92	18.2	0.65	1.67	3.20	6.95	0.98
132	21.9	0.60	1.67	3.29	7.67	1.24
GC41 (VMV, 2070 m depth, ~400 m away from VMV)						
Date of sampling: 15 June 2004						
13	8.81	0.83	1.59	3.07	7.00	1.13
28	17.4	0.61	1.67	3.29	7.88	1.33
43	26.4	0.50	1.64	3.35	7.95	1.38

† Noble gas concentrations are given in $\text{cm}^3\text{STP g}^{-1}$.

* Omitted due to experimental problems.

5

Exceptional mixing events in Lake Lugano, Switzerland, studied using environmental tracers

This chapter has been submitted for publication in *Limnology and Oceanography* and is currently under review (Holzner et al., 2008a).

Abstract The deep northern basin of Lake Lugano was permanently stratified over the last four decades due to mineralization in response to strong eutrophication. However, two consecutive cold and windy winters in 2004/2005 and 2005/2006 destabilised the water column and led to two exceptionally strong mixing events. The analysis of a time-series of CTD (conductivity, temperature and depth) data from 1995 to 2006 allows the evolution of the water body to be reconstructed that finally made deep convective mixing possible. Over the years 1995–2006, the stability of the water column decreased continuously in winter, reaching a neutral stability at the end of the study period. The Schmidt stability values observed in the winters 2004/2005 and 2005/2006 were virtually zero. Analyses of helium isotopes, tritium, sulfur hexafluoride and chlorofluorocarbons in water samples collected immediately after the two mixing events reveal large changes in the tracer concentration profiles and the apparent water ages in Lake Lugano compared to previous measurement data. The tracer concentration profiles became more homogeneous and approached atmospheric equilibrium concentrations. The tracer data, along with changes observed in the physical parameters of the water column, demonstrate that considerable deep-water renewal and gas exchange with the atmosphere has taken place.

5.1 Introduction

Lake Lugano is located on the border between Switzerland and Italy ($46^{\circ} 00' \text{ N}$, $9^{\circ} 00' \text{ E}$, 271 m above sea level, see Fig. 5.1). An artificial dam that was built on a moraine front in the first half of the 20th century separates the lake into two basins. This study focusses only on the deep northern basin ($z_{\text{max}} = 288 \text{ m}$), which can be treated as an individual lake with the connection to the southern basin acting as an outflow. The limited water throughflow with respect to the volume of the northern basin results in a relatively high hydrological residence time of $\sim 12.3 \text{ yr}$ (Barbieri and Polli, 1992).

During approximately 40 yr, the northern basin of Lake Lugano was meromictic and the water column was stagnant and anoxic below $\sim 100 \text{ m}$ depth (Aeschbach-Hertig et al., 2007; Barbieri and Mosello, 1992). Strong eutrophication during the second half of the 20th century caused chemical stratification of the water column (Wüest et al., 1992a). Environmental measures to reduce external phosphorus loading that were implemented in 1976 helped to bring about a significant improvement in the water quality of the uppermost 100 m (Barbieri and Mosello, 1992; Barbieri and Simona, 2001). In the deep water, however, phosphorus concentrations remained

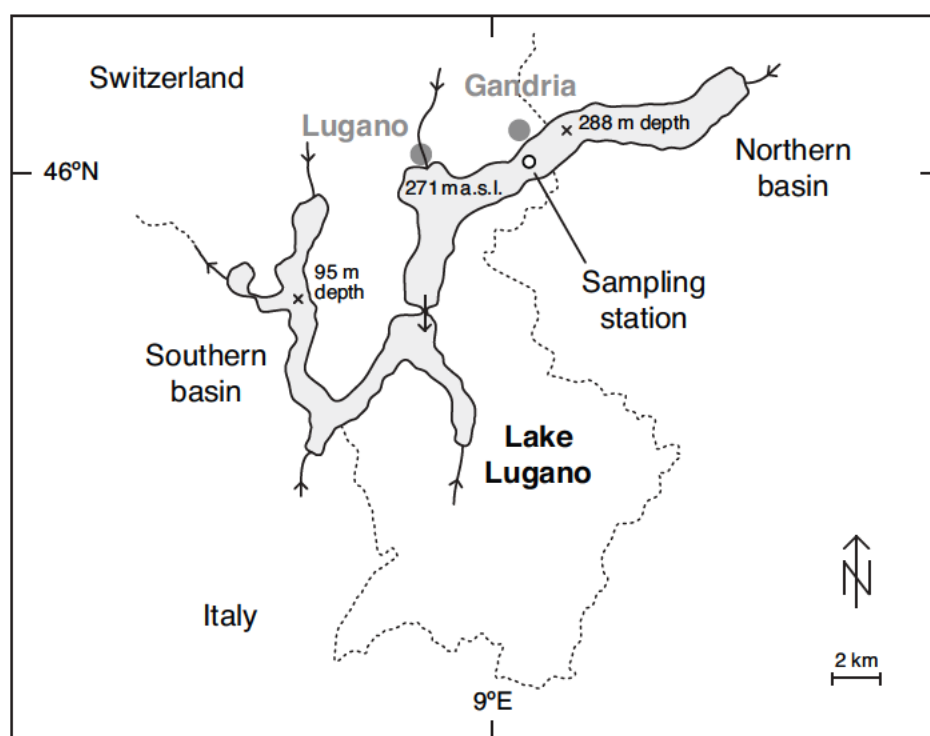


Figure 5.1 Map of Lake Lugano. The sampling station is located in the deepest part of the lake in the northern basin.

high and anoxic conditions continued to prevail. In winter 1998/1999, the first subtle signs of decreasing stability in the water column were observed. During the cold and windy winter of 2004/2005, convective mixing reached the bottom of the lake for the first time in decades. This exceptional mixing event erased the chemical stratification of the northern basin of Lake Lugano and facilitated even stronger deep-water renewal during the following winter of 2005/2006, which was unusually cold. In contrast, during the mild winter of 2006/2007 vertical mixing in the lake reached a maximum depth of only 80 m. Weak water exchange due to mild winters has also been reported in other Swiss lakes (Livingstone, 1997). Given the present warming trend in the climate, weak deep-water renewal due to high winter temperatures might become more frequent, potentially threatening lake water quality.

This study investigates the causes and effects of the recent exceptional mixing events in Lake Lugano. We use data on temperature, electrical conductivity and oxygen, which are recorded every two weeks as a part of the regular water quality monitoring of the lake, to illustrate the processes that led to the “lake overturn” in 2005 and 2006. The progressive vertical mixing is also reflected in the concentration changes of dissolved noble gases, sulfur hexafluoride (SF_6) and chlorofluorocarbons (CFCs), which were measured over a time period of five years.

Aeschbach-Hertig et al. (2007) presented an extensive environmental tracer study of Lake Lugano based on helium (He), tritium (^3H) and SF_6 data that documented the weak vertical mixing that occurred in the northern basin during 1990–2001. CFC data from 2001 and 2006 could not be used to analyze the dynamics of the water column because of CFC-12 contamination and CFC-11 degradation. No significant trend in the rate of deep-water renewal was found. New tracer data from May 2005 and April 2006, however, differ substantially from earlier data, indicating that considerable deep-water renewal and gas exchange has occurred recently.

5.2 Methods

5.2.1 Sampling

In this study, all CTD (conductivity, temperature and depth) profiles and water samples were taken at a station in the deepest part of Lake Lugano near the village of Gandria (Fig. 5.1). Profiles of temperature (T), electrical conductivity (κ_{20}) and oxygen (O_2) are measured every two weeks by the Ufficio Protezione e Depurazione Acque (UPDA) – formerly Laboratorio Study Ambientali (LSA) – and published in periodical reports (e.g. LSA, 1981–2000; UPDA, 2006). The CTD data used for this study cover the years 1995–2006, including unpublished measurements for 2006. CTD profiles were acquired using an Idronaut Ocean Seven 316 multi-parameter

probe (accuracy of $\pm 0.003^\circ\text{C}$ for T, $\pm 3 \mu\text{S cm}^{-1}$ for κ_{20} and $\pm 0.1 \text{ mg l}^{-1}$ for O_2 ; resolution of 0.0007°C for T, $1 \mu\text{S cm}^{-1}$ for κ_{20} and 0.01 mg l^{-1} for O_2).

Water samples for transient tracer analysis were taken using Niskin bottles. Any contact of the water samples with air during sampling was carefully avoided. The water samples for He and ^3H analyses were transferred to copper tubes on the ship, and the tubes were sealed gas-tight using pinch-off clamps. Samples for the analysis of SF_6 and CFC-12 were stored in stainless steel cylinders equipped with two plug valves. The transient tracer profiles sampled on 03 May 2001, 24 May 2005 and 25 April 2006 are discussed in this study (Tab. 5.1).

5.2.2 Transient tracers

Helium concentrations and isotope ratios were measured using noble gas mass spectrometry in the Noble Gas Laboratory at ETH Zürich (Beyerle et al., 2000). Tritium concentrations were determined by the ^3He ingrowth method (Clarke et al., 1976), using a high-sensitivity compressor-source noble gas mass spectrometer (Baur, 1999). Typical measurement precision is $\pm 0.5\%$ for He concentrations, $\pm 1.3\%$ for $^3\text{He}/^4\text{He}$ ratios and $\pm 5.1\%$ for ^3H . The determination of concentrations of ^3H and ^3He in the same water sample allow the apparent ^3H - ^3He water age to be calculated (Torgersen et al., 1977). For this calculation, the measured total ^3He concentration needs to be separated into the tritiogenic $^3\text{He}_{\text{tri}}$ (^3He produced by the decay of ^3H), atmospheric, and terrigenic components (Kipfer et al., 2002). Atmospheric equilibrium concentrations of He in the water column were calculated from the solubilities of Weiss (1971), as recommended by Kipfer et al. (2002), using the prevailing water temperature and salinity and the mean atmospheric pressure observed in Lugano (983.9 hPa; Aeschbach-Hertig et al., 2007). Salinity was calculated from the measured conductivity using a linear conversion of κ_{20} into S ($1 \mu\text{S cm}^{-1} = 0.89 \times 10^{-3} \text{ g kg}^{-1}$; Wüest et al., 1992a).

SF_6 and CFC-12 were analyzed simultaneously on a gas chromatograph equipped with an electron capture detector (GC-ECD) after extraction and purification in a vacuum line. Measurement precision for this method is $\pm 5\%$, as determined from the reproducibility of replicate samples with modern concentrations. Detection limits are $0.07 \text{ fmol kg}^{-1}$ for SF_6 and 2 fmol kg^{-1} for CFC-12. The temporal evolution of the atmospheric SF_6 and CFC-12 concentrations is imprinted in surface waters by gas exchange. As SF_6 and CFC-12 concentrations in lakes are not significantly affected by degradation processes or sources other than the atmosphere, the prevailing concentrations can be interpreted in terms of the time elapsed since a given water element was last in contact with the atmosphere. This time is called the water age (e.g. Hofer et al., 2002). To determine the apparent SF_6 and CFC-12 water ages, the atmospheric mixing ratios that correspond to solubility equilibrium with the observed

water column concentrations were calculated and compared with the temporal evolution of the atmospheric concentrations. Atmospheric equilibrium concentrations in Lake Lugano were determined using the atmospheric histories of Maiss and Breninkmeijer (1998) for SF₆ and of Walker et al. (2000) for CFC-12, and the solubility data of Bullister et al. (2002) for SF₆ and of Warner and Weiss (1985) for CFC-12.

5.3 Results and discussion

5.3.1 Temperature, conductivity and dissolved oxygen

The temporal evolution of temperature (T), electrical conductivity (κ_{20}) and oxygen concentration (O₂) in the water column from 1995 to 2006 is shown in Fig. 5.2. As already documented in our earlier work (Aeschbach-Hertig et al., 2007), the deep water temperature of Lake Lugano gradually increased during the 1990s. A first profound change in the temperature structure occurred in 1999, when winter mixing homogenized the water temperatures from the surface to 250 m depth. In response to this event, a temporary increase in the O₂ concentrations in the uppermost 100 m was detected, but the conductivity profiles, and thus the chemical stratification of the water column, were hardly affected. However, the cooling in 1999 seems to have been of great importance for the evolution of the mixing dynamics in the following years. After 1999, vertical homogenization of the water temperatures occurred almost every winter, which gradually reduced the strength of the stratification in the entire lake (see below).

Strong changes in both temperature and electrical conductivity occurred during the winters of 2004/2005 and 2005/2006, resulting in a persistent alteration of the water column stratification. A distinct mixing event at the beginning of March 2005 led to a cooling of the deep water by $\sim 0.3^\circ\text{C}$. Also, the distribution of dissolved solids in the water column changed dramatically. Before 2005, a strong gradient in electrical conductivity, and therefore in the concentration of dissolved solids, was present and stabilized the deep water body. The conductivity difference between 50 m and 250 m depth was $20\text{--}30\ \mu\text{S cm}^{-1}$. In March 2005, the electrical conductivity in the entire deep water mass below 50 m depth was set to $\sim 240\ \mu\text{S cm}^{-1}$ and remained virtually constant throughout 2005 and 2006. At the same time, traces of O₂ occurred at the bottom of the lake for the first time during the last ~ 40 years.

A subsequent mixing event occurred at the end of January 2006 which further cooled the deep water by an additional $\sim 0.2^\circ\text{C}$ and resulted in nearly uniform oxygen concentrations of $1.5\text{--}2.0\ \text{mg O}_2/\text{l}$ in the entire water column. The sudden drop in O₂ concentration in the surface water threatened sensitive fish species. Several dead fish were discovered in Lake Lugano shortly after the mixing event (CIPAIS, 2006).

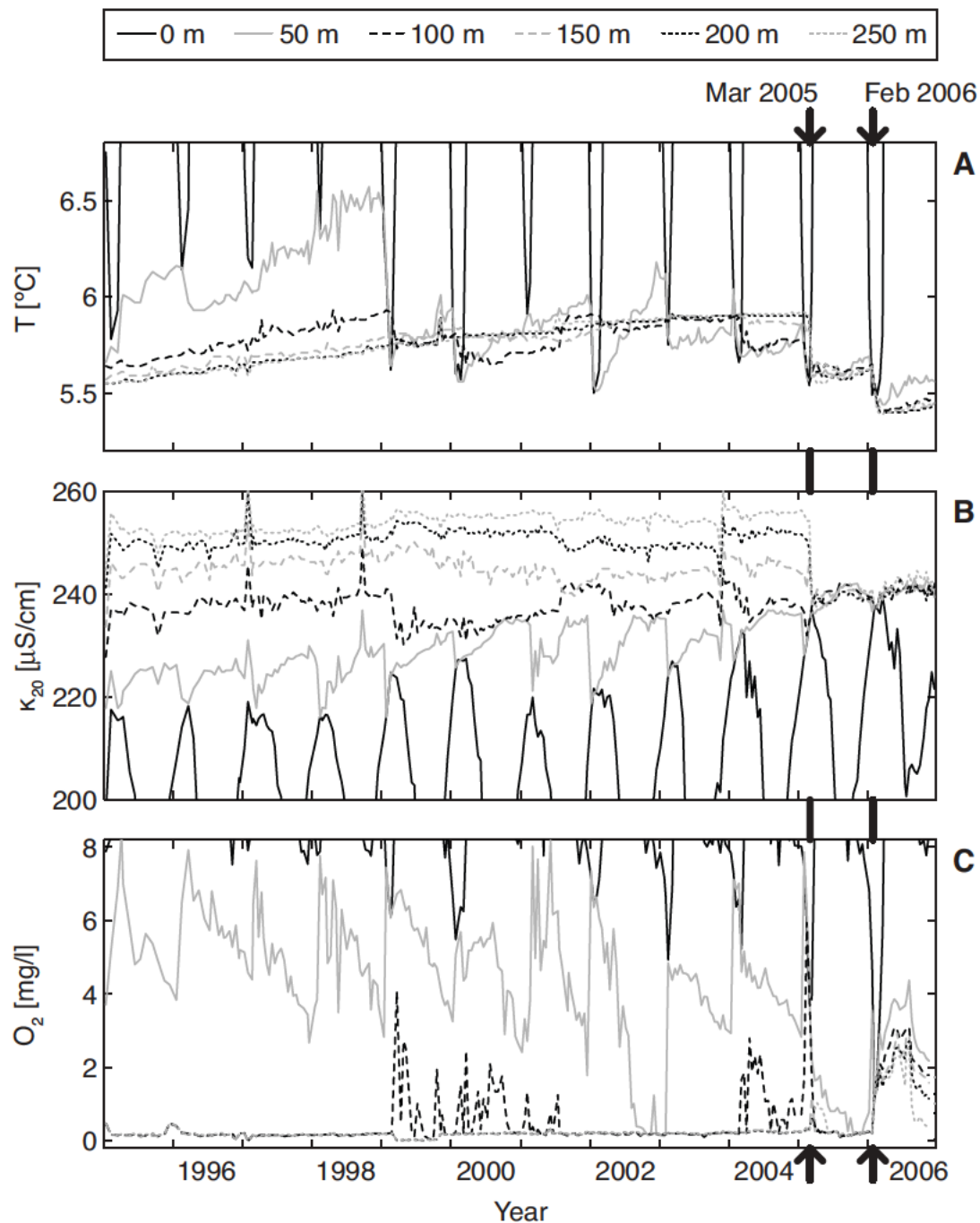


Figure 5.2 Temporal evolution of temperature T (A), electrical conductivity κ_{20} (B) and oxygen concentration O_2 (C) at selected depths. The dates of the two recent mixing events in 2005 and 2006 are shown as vertical arrows. Mixing in 1999 homogenized the water temperatures from the surface to 250 m depth and led to a temporary increase in the O_2 concentration at 100 m depth. The mixing events in 2005 and 2006 resulted in a decrease in the deep water temperature. Traces of O_2 occurred at the bottom of the lake for the first time in ~ 40 years. The electrical conductivities κ_{20} below 50 m converged during the 2005 mixing event and have remained virtually constant since then.

In the deep water, the non-zero O_2 concentrations prevailed until autumn, when the deepest layers turned anoxic again.

T and κ_{20} in the water column of Lake Lugano evolved from 1995 to 2005 in a way that reduced the stratification and gradually increased the probability of mixing. An increase in the deep water temperature during the 1990s due to geothermal heating and turbulent diffusion has already been identified by Aeschbach-Hertig et al. (2007). Apart from the cooling of the water column in 1999, which mainly affected the depth interval of 50–150 m, the increase in the deep-water temperature continued until early 2005. Additionally, κ_{20} above 100 m increased slightly after 1999, indicating higher exchange between deep and shallow water which weakened the chemical stratification. Summarizing, various events between 1995 and 2005 were responsible for reducing the vertical T and κ_{20} gradients to a point where the two consecutive cold and windy winters in 2004/2005 and 2005/2006 (CIP AIS, 2005, 2006) were finally able to initiate large-scale mixing events in Lake Lugano.

5.3.2 Density and stability

The time-series of water temperature and conductivity data were used to determine the density of the lake water and the stability of the water column during the last 11 years (Fig. 5.3). Prior to the recent mixing events, the water column of Lake Lugano was characterized by a strong density gradient (Fig. 5.3A). In February 1999 the density difference was reduced due to the cooling of the entire water column, which reached a virtually homothermal state. However, the water column remained stratified because of the large conductivity gradient. The density gradient below 50 m depth disappeared completely after the mixing event in March 2005. In February 2006, the density of the deep water increased slightly in response to further cooling of the deep water.

To assess the evolution of the density stratification of the entire water column, we computed the Schmidt stability ST (Idso, 1973; Schmidt, 1928) for each CTD profile (Fig. 5.3B). This quantity is defined as the work which would hypothetically be necessary to transform the observed density stratification into a vertically homogeneous density distribution by adiabatic mixing. A Schmidt stability value of zero means that the water column is not stratified and hence homogeneous, allowing vertical mixing to be triggered by a minimal input of turbulent kinetic energy. ST is computed as follows:

$$ST = \frac{g}{A_0} \int_{z=0}^{z_{max}} [z_V - z] [\rho_h - \rho(z)] A(z) dz \quad [J m^{-2}] \quad (5.1)$$

where g is the acceleration of gravity (9.81 m s^{-1}), A_0 is the surface area of Lake Lugano ($2.75 \times 10^7 \text{ m}^2$), z_{max} is the maximum depth of the lake (288 m), z_V is the depth of the center of volume of the lake (171 m), ρ_h is the hypothetical density of

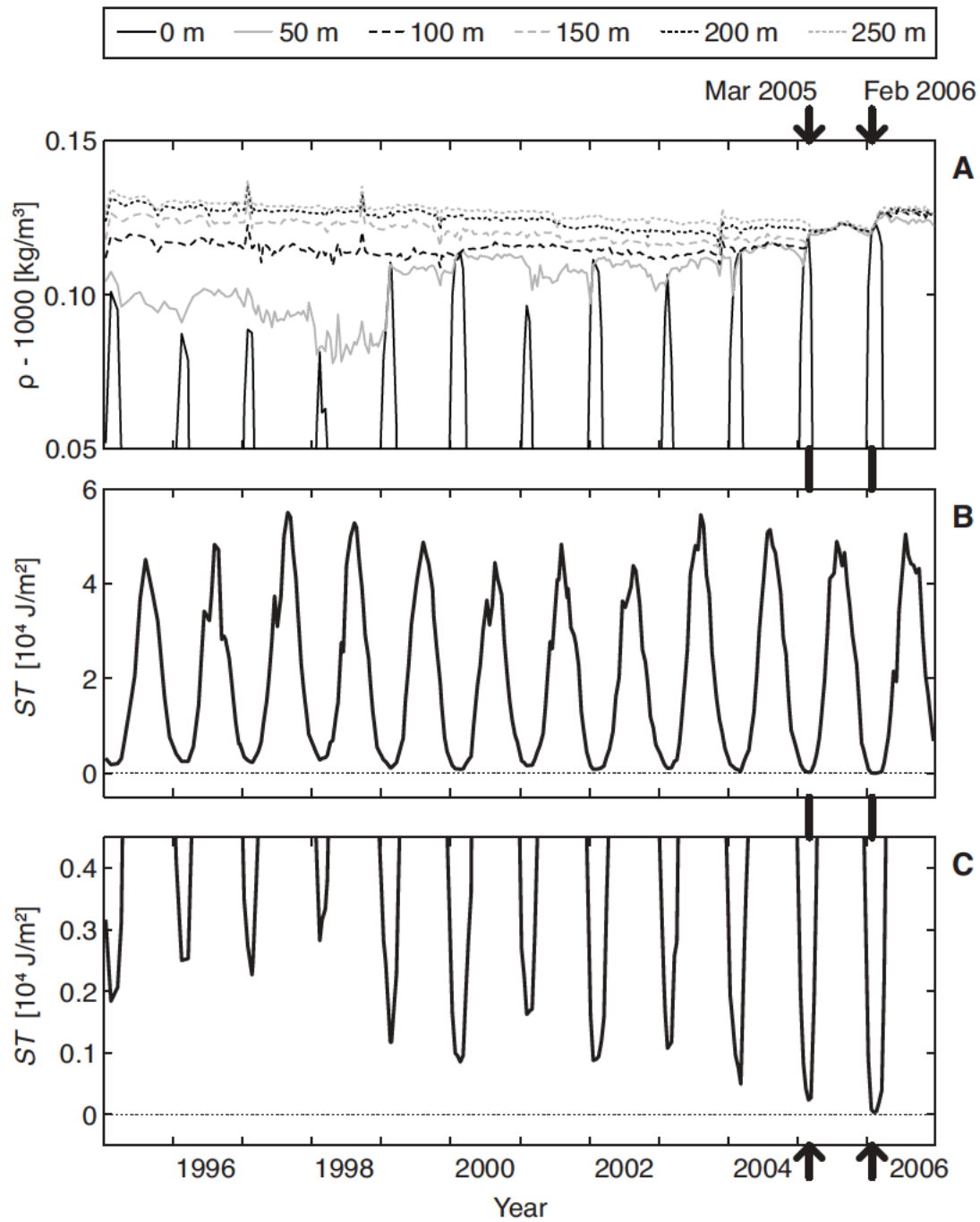


Figure 5.3 Temporal evolution of the water density ρ at selected depths (A), and of the Schmidt stability ST (B). (C) shows an enlargement of the Schmidt stability curve for $ST < 4500 \text{ J m}^{-2}$. At $ST = 0 \text{ J m}^{-2}$, the water column is not stratified and a minimal input of turbulent kinetic energy can trigger vertical mixing. The dates of the two recent mixing events are shown as vertical arrows.

the homogeneous lake after mixing, $\rho(z)$ is the observed density at depth z , and $A(z)$ is the isobath area at depth z . The Schmidt stability in Lake Lugano shows an annual cycle with the lowest values occurring in winter, when vertical density gradients are low due to seasonal cooling at the surface. Since 1995, the minimum Schmidt stabilities observed in winter (Fig. 5.3C) decreased substantially. A remarkable drop in the minimum Schmidt stability took place in February 1999, following the change in water temperatures shown in Fig. 5.2A. After 1999, the temperatures of the surface and deep water converged in winter, so temperature gradients did not stabilize the water column. However, the density stratification due to the concentration gradient of dissolved solids (reflected in conductivity) was present throughout that time and suppressed large-scale vertical water exchange. The ongoing warming of the deep water and a slight increase in the conductivity of the surface water (Fig. 5.2A–B) after 1999 gradually reduced the stratification in winter until the Schmidt stability approached zero during the winters of 2004/2005 and 2005/2006, and seasonal mixing homogenized the water column.

5.3.3 Transient tracer concentrations

Fig. 5.4 shows the concentrations of ^3H , ^3He and ^4He in the water column of Lake Lugano during spring 2001, 2005 and 2006. The corresponding concentration profiles of SF_6 and CFC-12 are presented in Fig. 5.5. The tracer data are listed in Tab. 5.1.

In 2001, the ^3H concentrations increased continuously from the surface to the deep water. This profile reflects the high ^3H input to the lake in the 1960s and 1970s

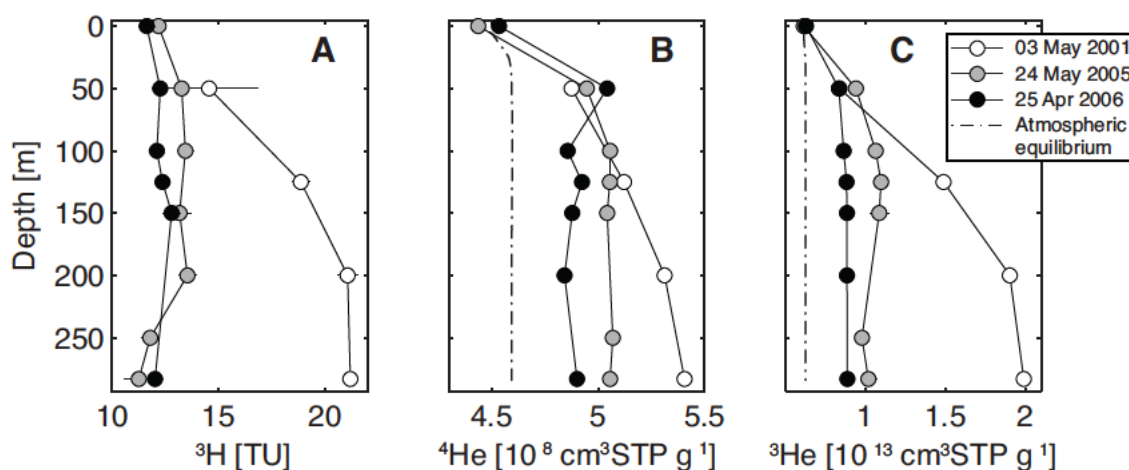


Figure 5.4 Depth profiles of ^3H (A), ^3He (B) and ^4He (C) concentrations. Data of 2001 from Aeschbach-Hertig et al. (2007). The atmospheric equilibrium concentrations for ^3He and ^4He are shown as broken lines.

Table 5.1 Concentrations of ^3H , He isotopes, SF_6 , CFC-12, apparent SF_6 ages and ^3H - ^3He ages in Lake Lugano. Data of 2001 from Aeschbach-Hertig et al. (2007).

Depth [m]	^3H [TU]	^4He [$10^{-8} \text{ cm}^3 \text{STP g}^{-1}$]	$^3\text{He}/^4\text{He}$ [10^{-6}]	SF_6 [fmol kg^{-1}]	CFC-12 [pmol kg^{-1}]	^3H - ^3He age [yr]	SF_6 age [yr]
Date of sampling: 03 May 2001							
0	–	–	–	2.02 ± 0.10	4.18 ± 0.21	–	<0
25	–	–	–	1.73 ± 0.09	5.22 ± 0.26	–	4.5 ± 0.8
50	14.6 ± 2.3	4.88 ± 0.01	1.72 ± 0.01	1.84 ± 0.09	5.62 ± 0.28	8.2 ± 1.0	4.0 ± 0.8
75	–	–	–	1.66 ± 0.08	6.08 ± 0.30	–	5.5 ± 0.7
100	–	–	–	1.26 ± 0.06	6.49 ± 0.32	–	9.3 ± 0.6
125	18.9 ± 0.4	5.12 ± 0.02	2.91 ± 0.01	1.33 ± 0.07	6.31 ± 0.32	18.5 ± 0.3	8.6 ± 0.7
150	–	–	–	1.16 ± 0.06	7.15 ± 0.36	–	10.3 ± 0.6
175	–	–	–	1.23 ± 0.06	6.81 ± 0.34	–	9.6 ± 0.6
200	21.0 ± 0.5	5.31 ± 0.01	3.58 ± 0.01	1.08 ± 0.05	7.00 ± 0.35	22.0 ± 0.3	11.1 ± 0.6
225	–	–	–	1.14 ± 0.06	6.70 ± 0.33	–	10.6 ± 0.6
250	–	–	–	0.99 ± 0.05	7.06 ± 0.35	–	12.3 ± 0.6
283	21.2 ± 0.3	5.41 ± 0.02	3.68 ± 0.01	0.94 ± 0.05	6.70 ± 0.33	22.7 ± 0.2	12.8 ± 0.6
Date of sampling: 24 May 2005							
0	12.2 ± 0.3	4.44 ± 0.03	1.39 ± 0.01	1.93 ± 0.10	3.15 ± 0.16	1.0 ± 0.3	<0
25	–	–	–	2.26 ± 0.11	4.87 ± 0.24	–	3.9 ± 0.9
50	13.3 ± 0.6	4.95 ± 0.03	1.90 ± 0.10	2.19 ± 0.11	5.23 ± 0.26	11.9 ± 1.4	5.5 ± 0.8
75	–	–	–	2.10 ± 0.10	5.23 ± 0.26	–	6.1 ± 0.8
100	13.4 ± 0.4	5.06 ± 0.03	2.10 ± 0.02	2.03 ± 0.10	5.36 ± 0.27	14.9 ± 0.3	6.6 ± 0.8
125	*	5.06 ± 0.03	2.17 ± 0.02	2.28 ± 0.11	5.60 ± 0.28	–	4.7 ± 0.8
150	13.2 ± 0.5	5.04 ± 0.03	2.16 ± 0.11	2.06 ± 0.10	5.52 ± 0.28	15.6 ± 1.3	6.4 ± 0.8
175	–	–	–	2.12 ± 0.11	5.44 ± 0.27	–	5.9 ± 0.8
200	13.5 ± 0.4	*	*	1.93 ± 0.10	5.18 ± 0.26	–	7.4 ± 0.8
225	–	–	–	2.14 ± 0.11	5.39 ± 0.27	–	5.8 ± 0.8
250	11.8 ± 0.4	5.07 ± 0.03	1.93 ± 0.01	2.21 ± 0.11	5.06 ± 0.25	14.0 ± 0.4	5.3 ± 0.8
283	11.3 ± 0.7	5.06 ± 0.03	2.01 ± 0.10	2.18 ± 0.11	5.42 ± 0.27	15.6 ± 1.5	5.6 ± 0.8
Date of sampling: 25 Apr 2006							
0	11.6 ± 0.4	4.54 ± 0.02	1.39 ± 0.01	2.36 ± 0.12	3.37 ± 0.17	1.4 ± 0.3	<0
50	12.3 ± 0.4	5.04 ± 0.03	1.65 ± 0.01	2.46 ± 0.12	4.83 ± 0.24	9.2 ± 0.3	4.5 ± 0.9
100	12.1 ± 0.3	4.86 ± 0.03	1.78 ± 0.01	2.00 ± 0.10	4.79 ± 0.24	10.3 ± 0.3	7.9 ± 0.8
125	12.4 ± 0.3	4.92 ± 0.03	1.79 ± 0.01	–	–	10.8 ± 0.3	–
150	12.8 ± 0.4	4.88 ± 0.03	1.81 ± 0.01	2.21 ± 0.11	4.60 ± 0.23	10.6 ± 0.3	6.4 ± 0.8
200	*	4.84 ± 0.03	1.83 ± 0.01	2.28 ± 0.11	4.93 ± 0.25	–	5.9 ± 0.8
250	*	*	*	2.25 ± 0.11	4.81 ± 0.24	–	6.1 ± 0.8
283	12.0 ± 0.4	4.90 ± 0.03	1.81 ± 0.01	2.07 ± 0.10	4.94 ± 0.25	11.1 ± 0.4	7.5 ± 0.8

– Not analyzed.

* Lost as a result of experimental problems.

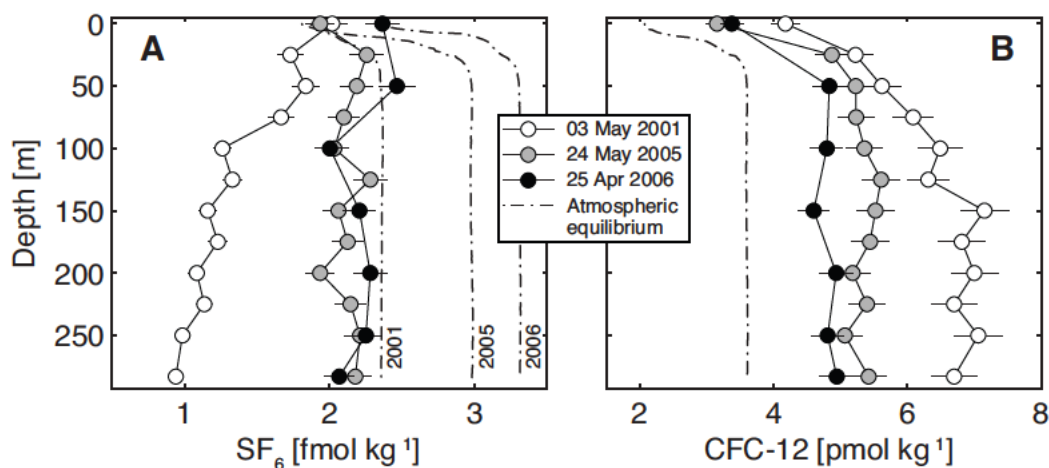


Figure 5.5 Depth profiles of SF_6 (A) and CFC-12 (B) concentrations. Data of 2001 from Aeschbach-Hertig et al. (2007). The atmospheric equilibrium concentrations for SF_6 and CFC-12 are shown as broken lines. Note the transient evolution of the SF_6 equilibrium concentrations caused by the continuous increase in atmospheric SF_6 concentrations.

from rivers and precipitation as a result of thermonuclear bomb tests in the atmosphere. As Lake Lugano became permanently stratified due to eutrophication at the time of high ^3H input, high concentrations of ^3H were stored in the isolated deep water and decayed continuously to ^3He . As a consequence, the tritiogenic ^3He that was generated accumulated in the stagnant deep water. In the surface water, the ^3H concentrations were also reduced by mixing with new inflow water that contained lower ^3H concentrations, and by exchange with atmospheric water vapor. The ^3H concentration profiles observed in 2005 and 2006 do not show substantial variation with depth. In the deep water, the concentrations are considerably lower than in 2001. The maximum ^3H concentrations near the bottom decreased from ~ 21 TU (1 TU = 1 tritium unit = 1 ^3H atom per 10^{18} ^1H atoms) in 2001 to 11–12 TU in 2005 and 2006. Note that the ^3H concentrations measured in 2005 and 2006 are significantly below the concentrations that would be expected if radioactive decay were the only process to remove ^3H from the deep water (16–17 TU). Therefore, the exchange with ^3H -poor surface water during the mixing events significantly reduced the observed ^3H concentrations in the deep water. During the 1990s, the ^3H concentrations in the deep water of Lake Lugano were already decreasing faster than expected due to the process of radioactive decay alone (Aeschbach-Hertig et al., 2007). An exponential fit to the data from 1990 to 2001 yields a decay rate of 0.077 yr^{-1} , which is higher than the radioactive decay rate of ^3H (0.056 yr^{-1}). However, this rate is considerably lower than the rate of 0.133 yr^{-1} that was determined by fitting the data from 2001 to 2006, during which the strong mixing events occurred. This implies that the perma-

nently stratified deep water of Lake Lugano was not completely isolated before 2005, and that turbulent mixing caused a significant deep-water renewal. But this turbulent water exchange rate was considerably smaller than the advective deep-water renewal rate in 2005 and 2006.

In all profiles, ^3He and ^4He in the deep water are supersaturated with respect to gas-partitioning equilibrium with the atmosphere. The He excess is caused by the accumulation of tritiogenic ^3He (produced by ^3H decay) and terrigenous ^4He (emanating from the solid Earth through the sediments) in the stagnant deep water body. Our earlier work (Aeschbach-Hertig et al., 2007) documented a continuous increase in the ^4He concentrations of the deep water of Lake Lugano during the 1990s and a slight decrease in the ^3He concentrations since 1992. In contrast, the helium concentrations below ~ 50 m decreased strongly between 2001 and 2005 and between 2005 and 2006. These changes indicate that the mixing events transported part of the excess He from the deep water to the surface, where it escaped to the atmosphere. A mass balance of excess He stored in the northern basin of Lake Lugano was calculated from interpolated profiles by integrating the product of the excess concentration $C^{\text{ex}}(z)$ with the volume $V(z)$ over depth z . The excess concentration is given as $C^{\text{ex}}(z) = C(z) - C^{\text{eq}}(z)$, where $C(z)$ is the observed noble gas concentration and $C^{\text{eq}}(z)$ is the atmospheric equilibrium concentration at depth z . These calculations allowed us to estimate the mass of excess He in the lake from each concentration profile; e.g. ~ 40 mg excess ^3He and ~ 4 kg excess ^4He in 2001. In comparison, the total dissolved masses of He in 2001 were ~ 80 mg ^3He and ~ 40 kg ^4He . The mass balance shows also that $\sim 48\%$ of the excess ^3He and $\sim 16\%$ of the excess ^4He degassed to the atmosphere between 2001 and 2005. From 2005 to 2006, the remaining excess of ^3He and ^4He decreased by a further $\sim 39\%$ and $\sim 23\%$, respectively. The relative loss of ^3He is much higher than the loss of ^4He because in 2001 ^3He was much more highly supersaturated than ^4He .

The SF_6 concentrations observed in 2001 decreased from the surface to the bottom of the lake due to gas exchange with the atmosphere and in response to the continuously increasing atmospheric SF_6 partial pressure (Maiss and Brenninkmeijer, 1998), and due to the limited vertical water exchange in Lake Lugano. In contrast, the SF_6 concentrations observed in 2005 and 2006 were nearly constant throughout the water column, again indicating extensive mixing and homogenization of the water column. The mixing events in March 2005 and February 2006 led to an increase in the SF_6 concentrations in the entire lake due to gas exchange with the increasingly “ SF_6 -rich” atmosphere. However, the SF_6 concentrations in the water column remained below the atmospheric equilibrium concentration, especially in the colder deep water, because the mixing events were too short to allow gas-partitioning equilibrium to be attained throughout the lake.

The deep water of Lake Lugano has been supersaturated with respect to CFC-12 for several years, presumably due to contamination (Aeschbach-Hertig et al., 2007). In 2001, the excess of dissolved CFC-12 in the lake water body was ~ 1.5 kg. This quantity of CFC-12 may have been introduced into Lake Lugano by accident or due to inappropriate disposal, as CFC-12 was widely used as cooling fluid in refrigerators and air conditioners before it was banned by the Montreal Protocol (Ozone Secretariat, 2000). The reduction in CFC-12 concentrations that occurred from 2001 to 2006 are the result of the increased upward transport of deep water rich in CFC-12, and the subsequent loss of CFC-12 to the atmosphere by gas exchange at the lake surface.

5.3.4 Apparent water ages

The apparent water ages derived from the ^3H , ^3He and SF_6 data for 2001, 2005 and 2006 are shown in Fig. 5.6 and Tab. 5.1. CFC-12 cannot be used to determine water ages in Lake Lugano, because the observed concentrations exceed the atmospheric equilibrium concentration. In 2001, both the ages calculated from ^3H - ^3He and from SF_6 increased considerably with depth, which indicates that vertical mixing in the water column was slow. However, the mixing events led to a distinct decrease in the apparent water ages in the deep water and to a reduction in the age difference between surface and deep water. The apparent ^3H - ^3He age close to the bottom of the lake decreased from ~ 23 yr in 2001 to ~ 16 yr in 2005 and ~ 11 yr in 2006. The apparent SF_6 age dropped from ~ 13 yr in 2001 to 6–7 yr in 2005 and 2006. Hence

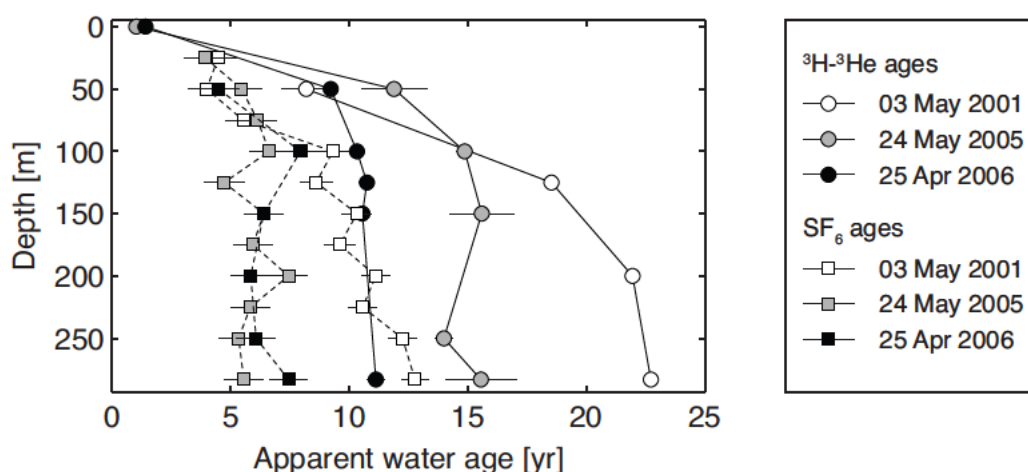


Figure 5.6 Depth profiles of the apparent SF_6 and ^3H - ^3He ages. Apparent tracer ages of 2001 from Aeschbach-Hertig et al. (2007).

both the ^3H - ^3He age and the SF_6 age were reduced by $\sim 50\%$, indicating considerable deep-water renewal.

SF_6 ages are systematically lower than ^3H - ^3He ages over the entire study period. The difference between the apparent water ages determined using different tracers is caused by the non-linear effect that mixing has on water age (Aeschbach-Hertig et al., 2007; Hofer et al., 2002; Jenkins and Clarke, 1976; Kipfer et al., 2002; Schlosser and Winckler, 2002; Vollmer et al., 2002). The mixture of two water volumes with different ages should ideally have the volume-weighted mean age; i.e., the “true” water age. However, mixing generates water containing volume-weighted mean tracer concentrations. As the tracer ages are non-linear functions of the tracer concentrations, the tracer age of the mixed water may deviate significantly from the “true” water age. The effect of mixing on tracer age depends on the tracer used for dating, the date of sampling, and the water age of the mixed water bodies. Aeschbach-Hertig et al. (2007) simulated the evolution of the apparent tracer ages in Lake Lugano over the last century using a simple mixed-reactor model. This analysis showed that SF_6 ages appear to underestimate the “true” water age, whereas ^3H - ^3He ages seem to overestimate it. Therefore, the “true” water age in Lake Lugano lies between the apparent SF_6 and ^3H - ^3He ages, and is not well constrained given the large differences in tracer ages. For this reason, to estimate the vertical water exchange that occurred during the recent mixing events we use the observed tracer concentrations rather than the water ages.

5.3.5 Quantification of deep-water renewal

Based on the mass balance of ^3He below 100 m depth, Aeschbach-Hertig et al. (2007) determined that between 1990 and 2001 about 8% of the deep water was exchanged with surface water annually. This relatively small renewal rate reflects the effect of the permanent stratification that prevailed before 2005, which limited vertical water exchange. Using the same ^3He mass balance approach for the time intervals 2001–2005 and 2005–2006 yields deep-water renewal rates of $\sim 75\%$ per year and $\sim 270\%$ per year, respectively. As expected, during these periods the deep-water renewal rates are considerably higher than those observed before 2001. However, the resulting rates cannot be directly related to the advective water exchange during the actual mixing events, because the approach used here yields mean exchange rates for the entire periods between successive samplings. As the time periods analyzed are much longer than the observed mixing events, the resulting rates appear considerably smaller than the effective water turnover during the mixing events in 2005 and 2006.

To better constrain the deep-water renewal that occurred during the mixing events in 2005 and 2006, we developed a dynamic three-box model for the northern basin of the lake (Fig. 5.7). The model simulates the temporal evolution of ^3H , ^3He , ^4He and

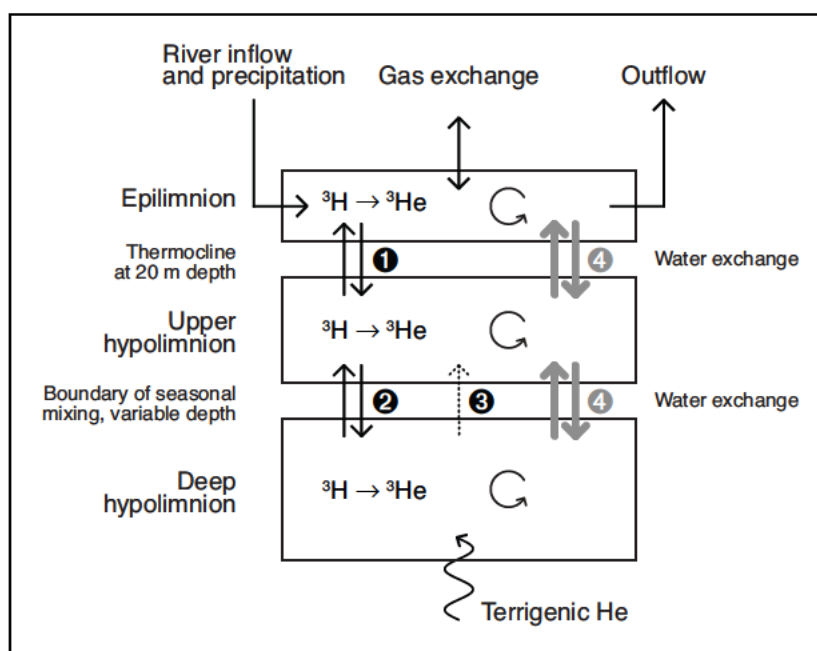


Figure 5.7 Illustration of the 3-box model of Lake Lugano. The vertical water exchange flows are labeled as follows: ❶ turbulent water exchange across the thermocline; ❷ weak renewal of the deep hypolimnion water (8% per year prior to 2005); ❸ water flow that compensates for the deepening of the boundary between the deep hypolimnion and the upper hypolimnion boxes; ❹ large vertical water exchange during the mixing events in 2005 and 2006.

SF_6 concentrations in the lake from 1990 to 2007, taking into account the processes of gas exchange at the water surface, tracer gain or loss due to water inflow and outflow, vertical water transport, ^3He production by the radioactive decay of ^3H , and terrigenous He input. The model was set up and numerically integrated using the simulation software AQUASIM (Reichert, 1994). The basin of Lake Lugano is modeled as three horizontal layers (epilimnion, upper hypolimnion and deep hypolimnion) representing zones of different mixing intensity. The epilimnion is assumed to be well-mixed by wind and undergoes gas exchange with the atmosphere. The upper hypolimnion undergoes seasonal mixing, while the deep hypolimnion corresponds to the deep water body that was permanently stratified before 2005. The three layers are modeled as mixed reactors, connected by water flows that represent the vertical transport processes.

Our main interest is focused on vertical transport during the mixing events in 2005 and 2006, expressed as water flow between the three boxes, which occurs only during the observed mixing periods. Apart from this exceptional water exchange, the model also accounts for the turbulent exchange across the thermocline described by a constant exchange rate between the epilimnion and the upper hypolimnion (of 60%

of the upper hypolimnion volume per year; Dzambas and Ulrich, 1994). Correspondingly, prior to 2005, for the deep hypolimnion a water renewal rate of 8% per year was assumed (Aeschbach-Hertig et al., 2007). The duration of the mixing events, the depth of the thermocline (considered to be the boundary between epilimnion and hypolimnion), and the depth of the boundary between the upper hypolimnion and the deep hypolimnion were estimated from the time-series of CTD profiles from 1995 to 2005. We assumed that the epilimnion corresponds to the surface layer that becomes warmer than 10°C in summer. Applying this criterion, the thermocline depth remained virtually constant at about 20 m, the value used in the model. The maximum depth of seasonal mixing, i.e. the boundary between the upper hypolimnion and the deep hypolimnion, is assumed to correspond to the maximum depth at which oxygen is detected during regular lake monitoring in a particular year. This depth gradually increased from 85 m in 1995 to 110 m in 2004. In the model, the depth of the boundary increases with time at a constant rate. It results in a corresponding upward net water flow from the deep hypolimnion to the upper hypolimnion box.

We used the tracer data given in Tab. 5.1 and earlier data from Aeschbach-Hertig et al. (2007) to constrain the model parameters. For each box, we calculated volume-weighted mean concentrations of the tracers from interpolated profiles. The 1990 data were used as initial conditions. The inverse fitting tools of AQUASIM were applied to tune the gas exchange velocities of He and SF₆ and to estimate the vertical water transport during the mixing events in 2005 and 2006.

The modeled histories of ³H and ³He are in reasonably good agreement with the tracer measurements (Fig. 5.8). In particular, the dramatic changes in the tracer concentrations during the mixing events in 2005 and 2006 are adequately reproduced. For ⁴He and SF₆ the model results (not shown) deviate from the observations, because the input of these tracers into Lake Lugano cannot be adequately reconstructed. Aeschbach-Hertig et al. (2007) propose that elevated SF₆ concentrations in the local air might explain the slight supersaturation with respect to SF₆ found for the surface sample in 2001. However, the magnitude and temporal evolution of the proposed atmospheric SF₆ excess remains unclear and cannot be appropriately modeled. The terrigenous input of ⁴He into lakes depends on the underlying geological structures and may be spatially non-uniform (Ballentine and Burnard, 2002; Brennwald, 2004; Mamyrin and Tolstikhin, 1984; Tomonaga et al., 2007). A clear allocation of the terrigenous ⁴He input to each of the three boxes of the model is therefore not possible, leading to uncertainties in the modeled ⁴He evolution.

The total water volumes exchanged during the mixing events and the corresponding gas exchange velocities for He and SF₆ are summarized in Tab. 5.2. Note that the mixing events of 2005 and 2006 are characterized by exchanged water volumes that exceed the volume of the deep hypolimnion by factors of about 2 and 7, respectively. As expected, these rates are considerably higher than the ones determined using a

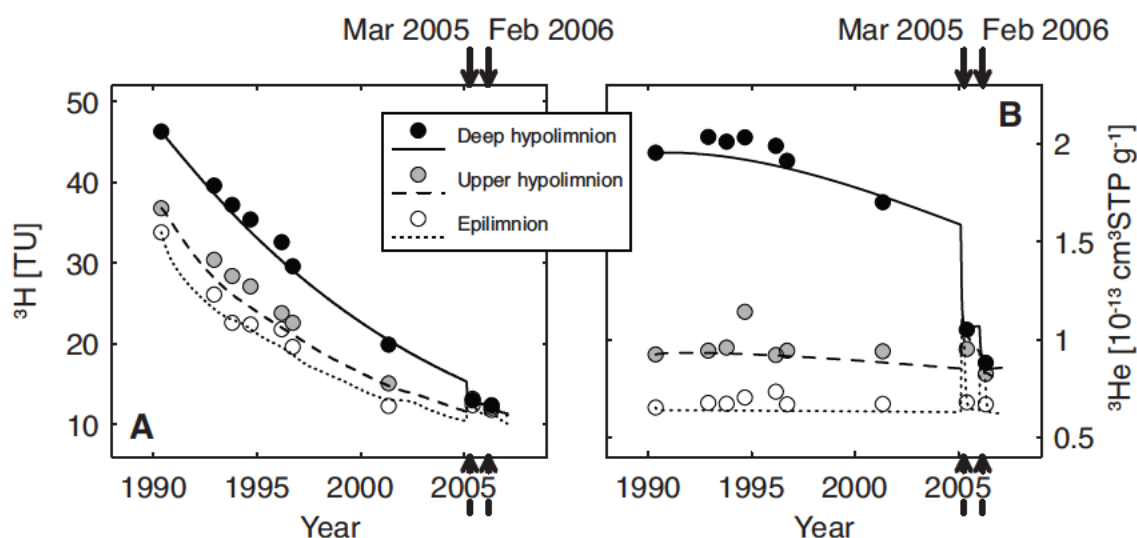


Figure 5.8 Results of the 3-box model calculations. (A) Measured and modeled ^3He concentrations. (B) Measured and modeled ^3H concentrations. Tracer data are from Aeschbach-Hertig et al. (2007) and this study. The dates of the two recent mixing events are shown as vertical arrows.

simple mass balance of ^3He for the deep water (see above). The fairly large uncertainties are due to the fact that the tracer concentration gradients below 50 m depth become virtually zero during the mixing events, making the outcome of the model only weakly dependent on the vertical water exchange.

The estimated gas exchange velocities (Tab. 5.2) are about 30–40% higher than the theoretical velocities calculated from the mean wind speed measured at the meteorological station in Lugano and the mean annual surface water temperature of the lake. These differences are likely due to the fact that the effective wind speeds on the lake are significantly higher than those measured in Lugano. Furthermore, gas exchange velocities calculated using the mean wind speed tend to underestimate the actual exchange due to the non-linear effect of wind-speed variability on gas transfer (Livingstone and Imboden, 1993). We used the estimated gas exchange velocity for SF_6 to calculate the corresponding velocity for O_2 . Combined with the T and O_2 data from the CTD measurements (see Fig. 5.2), our estimate of the O_2 gas exchange velocity can be used to calculate the flux of O_2 into the northern basin of Lake Lugano. For instance, during the second mixing event in February 2006, which lasted ~ 60 days, about 80 tonnes of O_2 per day were injected into the lake. This input corresponds to a concentration increase of only $\sim 1 \text{ mg l}^{-1} \text{ O}_2$ for the entire lake volume. Consequently, the O_2 concentrations in the entire water column remained low ($< 5 \text{ mg l}^{-1}$) until the onset of stratification in April 2006, due to the continuing

Table 5.2 Results of the three-box model. The total volumes of water exchanged and the gas exchange velocities were determined using inverse fitting methods.

Deep-water renewal		
Year	V_{ex} [m ³]	V_{ex}/V_d
2005	$(6 \pm 4) \times 10^9$	2.3 ± 1.4
2006	$(17 \pm 11) \times 10^9$	6.8 ± 4.3
V_{ex} : water exchanged during the mixing events, estimated using inverse fitting.		
V_d : mean volume of the deep hypolimnion box (2.5×10^9 m ³).		
Gas exchange velocities v_i [m d ⁻¹]		
Gas i	modeled *	theoretical **
SF ₆	0.23	0.16
³ He	0.84	0.64
⁴ He	0.76	0.58
O ₂	0.32	0.24

* The gas exchange velocity for SF₆ is estimated in the model using inverse fitting. The other velocities are calculated using $v_i/v_j = (D_i/D_j)^{2/3}$ (Schwarzenbach et al., 2003). Estimated errors in the gas exchange velocities are $\sim 10\%$.

** Theoretical gas exchange velocities v_i are calculated according to Wanninkhof (1992) for the mean wind speed measured at the MeteoSwiss station in Lugano in the period from 1971 to 2000 (1.75 m s^{-1}) and for the mean annual surface water temperature from the CTD measurements (14°C).

mixing and fast O₂ consumption by the large reservoir of reducing substances in the deep water (e.g. Barbieri and Mosello, 1992; UPDA, 2006).

5.4 Conclusions

The transient tracer profiles and the time series of CTD data from Lake Lugano record substantial changes in the physical and chemical properties of the water column in response to two strong convective mixing events during the winters of 2004/2005 and 2005/2006. Before 2005, the deep water of Lake Lugano had been permanently stratified for ~ 40 yr and the physical and chemical state of this water body had undergone only minor changes due to limited turbulent transport. Turbulent diffusion and geothermal heating gradually warmed the deep water over the last decade and reduced the conductivity gradient in the water column slightly. This evolution reduced the strength of the stratification to a point where a large-scale convective mixing event (“overturn”) of the entire water column was able to take place. The onset of the recent mixing events in Lake Lugano was favored by exceptionally cold and windy

conditions that had occurred during the preceding winters. The considerable deep-water renewal (a vertical water exchange of more than the total deep water volume) and extensive gas exchange that occurred in 2005 and 2006 is clearly documented by transient tracer concentrations, obtained immediately after the two mixing events, which differ substantially from earlier data.

The environmental tracer data collected for this work, along with previously published data, form a 15-yr time series of tracer measurements in the northern basin of Lake Lugano. These data provide a record of the mixing dynamics of the lake from 1990–2006. During this period, the deep-water renewal rates in the lake increased by a factor greater than 10 due to the two strong winter mixing events. Our work demonstrates that long time-series of environmental tracer data are useful for analyzing transitions in the mixing regimes of lakes in response to environmental and climatic changes. For this purpose, the time period covered by a tracer study needs to be long enough to cover typical time scales of the mixing dynamics that are representative of the particular lake concerned.

Compared to dissolved oxygen concentrations or to the temperature and conductivity of the lake water, the effects of mixing on the environmental tracer concentrations (noble gases, SF₆ and CFCs) are more pronounced and the resulting tracer signals are detectable over a longer time, because these tracers are biochemically conservative in lakes. Transport within the lake and gas exchange with the atmosphere are therefore the main processes that affect the observed tracer concentrations and the data collected are suitable for quantifying the corresponding process rates. As an example, lake monitoring based on noble gas analyses allows the exchange of dissolved gases with the anoxic deep water during a mixing event to be documented, while oxygen cannot be used as a tracer due to the fast oxygen consumption.

Acknowledgements We appreciate the support in the laboratory given by H. Amaral, M. S. Brennwald, M. Hofer, S. Klump and Y. Tomonaga from the Environmental Isotopes Group at Eawag (Swiss Federal Institute of Aquatic Science and Technology), as well as by H. Baur and U. Menet from ETH (Swiss Federal Institute of Technology Zurich). We thank D. M. Livingstone for his support in interpreting the CTD (conductivity, temperature and depth) time-series and for his detailed comments that improved our manuscript. Funding for C. P. H. was provided by the Swiss Federal Office of Education and Science (Contract no. 02.0247) within the framework of the European Union project CRIMEA (Contribution of high-intensity gas seeps in Black Sea to the methane emission to the atmosphere, Contract no. EVK2-CT-2002-00162). Further financial support came from the ETH research cluster TUMSS (Towards an improved understanding of methane sources and sinks) to C. P. H. and R. K. and from the Swiss National Science Foundation to R. K. (Grants 200020-101725 and 200020-105263).

Synthesis and outlook

The three case studies of this thesis document different novel applications of noble gases to study gas exchange and mixing processes in lakes and oceans. Especially deviations of the dissolved noble gas concentrations from their respective atmospheric equilibrium concentrations – so-called noble gas concentration anomalies – were found to be informative evidence of past or ongoing physical processes. The magnitude of the noble gas concentration anomalies observed in the studied water bodies allow the rates of the involved physical processes to be estimated.

The study of Lake Hallwil confirms that noble gases can be used to trace secondary gas exchange processes induced by bubbles which are injected from an aeration system (Chapter 3). The enrichment of dissolved noble gases found in the lake is shown to reflect the operation of the aeration system and the composition of the aeration gas (which is enriched in noble gases). It is demonstrated that the collected noble gas concentration profiles can in principle be used to quantify the total gas mass injected from the aeration system into the lake during the aeration period. To further constrain the estimate of the aeration gas mass input, a refined sampling strategy that covers the entire aeration period is proposed. The analysis of noble gas concentrations in the pore waters of the sediments of Lake Hallwil could complement the measurements in the water column. Noble gases in the pore water of lake sediments have been shown to preserve information on the history of the physical conditions prevailing in the overlaying water column (Brennwald, 2004). The noble gas concentrations in pore waters of the Lake Hallwil sediments are therefore expected to record effects of the aeration operation since its implementation about 20 years ago.

In the Black Sea, noble gas data were employed to determine vertical mixing in the water column and He input from terrigenous sources (Chapter 4). Furthermore,

specific noble gas anomalies were discovered in the water column above active CH₄ gas seeps. The observed noble gas depletions cannot be solely explained by secondary gas exchange processes (stripping and dissolution) with the injected bubbles. They rather indicate the presence of a rising plume of water depleted with respect to noble gases, which is emitted together with gas bubbles from the CH₄ seeps. Presumably, the flow of gas bubbles emitted from the studied seeps is too weak to make the noble gas concentration effect of stripping and dissolution by the injected CH₄ gas bubbles detectable in the water column. To successfully study the effect of noble-gas exchange between the rising bubbles and the surrounding water, seeps with higher gas-emission rates or aeration systems that inject noble-gas free bubbles should be analyzed in future studies. In such a setting, the direct effects of the secondary gas exchange processes on the dissolved noble gases, as predicted by models (Graser, 2006), should become more apparent.

In Lake Lugano, time-series of noble gas data and physical parameters of the water column (temperature and electrical conductivity) clearly document a recent increase of vertical mixing and deep water renewal that culminated in a sudden and complete overturn of the water column (Chapter 5). A numerical lake mixing model that was calibrated using the noble gas data yields quantitative estimates of the deep water renewal. The study on Lake Lugano highlights the relevance of time-series to study transitions in the physical conditions (e.g. in the mixing regime) prevailing in lakes and oceans. As such transitions may occur more frequently in the course of the changing climate, long time-series will become even more valuable.

In analogy to the presented case studies, the use noble of gases to analyze gas exchange and mixing processes can contribute to various surveys in lakes and oceans. Future work could for instance focus on the following topics:

- *Incorporate noble gases in process-oriented numerical models:* The noble gas data from the studies on gas injection into lake Hallwil and into the Black Sea should be combined with current work on single-bubble and bubble-plume models being developed to study the gas exchange and mixing processes that are induced by bubbles in these water bodies (e.g. McGinnis et al., 2004, 2006b). This approach would help to better understand the observed noble gas anomalies and would also allow the models to be better calibrated with actual data.
- *New field studies:* The experiences from the studies on aeration systems and marine gas seeps are useful to plan well directed field studies in the future. The sampling strategy can be chosen more adequately based on the knowledge, which effects on the noble gas concentrations in the water column have to be expected.

It is therefore intended to continue the study of the aeration system in Lake Hallwil to gain a more comprehensive budget of the injected aeration gas mass from the concentrations of dissolved noble gases in the water body.

In collaboration with IFM-GEOMAR and various other institutes, or group is currently involved in a study of CH₄ gas seeps in the Pacific, offshore New Zealand (Faure et al., 2006; IFM-GEOMAR, 2007). The study has great similarities to the work in the Black Sea and may therefore benefit from the findings of this thesis.

At present, researchers from Eawag are investigating the large concentrations of dissolved gases (CH₄ and CO₂) stored in the deep water of Lake Kivu, which is located on the boundary between Rwanda and the Democratic Republic of the Congo (Eawag, 2008). The potential release of these gases to the atmosphere due to an event that disrupts the density stratification of the water column (e.g. following a volcanic eruption or a major earthquake) poses a severe hazard to the local residents and to the environment. Like in the studies of Lake Lugano and of the Black Sea, noble gases could be used to analyze the water dynamics and the processes of gas injection and accumulation in Lake Kivu.

- *New experimental developments:* A new system to analyze simultaneously noble gas concentrations in water samples (except the ³He/⁴He isotopic composition) together with the concentrations of SF₆ and CFCs, using GC-ECD and GC-MS, is being developed at Eawag. The first results are promising (M. Hofer, pers. comm.). This system will facilitate combined transient tracer studies and will allow faster analyses of the tracer concentrations in water samples. It might be particularly useful in gas-exchange studies like at Lake Hallwil, where the contributions of non-atmospheric noble gases (especially ³He and ⁴He) are irrelevant.

These are just few suggestions for potential future directions in studies of noble gases in lakes and oceans. The presented results, as well as the new questions that emerged in the course of the work, emphasize the relevance of noble gases as environmental tracers for gas exchange and mixing processes in surface water bodies and are expected to stimulate future research in this field.

Bibliography

- Aeschbach-Hertig W. *Helium und Tritium als Tracer für physikalische Prozesse in Seen*. Diss. ETH Nr. 10714, ETH Zürich, 1994. URL <http://e-collection.ethbib.ethz.ch/show?type=diss&nr=10714>.
- Aeschbach-Hertig W., Kipfer R., Hofer M., Imboden D. M., and Baur H. Density-driven exchange between the basins of Lake Lucerne (Switzerland) traced with the ^3H - ^3He method. *Limnol. Oceanogr.*, 41(4):707–721, 1996.
- Aeschbach-Hertig W., Peeters F., Beyerle U., and Kipfer R. Interpretation of dissolved atmospheric noble gases in natural waters. *Water Resour. Res.*, 35(9):2779–2792, 1999.
- Aeschbach-Hertig W., Hofer M., Schmid M., Kipfer R., and Imboden D. M. The physical structure and dynamics of a deep, meromictic crater lake (Lac Pavin, France). *Hydrobiol.*, 487(1):111–136, 2002. doi: 10.1023/A:1022942226198.
- Aeschbach-Hertig W., Holzner C. P., Hofer M., Simona M., Barbieri A., and Kipfer R. A time series of environmental tracer data from deep meromictic Lake Lugano, Switzerland. *Limnol. Oceanogr.*, 52(1):257–273, 2007.
- AfU (Abteilung für Umwelt, Kanton Aargau). Sanierung Hallwilersee., 2007. URL http://www.ag.ch/umwelt/de/pub/themen/wasser/sanierung_hallwilersee.htm. Accessed: 5 Oct 2007.
- Artemov Y. G. Software support for investigation of natural methane seeps by hydroacoustic method. *Mar. Ecol. Journal*, 1:57–71, 2006.
- Ballentine C. J. and Burnard P. G. Production, release and transport of noble gases in the continental crust. In Porcelli D., Ballentine C. J., and Wieler R., editors, *Noble gases in geochemistry and cosmochemistry*, volume 47 of *Rev. Mineral. Geochem.*, pages 481–538. Mineralogical Society of America, Geochemical Society, 2002.
- Barbieri A. and Mosello R. Chemistry and trophic evolution of Lake Lugano in relation to nutrient budget. *Aquat. Sci.*, 54(3/4):219–237, 1992. doi: 10.1007/BF00878138.
- Barbieri A. and Polli B. Description of Lake Lugano. *Aquat. Sci.*, 54(3/4):181–183, 1992. doi: 10.1007/BF00878135.

- Barbieri A. and Simona M. Trophic evolution of Lake Lugano related to external load reduction: Changes in phosphorus and nitrogen as well as oxygen balance and biological parameters. *Lakes & Reservoirs: Research and Management*, 6(1):37–47, 2001. doi: 10.1046/j.1440-1770.2001.00120.x.
- Baur H. A noble-gas mass spectrometer compressor source with two orders of magnitude improvement in sensitivity. In *American Geophysical Union, Fall Meeting*, volume 80 of *EOS, Trans. Am. Geophys. Union*, page F1118, San Francisco, 1999. American Geophysical Union.
- Beyerle U., Aeschbach-Hertig W., Imboden D. M., Baur H., Graf T., and Kipfer R. A mass spectrometric system for the analysis of noble gases and tritium from water samples. *Environ. Sci. Technol.*, 34(10): 2042–2050, 2000. doi: 10.1021/es990840h.
- Bieri R. H., Koide M., and Goldberg E. D. The noble gas contents of Pacific seawaters. *J. Geophys. Res.*, 71(22):5243–5265, 1966.
- Bohrmann G., Ivanov M., Foucher J. P., Spiess V., Bialas J., Greinert J., Weinrebe W., Abegg F., Aloisi G., Artemov Y., Blinova V., Drews M., Heidersdorf F., Krabbenhöft A., Klaucke I., Krastel S., Leder T., Polikarpov I., Saburova M., Schmale O., Seifert R., Volkonskaya A., and Zillmer M. Mud volcanoes and gas hydrates in the Black Sea: New data from Dvurechenskii and Odessa mud volcanoes. *Geo-Mar. Lett.*, 23(3):239–249, 2003. doi: 10.1007/s00367-003-0157-7.
- Brennwald M. S. *The use of noble gases in lake sediment pore water as environmental tracers*. Diss. ETH Nr. 15629, ETH Zürich, 2004. URL <http://e-collection.ethbib.ethz.ch/show?type=diss&nr=15629>.
- Brennwald M. S., Hofer M., Peeters F., Aeschbach-Hertig W., Strassmann K., Kipfer R., and Imboden D. M. Analysis of dissolved noble gases in the pore water of lacustrine sediments. *Limnol. Oceanogr. Methods*, 1:51–62, 2003.
- Broecker W. S., Cromwell J., and Li Y. H. Rates of vertical eddy diffusion near the ocean floor based on measurements of the distribution of excess ^{222}Rn . *Earth Planet. Sci. Lett.*, 5:101–105, 1968. doi: 10.1016/S0012-821X(68)80022-6.
- Bullister J. L., Wisegarver D. P., and Menzia F. A. The solubility of sulfur hexafluoride in water and seawater. *Deep-Sea Res. I*, 49(1):175–187, 2002. doi: 10.1016/S0967-0637(01)00051-6.
- Chung Y. and Craig H. Excess-radon and temperature profiles from the Eastern Equatorial Pacific. *Earth Planet. Sci. Lett.*, 14(1):55–64, 1972. doi: 10.1016/0012-821X(72)90079-9.
- CIP AIS (Commissione Internazionale per la Protezione delle Acque Italo-Svizzere). Stato limnologico del Lago di Lugano: Circolazione invernale 2004–2005. Bolletino dei Laghi Maggiore e Lugano no. 6, 2005.
- CIP AIS (Commissione Internazionale per la Protezione delle Acque Italo-Svizzere). Stato limnologico del Lago di Lugano: Circolazione invernale 2005–2006. Bolletino dei Laghi Maggiore e Lugano no. 7, 2006.
- Clark J. F., Leifer I., Washburn L., and Luyendyk B. P. Compositional changes in natural gas bubble plumes: observations from the Coal Oil Point marine hydrocarbon seep field. *Geo-Mar. Lett.*, 23(3): 187–193, 2003. doi: 10.1007/s00367-003-0137-y.
- Clarke W. B., Beg M. A., and Craig H. Excess ^3He in the sea: Evidence for terrestrial primordial helium. *Earth Planet. Sci. Lett.*, 6:213–220, 1969. doi: 10.1016/0012-821X(69)90093-4.

- Clarke W. B., Jenkins W. J., and Top Z. Determination of tritium by mass spectrometric measurement of ^3He . *Int. J. appl. Radiat. Isotopes*, 27:515–522, 1976.
- Clever H. L., editor. *Krypton, xenon and radon – gas solubilities*, volume 2 of *Solubility data series*. Pergamon Press, Oxford, 1979.
- Colman J. A. and Armstrong D. E. Vertical eddy diffusivity determined with Rn-222 in the benthic boundary-layer of ice-covered lakes. *Limnol. Oceanogr.*, 32(3):577–590, 1987.
- Craig H. and Lal D. The production rate of natural tritium. *Tellus*, 13(1):85–105, 1961.
- Craig H. and Weiss R. F. Dissolved gas saturation anomalies and excess helium in the ocean. *Earth Planet. Sci. Lett.*, 10(3):289–296, 1971. doi: 10.1016/0012-821X(71)90033-1.
- Craig H., Clarke W. B., and Beg M. A. Excess ^3He in deep water on the East Pacific Rise. *Earth Planet. Sci. Lett.*, 26(2):125–132, 1975. doi: 10.1016/0012-821X(75)90079-5.
- CRIMEA Project. Contribution of high-intensity gas seeps in black sea to the methane emission to the atmosphere. Final scientific report, EC project EVK-2-CT-2002-00162, 2006. URL <http://crimea-info.org/>.
- Danckwerts P. V. Significance of liquid-film coefficients in gas absorption. *Indust. Eng. Chem.*, 43: 1460–1467, 1951. doi: 10.1021/ie50498a055.
- Deacon E. L. Gas transfer to and across an air-water interface. *Tellus*, 29:363–374, 1977.
- Der Schweizerische Bundesrat. Gewässerschutzverordnung vom 28. Oktober 1998 (GSchV). SR-No. 814.201, 1998. URL http://www.admin.ch/ch/d/sr/c814_201.html.
- Dzambas Z. and Ulrich M. MASAS library files for Swiss lakes. Technical report, Eawag/ETH, 1994.
- Eawag. Turning a risk into a resource, 2008. URL http://www.eawag.ch/media/20071011/index_EN. Accessed: 13 Mar 2008.
- Eawag/SIAM. AQUASIM: Computer program for the identification and simulation of aquatic systems., 2007. URL <http://www.eawag.ch/organisation/abteilungen/siam/software/aquasim/>. Accessed: 8 Nov 2007.
- Edmonds T. and Singleton V. Field testing report Lake Hallwil (July 11-15, 2005). Unpublished report, Civil and Environmental Engineering, Virginia Polytechnic Institute and State University, Blacksburg, VA, USA, 2005.
- Faure K., Greinert J., Pecher I. A., Graham I. J., Massoth G. J., de Ronde C. E. J., Wright I. C., Baker E. T., and Olson E. J. Methane seepage and its relation to slumping and gas hydrate at the Hikurangi margin, New Zealand. *New Zealand J. Geol. Geophys.*, 49:503–516, 2006.
- Gächter R. and Stadelmann P. Gewässerschutz und Seeforschung. In Ruoss E., editor, *Der Sempachersee*, volume 33 of *Mitt. Naturforsch. Ges. Luzern*, pages 343–377. Naturforsch. Ges., Luzern, Switzerland, 1993.
- Graser N. *Edelgase als Tracer bei der Untersuchung der Gasblasenauflösung in natürlichen Gewässern*. Diploma thesis, Eawag Dübendorf / ETH Zürich, 2006.

- Greinert J., Artemov Y., Egorov V., De Batist M., and McGinnis D. 1300-m-high rising bubbles from mud volcanoes at 2080 m in the Black Sea: Hydroacoustic characteristics and temporal variability. *Earth Planet. Sci. Lett.*, 244(1-2):1–15, 2006. doi: 10.1016/j.epsl.2006.02.011.
- Higbie R. The rate of absorption of a pure gas into a still liquid during a short time of exposure. *Trans. Am. Inst. Chem. Eng.*, 31(2):365–389, 1935.
- Hofer M., Peeters F., Aeschbach-Hertig W., Brennwald M. S., Holocher J., Livingstone D. M., Romanovski V., and Kipfer R. Rapid deep-water renewal in Lake Issyk-Kul (Kyrgyzstan) indicated by transient tracers. *Limnol. Oceanogr.*, 47(4):1210–1216, 2002.
- Hohmann R., Hofer M., Kipfer R., Peeters F., and Imboden D. M. Distribution of helium and tritium in Lake Baikal. *J. Geophys. Res.*, 103(C6):12823–12838, 1998.
- Hohmann R., Schlosser P., Jacobs S., Ludin A., and Weppernig R. Excess helium and neon in the southeast Pacific: Tracers for glacial meltwater. *J. Geophys. Res.*, 107(C11):3198, 2002. doi: 10.1029/2000JC000378.
- Holocher J. *Investigations of gas exchange in quasi-saturated porous media using noble gases as conservative tracers*. Diss. ETH Nr. 14588, ETH Zürich, 2002. URL <http://e-collection.ethbib.ethz.ch/show?type=diss&nr=14588>.
- Holocher J., Peeters F., Aeschbach-Hertig W., Kinzelbach W., and Kipfer R. Kinetic model of gas bubble dissolution in groundwater and its implications for the dissolved gas composition. *Environ. Sci. Technol.*, 37:1337–1343, 2003.
- Holzner C. *Untersuchung der Tiefenwassererneuerung in meromiktischen Seen mittels transienter Tracer und numerischer Modellierung*. Diploma thesis, Eawag Dübendorf / ETH Zürich, 2001.
- Holzner C. P., Amaral H., Brennwald M. S., Hofer M., Klump S., and Kipfer R. Methane bubble streams in the Black Sea traced by dissolved noble gases. In *EGU General Assembly*, volume 7 of *Geophysical Research Abstracts*, page 03846, Vienna, Austria, 2005. European Geosciences Union.
- Holzner C. P., Graser N., Brennwald M. S., and Kipfer R. Noble gases as tracers for gas-exchange processes at bubble-streams in lakes and oceans. In *16th Annual V. M. Goldschmidt Conference*, volume 70 (18, Suppl. 1), page A262, Melbourne, Australia, 2006. *Geochim. Cosmochim. Acta*. doi: 10.1016/j.gca.2006.06.526.
- Holzner C. P., Aeschbach-Hertig W., Simona M., Veronesi M., Kipfer R., and Imboden D. M. Exceptional mixing events in Lake Lugano, Switzerland, studied using environmental tracers. *Limnol. Oceanogr.*, submitted, 2008a.
- Holzner C. P., McGinnis D. F., Schubert C. J., Kipfer R., and Imboden D. M. Noble gas anomalies related to high-intensity methane gas seeps in the Black Sea. *Earth Planet. Sci. Lett.*, 265(3-4):396–409, 2008b. doi: 10.1016/j.epsl.2007.10.029.
- Hornafius J. S., Quigley D., and Luyendyk B. P. The world's most spectacular marine hydrocarbon seeps (Coal Oil Point, Santa Barbara Channel, California): Quantification of emissions. *J. Geophys. Res.*, 104(C9):20703–20712, 1999. doi: 10.1029/1999JC900148.
- IAEA/WMO. Global network of isotopes in precipitation. The GNIP database., 2004. URL <http://isohis.iaea.org>. Accessed: 7 Nov 2007.
- Idso S. B. On the concept of lake stability. *Limnol. Oceanogr.*, 18(4):681–683, 1973.

- IFM-GEOMAR. NEW VENTS / New Zealand cold vents, 2007. URL <http://www.ifm-geomar.de/index.php?id=newvents&L=1>. Accessed: 17 Mar 2008.
- Imboden D. M. Natural radon as a limnological tracer for the study of vertical and horizontal eddy diffusion. In IAEA, editor, *Isotopes in lake studies*, pages 213–218, Vienna, 1977. IAEA.
- Imboden D. M. and Emerson S. Natural radon and phosphorus as limnologic tracers: Horizontal and vertical eddy diffusion in Greifensee. *Limnol. Oceanogr.*, 23(1):77–90, 1978.
- Imboden D. M. and Joller T. Turbulent mixing in the hypolimnion of Baldeggersee (Switzerland) traced by natural radon-222. *Limnol. Oceanogr.*, 29(4):831–844, 1984.
- Imboden D. M. and Wüest A. Mixing mechanisms in lakes. In Lerman A., Imboden D. M., and Gat J. R., editors, *Physics and chemistry of lakes*, pages 83–138. Springer, Berlin, 2nd edition, 1995.
- Jähne B., Heinz G., and Dietrich W. Measurement of the diffusion coefficients of sparingly soluble gases in water. *J. Geophys. Res.*, 92(C10):10767–10776, 1987.
- Jenkins W. J. ^3H and ^3He in the Beta Triangle: Observations of gyre ventilation and oxygen utilization rates. *J. Phys. Oceanogr.*, 17:763–783, 1987.
- Jenkins W. J. and Clarke W. B. The distribution of ^3He in the western Atlantic Ocean. *Deep-Sea Res.*, 23(6):481–494, 1976. doi: 10.1016/0011-7471(76)90860-3.
- Judd A. G. Natural seabed gas seeps as sources of atmospheric methane. *Env. Geol.*, 46(8):988–996, 2004. doi: 10.1007/s00254-004-1083-3.
- Keeling R. F. On the role of large bubbles in air-sea gas exchange and supersaturation in the ocean. *J. Marine Res.*, 51:237–271, 1993. doi: 10.1357/0022240933223800.
- Kipfer R., Aeschbach-Hertig W., Beyerle U., Goudsmit G., Hofer M., Peeters F., Klerkx J., Plisnier J.-P., Kliebe E. A., and Ndhlovu R. New evidence for deep water exchange in Lake Tanganyika. In *2000 Ocean Sciences Meeting*, volume 80 of *EOS, Transactions, American Geophysical Union*, page OS239, San Antonio, 2000. AGU.
- Kipfer R., Aeschbach-Hertig W., Peeters F., and Stute M. Noble gases in lakes and ground waters. In Porcelli D., Ballentine C. J., and Wieler R., editors, *Noble gases in geochemistry and cosmochemistry*, volume 47 of *Rev. Mineral. Geochem.*, pages 615–700. Mineralogical Society of America, Geochemical Society, 2002.
- Klump S. *The formation of excess air in groundwater studied using noble gases as conservative tracers in laboratory and field experiments*. Diss. ETH Nr. 17168, ETH Zürich, 2007. URL <http://e-collection.ethbib.ethz.ch/show?type=diss&nr=17168>.
- Korotaev G., Oguz T., and Riser S. Intermediate and deep currents of the Black Sea obtained from autonomous profiling floats. *Deep-Sea Res. II*, 53:1901–1910, 2006.
- Kourtidis K., Kioutsioukis I., McGinnis D. F., and Rapsomanikis S. Effects of methane outgassing on the Black Sea atmosphere. *Atmos. Chem. Phys.*, 6:5173–5182, 2006.
- Krastel S., Spiess V., Ivanov M., Weinrebe W., Bohrmann G., Shashkin P., and Heidersdorf F. Acoustic investigations of mud volcanoes in the Sorokin Trough, Black Sea. *Geo-Mar. Lett.*, 23(3):230–238, 2003. doi: 10.1007/s00367-003-0143-0.

- Kutas R. I., Paliy S. I., and Rusakov O. M. Deep faults, heat flow and gas leakage in the northern Black Sea. *Geo-Mar. Lett.*, 24(3):163–168, 2004. doi: 10.1007/s00367-004-0172-3.
- Leifer I. and Judd A. G. Oceanic methane layers: The hydrocarbon seep bubble deposition hypothesis. *Terra Nova*, 14(6):417–424, 2002. doi: 10.1046/j.1365-3121.2002.00442.x.
- Leifer I. and Patro R. K. The bubble mechanism for methane transport from the shallow sea bed to the surface: A review and sensitivity study. *Cont. Shelf Res.*, 22(16):2409–2428, 2002.
- Leifer I., Clark J. F., and Chen R. F. Modifications of the local environment by natural marine hydrocarbon seeps. *Geophys. Res. Lett.*, 27(22):3711–3714, 2000. doi: 10.1029/2000GL011619.
- Leifer I., Luyendyk B. P., Boles J., and Clark J. F. Natural marine seepage blowout: Contribution to atmospheric methane. *Global Biogeochem. Cycles*, 20:GB3008, 2006. doi: 10.1029/2005GB002668.
- Lide D. R., editor. *CRC handbook of chemistry and physics*. CRC Press, Boca Raton, Ann Arbor, London, Tokyo, 75th edition, 1994.
- Liss P. S. and Merlivat L. Air-sea gas exchange rates: Introduction and synthesis. In Buat-Ménard P., editor, *The role of air-sea exchange in geochemical cycling*, pages 113–127. D. Reidel publishing company, Dordrecht, 1986.
- Livingstone D. M. An example of the simultaneous occurrence of climate-driven “sawtooth” deep-water warming/cooling episodes in several Swiss lakes. *Verh. Internat. Verein. Limnol.*, 26:822–828, 1997.
- Livingstone D. M. and Imboden D. M. The non-linear influence of wind-speed variability on gas transfer in lakes. *Tellus*, 45B(3):275–295, 1993.
- Livingstone D. M. and Lotter A. F. The relationship between air and water temperatures in lakes of the Swiss Plateau: A case study with palaeolimnological implications. *J. Paleolimnol.*, 19:181–198, 1998. doi: 10.1023/A:1007904817619.
- Livingstone D. M., Lotter A. F., and Walker I. R. The decrease in summer surface water temperature with altitude in Swiss Alpine lakes: A comparison with air temperature lapse rates. *Arctic Antarctic Alpine Res.*, 31(4):341–352, 1999.
- LSA (Laboratorio Studi Ambientali). Ricerche sull’evoluzione del Lago di Lugano; aspetti limnologici. Campagne annuali 1980-1999. Technical report, Commissione Internazionale per la Protezione delle Acque Italo-Svizzere, 1981-2000.
- Lucas L. L. and Unterwieser M. P. Comprehensive review and critical evaluation of the half-life of tritium. *J. Res. Nat. Inst. Stand. Technol.*, 105(4):541–549, 2000.
- Lüdmann T., Wong H. K., Konerding P., Zillmer M., Petersen J., and Flüh E. Heat flow and quantity of methane deduced from a gas hydrate field in the vicinity of the Dnieper Canyon, northwestern Black Sea. *Geo-Mar. Lett.*, 24(3):182–193, 2004. doi: 10.1007/s00367-004-0169-y.
- Maiss M. and Brenninkmeijer C. A. M. Atmospheric SF₆: Trends, sources, and prospects. *Environ. Sci. Technol.*, 32:3077–3086, 1998.
- Mamyrin B. A. and Tolstikhin I. N. *Helium isotopes in nature*, volume 3 of *Developments in Geochemistry*. Elsevier, Amsterdam, Oxford, New York, Tokyo, 1st edition, 1984.
- Märki E. and Schmid M. Der Zustand des Hallwilersees. *Wasser, Energie, Luft*, 75(4):105–112, 1983.

- McDougall T. J. Bubble plumes in stratified environments. *J. Fluid Mech.*, 85(4):655–672, 1978.
- McGinnis D. F. and Little J. C. Predicting diffused-bubble oxygen transfer rate using the discrete-bubble model. *Water Res.*, 36(18):4627–4635, 2002. doi: 10.1016/S0043-1354(02)00175-6.
- McGinnis D. F., Lorke A., Wüest A., Stöckli A., and Little J. C. Interaction between a bubble plume and the near field in a stratified lake. *Water Resour. Res.*, 40:W10206, 2004. doi: doi:10.1029/2004WR003038.
- McGinnis D. F., Greinert J., Artemov Y., Beaubien S. E., and Wüest A. Fate of rising methane bubbles in stratified waters: How much methane reaches the atmosphere? *J. Geophys. Res.*, 111:C09007, 2006a. doi: 10.1029/2005JC003183.
- McGinnis D. F., Holzner C. P., Kipfer R., and Wüest A. Vertical methane fluxes in the black sea deep-water: Are there plumes? In *Proceedings of the 6th International Conference on Stratified Flows*, pages 787–792, Perth, Australia, 2006b.
- Naudts L., Greinert J., Artemov Y., Staelens P., Poort J., Van Rensbergen P., and De Batist M. Geological and morphological setting of 2778 methane seeps in the Dnepr paleo-delta, northwestern Black Sea. *Marine Geol.*, 227(3-4):177–199, 2006. doi: 10.1016/j.margeo.2005.10.005.
- Ozima M. and Podosek F. A. *Noble gas geochemistry*. Cambridge University Press, Cambridge, 2nd edition, 2002.
- Ozone Secretariat. *The Montreal Protocol on Substances that Deplete the Ozone Layer*. United Nations Environment Programme, Nairobi, Kenya, 2000.
- Özsoy E., Rank D., and Salihoglu I. Pycnocline and deep mixing in the Black Sea: Stable isotope and transient tracer measurements. *Estuar. Coast. Shelf Sci.*, 54(3):621–629, 2002. doi: 10.1006/ecss.2000.0669.
- Peeters F., Kipfer R., Hohmann R., Hofer M., Imboden D. M., Kodenev G. G., and Khozder T. Modelling transport rates in Lake Baikal: gas exchange and deep water renewal. *Environ. Sci. Technol.*, 31(10): 2973–2982, 1997.
- Peeters F., Kipfer R., Achermann D., Hofer M., Aeschbach-Hertig W., Beyerle U., Imboden D. M., Rozanski K., and Fröhlich K. Analysis of deep-water exchange in the Caspian Sea based on environmental tracers. *Deep-Sea Res. I*, 47(4):621–654, 2000a. doi: 10.1016/S0967-0637(99)00066-7.
- Peeters F., Kipfer R., Hofer M., Imboden D. M., and Domysheva V. M. Vertical turbulent diffusion and upwelling in Lake Baikal estimated by inverse modeling of transient tracers. *J. Geophys. Res.*, 105 (C2):3451–3464, 2000b. doi: 10.1029/1999JC900293.
- Reeburgh W. S., Ward B. B., Whalen S. C., Sandbeck K. A., Kilpatrick K. A., and Kerkhof L. J. Black Sea methane geochemistry. *Deep-Sea Res.*, 38(Suppl. 2):S1189–S1210, 1991.
- Rehder G., Brewer P. W., Peltzer E. T., and Friederich G. Enhanced lifetime of methane bubble streams within the deep ocean. *Geophys. Res. Lett.*, 29(15):1731, 2002. doi: 10.1029/2001GL013966.
- Reichert P. Aquasim – a tool for simulation and data analysis of aquatic systems. *Wat. Sci. Tech.*, 30(2): 21–30, 1994.
- Ro K. S. and Hunt P. G. A new unified equation for wind-driven surficial oxygen transfer into stationary water bodies. *Trans. ASABE*, 49(5):1615–1622, 2006.

- Ro K. S., Hunt P. G., and Poach M. E. Wind-driven surficial oxygen transfer. *Crit. Rev. Environ. Sci. Technol.*, 37(6):539 – 563, 2007. doi: 10.1080/10643380601174749.
- Roether W. On oceanic boundary conditions for tritium, on tritiogenic ^3He and on the tritium- ^3He age concept. In Anderson D. L. T. and Willebrand J., editors, *Oceanic circulation models: Combining data and dynamics*, pages 377–407. Kluwer Academic Press, 1989.
- Ross D. A., Neprochnov Y. P., and the Scientific Party of DSDP Leg 42B . *Initial reports of the Deep Sea Drilling Project*, volume 42, Part 2. U.S. Government Printing Office, Washington, 1978.
- Schaffner U. Belüftung des Hallwilersees. *Schweizer Ingenieur und Architekt*, 23:660–663, 1987.
- Scheidegger A., Stöckli A., and Wüest A. Einfluss der internen Sanierungsmassnahmen auf den Stoffhaushalt im Hallwilersee. *Wasser, Energie, Luft*, 86(5/6):126–131, 1994.
- Schlosser P. Helium: a new tracer in Antarctic oceanography. *Nature*, 321:233–235, 1986. doi: 10.1038/321233a0.
- Schlosser P. and Winckler G. Noble gases in ocean waters and sediments. In Porcelli D., Ballentine C., and Wieler R., editors, *Noble gases in geochemistry and cosmochemistry*, volume 46 of *Rev. Mineral. Geochem.*, pages 701–730. Mineralogical Society of America, Geochemical Society, 2002.
- Schlosser P., Bayer R., Foldvik A., Gammelsrød T., Rohardt G., and Münnich K. O. Oxygen 18 and helium as tracers of ice shelf water and water/ice interaction in the Wedell Sea. *J. Geophys. Res.*, 95 (C3):3253–3263, 1990.
- Schlosser P., Bonisch G., Rhein M., and Bayer R. Reduction of deepwater formation in the Greenland Sea during the 1980s: Evidence from tracer data. *Science*, 251(4997):1054–1056, 1991a. doi: 10.1126/science.251.4997.1054.
- Schlosser P., Bullister J. B., and Bayer R. Studies of deep water formation and circulation in the Weddell Sea using natural and anthropogenic tracers. *Marine Chem.*, 35:97–122, 1991b.
- Schmale O., Greinert J., and Rehder G. Methane emission from high-intensity marine gas seeps in the Black Sea into the atmosphere. *Geophys. Res. Lett.*, 32:L07609, 2005. doi: 10.1029/2004GL021138.
- Schmidt W. Über die Temperatur- und Stabilitätsverhältnisse von Seen. *Geogr. Ann.*, 10:145–177, 1928.
- Schubert C. J., Durisch-Kaiser E., Holzner C. P., Klauser L., Wehrli B., Schmale O., Greinert J., McGinnis D. F., De Batist M., and Kipfer R. Methanotrophic microbial communities associated with bubble plumes above gas seeps in the Black Sea. *Geochem. Geophys. Geosyst.*, 7(4):Q04002, 2006a. doi: 10.1029/2005GC001049.
- Schubert C. J., Durisch-Kaiser E., Klauser L., Wehrli B., Holzner C. P., Kipfer R., Schmale O., Greinert J., and Kuypers M.M.M. Recent studies on sources and sinks of methane in the Black Sea. In Neretin L.N., Jørgensen B.B., and Murray J. W., editors, *Past and Present Water Column Anoxia*, Nato Science Series: Earth and Environmental Sciences, pages 419–441. Kluwer-Springer, 2006b.
- Schwarzenbach R. P., Gschwend P. M., and Imboden D. M. *Environmental Organic Chemistry*. John Wiley & Sons, Inc., New York, 2nd edition, 2003.
- Sorokin Y. I. *The Black Sea: Ecology and oceanography*. Biology of inland waters. Backhuys Publishers, Leiden, 2002.

- Stanev E. V., Staneva J., Bullister J. L., and Murray J. W. Ventilation of the Black Sea pycnocline. Parameterization of convection, numerical simulations and validations against observed chlorofluorocarbon data. *Deep-Sea Res. I*, 51(12):2137–2169, 2004. doi: 10.1016/j.dsr.2004.07.018.
- Stöckli A. Der Hallwilersee wird bald wieder gesund. *Umwelt Aargau – Umweltinformation Kanton Aargau*, Special Issue 20, 2005.
- Stöckli A. and Schmid M. Die Sanierung des Hallwilersees: Erste Erfahrungen mit Zwangszirkulation und Tiefenwasserbelüftung. *Wasser, Energie, Luft*, 79(7/8):143–149, 1987.
- Strassmann K. M., Brennwald M. S., Peeters F., and Kipfer R. Dissolved noble gases in porewater of lacustrine sediments as palaeolimnological proxies. *Geochim. Cosmochim. Acta*, 69(7):1665–1674, 2005. doi: 10.1016/j.gca.2004.07.037.
- Tolstikhin I. N. and Kamenskiy I. L. Determination of ground-water ages by the T-³He method. *Geochem. Internat.*, 6:810–811, 1969.
- Tomonaga Y., Brennwald M. S., and Kipfer R. Spatial variability in the release of terrigenous He from the sediments of Lake Van (Turkey). In *17th Annual V. M. Goldschmidt Conference*, volume 71 (15, Suppl. 1), page A1029, Cologne, Germany, 2007. *Geochim. Cosmochim. Acta*. doi: 10.1016/j.gca.2007.06.027.
- Top Z. and Clarke W. B. Helium, neon and tritium in the Black Sea. *J. Marine Res.*, 41(1):1–17, 1983.
- Top Z., Clarke W. B., Eismont W. C., and Jones E. P. Radiogenic helium in Baffin Bay bottom water. *Econ. Geol.*, 38(3):435–452, 1981.
- Top Z., Izdar E., Ergün M., and Konuk T. Evidence of tectonism from ³He and residence time of helium in the Black Sea. *Eos*, 71:1020–1021, 1990.
- Top Z., Östlund G., Pope L., and Grall C. Helium isotopes, neon and tritium in the Black Sea, a comparison with the 1975 observations. *Deep-Sea Res.*, 38(Suppl. 2):S747–S759, 1991.
- Torgersen T., Top Z., Clarke W. B., Jenkins W. J., and Broecker W.S. A new method for physical limnology – tritium-helium-3 ages – results for Lakes Erie, Huron and Ontario. *Limnol. Oceanogr.*, 22(2):181–193, 1977.
- Torgersen T., Clarke W. B., and Jenkins W. J. The tritium/helium-3 method in hydrology. In *Isotope Hydrology 1978*, pages 917–930. IAEA, Vienna, 1979.
- Torgersen T., Hammond D. E., Clarke W. B., and Peng T.-H. Fayetteville, Green Lake, New York: ³H-³He water mass ages and secondary chemical structure. *Limnol. Oceanogr.*, 26(1):110–122, 1981.
- UPDA (Ufficio Protezione e Depurazione Acque). Ricerche sull'evoluzione del Lago di Lugano; aspetti limnologici. Programma quinquennale 2003–2007. Campagna 2004 e 2005. Technical report, Commissione Internazionale per la Protezione delle Acque Italo-Svizzere (Ed.), 2006.
- Vollmer M. K., Weiss R. F., Schlosser P., and Williams R. T. Deep-water renewal in Lake Issyk-Kul. *Geophys. Res. Lett.*, 29(8):124/1 –124/4, 2002. doi: 10.1029/2002GL014763.
- Walker S. J., Weiss R. F., and Salameh P. K. Reconstructed histories of the annual mean atmospheric mole fractions for the halocarbons CFC-11, CFC-12, CFC-113, and carbon tetrachloride. *J. Geophys. Res.*, 105(C6):14285–14296, 2000.

- Walter K. M., Zimov S. A., Chanton J. P., and Chapin III F. S. Methane bubbling from Siberian thaw lakes as a positive feedback to climate warming. *Nature*, 443:71–75, 2006. doi: 10.1038/nature05040.
- Wanninkhof R. Relationship between wind speed and gas exchange over the ocean. *J. Geophys. Res.*, 97(C5):7373–7382, 1992.
- Warner M. J. and Weiss R. F. Solubilities of chlorofluorocarbons 11 and 12 in water and seawater. *Deep-Sea Res. I*, 32(12):1485–1497, 1985. doi: 10.1016/0198-0149(85)90099-8.
- Wehrli B. and Wüest A. Zehn Jahre Seenbelüftung: Erfahrungen und Optionen. Schriftenreihe der Eawag Nr. 9, Eawag, 1996.
- Weiss R. F. Solubility of helium and neon in water and seawater. *J. Chem. Eng. Data*, 16(2):235–241, 1971.
- Weiss R. F. The solubility of nitrogen, oxygen and argon in water and seawater. *Deep-Sea Res.*, 17(4): 721–735, 1970. doi: 10.1016/0011-7471(70)90037-9.
- Weiss R. F. and Kyser T. K. Solubility of krypton in water and seawater. *J. Chem. Eng. Data*, 23(1): 69–72, 1978. doi: 10.1021/je60076a014.
- Weiss W., Bullacher J., and Roether W. Evidence of pulsed discharges of tritium from nuclear energy installations in central european precipitation. In IAEA , editor, *Behaviour of tritium in the environment*, Proceedings Series, pages 17–30, San Francisco, 16-20 Oct. 1978, 1979. IAEA.
- Weiss W., Zapf T., Baitter M., Kromer B., Fischer K. H., Schlosser P., Roether W., and Münnich K. O. Subsurface horizontal water transport and vertical mixing in Lake Constance traced by radon-222, tritium, and other physical and chemical tracers. In IAEA , editor, *Isotope Hydrology 1983*, volume IAEA-SM-270/7 of *Isotope Hydrology*, pages 43–54, Vienna, 1984. IAEA.
- Whitman W. G. The two-film theory of gas absorption. *Chem. Met. Eng.*, 29:146–148, 1923.
- Winckler G., Aeschbach-Hertig W., Holocher J., Kipfer R., Levin I., Poss C., Rehder G., Suess E., and Schlosser P. Noble gases and radiocarbon in natural gas hydrates. *Geophys. Res. Lett.*, 29(10):1423, 2002. doi: 10.1029/2001GL014013.
- Wüest A., Aeschbach-Hertig W., Baur H., Hofer M., Kipfer R., and Schurter M. Density structure and tritium-helium age of deep hypolimnetic water in the northern basin of Lake Lugano. *Aquat. Sci.*, 54 (3/4):205–218, 1992a. doi: 10.1007/BF00878137.
- Wüest A., Brooks N. H., and Imboden D. M. Bubble plume modeling for lake restoration. *Water Resour. Res.*, 28(12):3235–3250, 1992b.
- Zenger A., Ilmberger J., Heinz G., Schimmele M., Schlosser P., Imboden D., and Münnich K. O. Behaviour of a medium-sized basin connected to a large lake. In Tilzer M. M. and Serruya C., editors, *Large Lakes: Ecological Structure and Function*, Brock/Springer Series in Contemporary Bioscience, pages 133–155. Springer-Verlag, Berlin, Heidelberg, 1990.

Curriculum vitae

Christian Peter Holzner

14 July 1972	Born in Zürich, Switzerland
1980 – 1986	Primary school in Uitikon-Waldegg
1986 – 1989	Secondary school in Uitikon-Waldegg
1989 – 1994	High school in Zürich School-leaving exam (Matura)
1994 – 1996	Studies in Architecture Swiss Federal Institute of Technology Zürich (ETH)
1996 – 2001	Studies in Environmental Sciences Swiss Federal Institute of Technology Zürich (ETH)
2001	Diploma in environmental sciences (Dipl. Umwelt-Natw. ETH)
2002 – 2003	Research and teaching assistant Swiss Federal Institute of Aquatic Science and Technology (Eawag)
2003 – 2008	PhD student and research assistant in the Department of Environmental Sciences of the Swiss Federal Institute of Technology Zürich (ETH), Zürich and in the Department of Water Resources and Drinking Water of the Swiss Federal Institute of Aquatic Science and Technology (Eawag), Dübendorf

